Catalytic Pyrolysis of Thermally Pre-treated Biomass for Aromatic Production

by

Vaishnavi Srinivasan

A thesis submitted to the Graduate Faculty of
Auburn University
in partial fulfillment of the
requirements for the Degree of
Master of Science

Auburn, Alabama
August 3, 2013

Keywords: biomass, torrefaction, pyrolysis, bio-oil, catalyst,

Approved by

Sushil Adhikari, Chair, Associate professor of Biosystems Engineering
Oladiran Fasina, Professor of Biosystems Engineering
Maobing Tu, Associate Professor, School of Forestry and Wildlife Science

Abstract

Torrefaction, a biomass pre-treatment process, is considered to be a promising way to improve biomass properties, aiding in producing highly deoxygenated biofuel. Among several techniques available to convert biomass to bio-fuel, fast pyrolysis has attracted a lot of interest due to its high yield of liquid product, bio-oil. However, the liquid product has certain negative properties such as high oxygen content, high acidity, and low heating value, which make it unfit as an alternate transportation fuel. Among these, the primary property that has to be upgraded is its high oxygen content, as it restricts bio-oil miscibility with hydrocarbon fuels. Catalytic pyrolysis, a promising upgrading technique, focuses on selectively eliminating or reducing oxygen content present in the bio-oil.

Hence, the current study is focused on the effect of torrefaction on the aromatic hydrocarbon yield produced from catalytic pyrolysis of biomass and its individual components. A brief introduction and detailed background information are documented in Chapter 1 and Chapter 2, respectively.

The combined effect of torrefaction and shape selective catalyst (ZSM-5) on the hydrocarbon yield from pyrolysis of pine wood is discussed in Chapter 3. Pine wood chips were torrefied and the resultant was pyrolyzed at four different temperatures with three different biomass to catalyst ratios. Bio-oil vapors produced from catalytic pyrolysis

of torrefied biomass resulted in high aromatic hydrocarbon yield. Guaicols and furans were found to be a possible intermediate in aromatic hydrocarbon production. In addition to this, the presence of certain metals on the catalyst also favored the yield of aromatic hydrocarbons. The effect of torrefaction on individual components of the biomass, namely cellulose and lignin, was studied (Chapter 4 and Chapter 5) along with the influence of catalyst acidity and pyrolysis temperature on pyrolysis products of raw and torrefied cellulose and lignin. Pyrolysis of torrefied cellulose resulted in a significant amount (~10 wt.%) of aromatic hydrocarbons, which were completely absent from raw cellulose pyrolysis. Torrefaction in lignin resulted in more condensed guaiacyl linkages, which are attributed to decreased guaiacols and increased phenol yield from pyrolysis. For both cellulose and lignin, ZSM-5 catalyst acidity played a pivotal role in promoting aromatic hydrocarbon yield.

Acknowledgments

Firstly, I would like to thank my advisor, Dr. Sushil Adhikari, for his constant guidance and motivation. Without his help, this thesis could have never achieved its current form. I would like to express my gratitude for my committee members, Dr. Olaridan Fasina and Dr. Maobing Tu, for their comments and suggestions.

I would also like to thank Southeastern Sun Grant and the Auburn University Office of Vice President for Research for providing necessary funds for this work. I would like to express my special gratitude for Ms. Suchithra Thangalazhy Gopakumar for helping me carry out initial experiments for this work. Special thanks to my friends Shyamsundar Ayalur Chattanathan, Avanti Kulkarni, Nourrrdine Abdoulmoumine and Gurdeep Hehar for their help during my graduate study.

I owe all my success to my parents Srinivasan and Kalyani for their support and love. Above all, I would like to thank my brother Anantha Narasimhan Srinivasan for his constant encouragement and motivation.

Table of Contents

List of Tables

List of Figures

Chapter 1- Introduction

Growing energy thirst has called for extensive research in various types of alternate energy sources throughout the world. Among several renewable sources of energy, biomass is attractive because of its flexibility to be converted into heat, electricity and liquid fuel. Recently, biomass torrefaction, a pre-treatment process, has gained research interest as it aids in improving (either "aids in improving" or "helps to improve") several biomass properties such as increasing calorific value, lowering grinding energy, and decreasing O/C ratio. Torrefaction is a mild thermal degradation process that takes place at around 200-300°C in inert condition. One of the major advantages of this process is that it helps in removing - or rather lowering - the oxygen present in the biomass. The presence of oxygen poses several challenges on the application of biomass-derived fuels, hence the advantage of decreased levels. Biomass can be converted into energy through several thermochemical and biochemical approaches. Among these methods, fast pyrolysis, a thermochemical biomass conversion technique, is gaining a lot of attention because of its high yield of liquid product. Fast pyrolysis involves thermal decomposition of biomass between 400-700°C, resulting in three products: solid (chars), condensable vapors and gases. Liquid obtained by cooling the condensable vapors is the desired product: "bio-oil". Bio-oil is considered to have several potential applications such as heat generation, transportation fuel, and

feedstock for various commodity chemicals. However, certain properties of bio-oil such as high oxygen content (~35 wt.%), high acidity, and high viscosity restrict its wide spread application. The oxygen content of bio-oil has to be lowered for it to be used as an excellent alternate transportation fuel since high oxygen content makes bio-oil immiscible with conventional hydrocarbon fuel. There are different techniques available to upgrade bio-oil such as catalytic cracking, catalytic hydrodeoxygenation and solvent addition. Catalytic cracking and hydrodeoxygenation are two major techniques to produce high yield of hydrocarbons. Catalytic cracking can either be done by passing pyrolytic vapors through a bed of catalyst or by incorporating catalyst along with biomass in the pyrolysis step. Incorporation of catalyst in the pyrolysis step helps in reducing a number of upgrading steps and also produces more deoxygenated bio-oil. In addition to these upgrading techniques, the torrefaction process followed by pyrolysis is also gaining importance in the area of energy and fuels.

1.1 Research Objectives

Since oxygen content has to be reduced in the bio-oil in order to increase the hydrocarbon yield, production of aromatic hydrocarbon from torrefaction followed by catalytic pyrolysis of biomass and its individual components is considered as the main objective in this work. However, the overall objective is divided into three specific objectives. For each specific objective, pyrolysis vapors were analyzed using gas chromatography coupled with mass spectrometer (GC/MS).

1.1.1. Catalytic Pyrolysis of Torrefied Biomass for Aromatic Hydrocarbon Production

This study was focused on aromatic hydrocarbon production through catalytic pyrolysis of torrefied pine wood chips. The effect of torrefaction on aromatic yield from pyrolysis process was analyzed. Catalytic pyrolysis of torrefied biomass was studied at four temperatures and three biomass to catalyst ratios in order to study the effect of temperature and catalyst amount.

1.1.2. Catalytic Pyrolysis of Raw and Torrefied Cellulose

This study was performed in order to analyze the individual behavior of cellulose, the major constituent of biomass, during torrefaction and pyrolysis. Catalytic pyrolysis of both feedstock was studied at three different pyrolysis temperatures with zeolite catalyst of varying acidity. The zeolite catalyst acidity was controlled by changing its silica to alumina ratio. This helped in analyzing the effect of catalytic acidity and pyrolysis temperature on the product distribution from pyrolysis of raw and torrefied cellulose.

1.1.3. Catalytic Pyrolysis of Raw and Torrefied Lignin

This study was proposed to understand the behavior of lignin, the second major constituent of biomass, during torrefaction and pyrolysis. An FTIR study was performed to analyze the structural changes in lignin during torrefaction process. Zeolite catalyst with varying acidity were used to study the effect of catalyst acidity during pyrolysis of raw and torrefied lignin. Additionally, pyrolysis was performed at three temperatures for both raw and torrefied lignin.

Chapter 2 – Literature Review

2.1. Energy Utilization and Demand

Fossil fuels play a critical role in the world's energy market. The demand for energy has been sustained in the past due to affordable energy prices and a high reliance on oil and electricity sources. Due to the hike in oil prices and the exponential increase in population size, the demand for energy is also continuously rising. In the 20th century, the population quadrupled, and our energy demand rose to a level 16 times greater than the previous century. The greater demand began exhausting the fossil fuel supply at an alarming rate. Currently about 13 terawatts (TW) of energy is needed to support (or sustain) the population of 6.5 billion people worldwide (Kamat, 2007). In 2030, approximately 84% of the energy demand will be met by fossil fuels as reported by the World Energy Outlook (WEO) (Shafiee & Topal, 2009) . By year 2050, we will need an additional 10 TW of clean energy to maintain our current lifestyle. The ever-increasing requirement for energy and depletion of fossil fuels has aggravated the energy crisis in recent years. According to International Energy Agency statistics, 60% of the world's oil consumption is by the transportation sector. New bio-fuels have been explored for energy generation purposes, as they reduce greenhouse gas emissions and replace petroleum fuels. This in turn mitigates pollution issues (Demirbas & Balat, 2006). Bio-fuels are referred as the fuels for electricity production through direct combustion, but it is

popularly used as liquid fuels in transportation sector (Balat & Balat, 2009). Figure 2.1 (EIA, 2013) shows the U.S. primary consumption by fuel from the year 1980 to 2040. It can be seen that total energy consumption increases from 98 quadrillion BTU in 2011 to 104 quadrillion BTU in 2035 and continues to 108 quadrillion BTU in 2040. Examining the various sources of energy, fossil fuel consumption shows a decline from 82% in 2011 to 78% in 2040 while bio-fuels consumption shows an increase from 1.3 quadrillion in 2011 to 2.1 quadrillion in 2040. Figure 2.2 (EIA, 2013) shows the U.S. energy-related carbon dioxide emissions in recent *AEO* (Annual Energy Outlook) reference cases. The projected growth rate for U.S. energy-related CO_2 emissions has declined in each year since 2005, reflecting the adoption of higher economy fuel standards and the shift to less carbon-intensive fuels. Biofuels are gaining a lot of attraction to serve as an excellent alternate liquid fuels. (Balat & Balat, 2009).

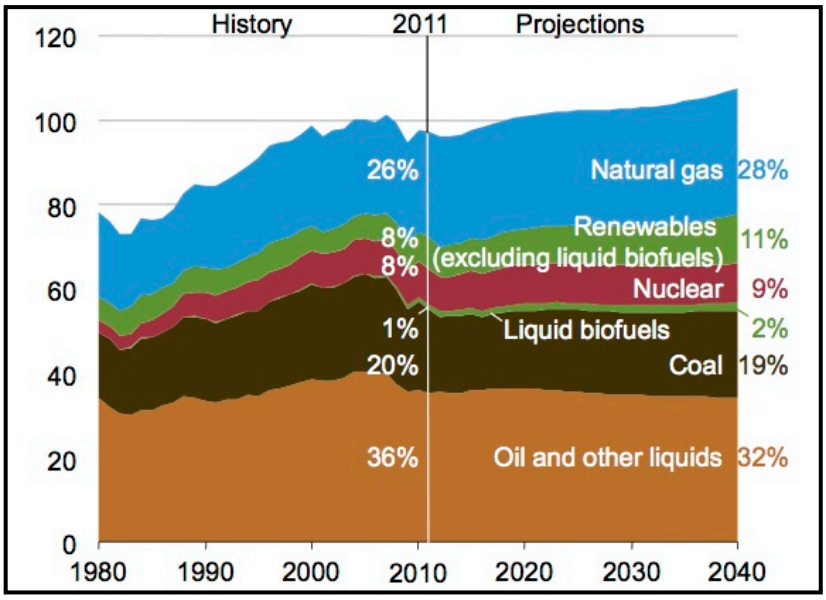

Figure 2.1: U.S. primary energy consumption by fuel, 1980-2040

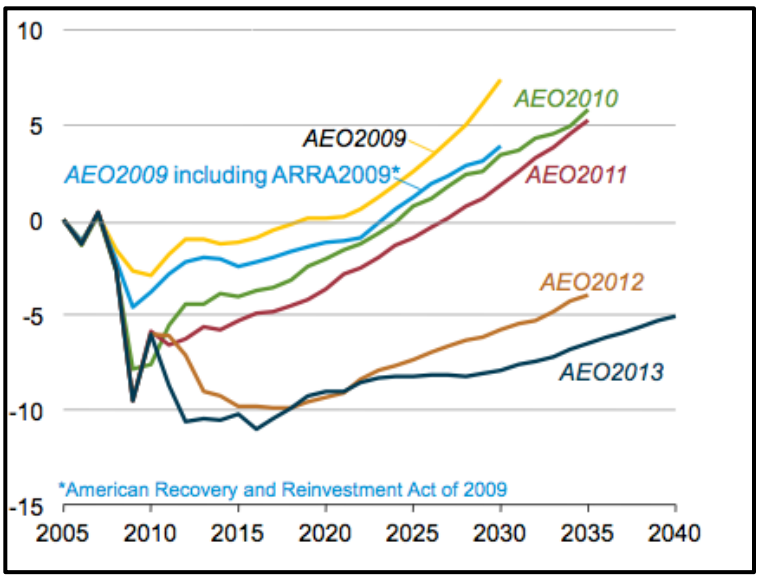

Figure 2.2: U.S energy related carbon dioxide emissions in recent AEO reference cases (percent change from 2005)

2.2. Biomass

Among several sources of renewable energy, biomass is increasing in popularity , as it is the only available renewable energy source for liquid fuels production. Biomass includes wood, plant and animal wastes, agricultural crops and other wastes (Balat, 2005). Energy from biomass is used for various purposes such as power and heat generation and production of valuable chemicals including ethanol and methanol. In addition to this, biomass is CO_2 neutral and has a very low content of sulfur and nitrogen; hence the fuel obtained from biomass is clean with very minimal emission of NO_x (Antolín et al., 1996).

Biomass is primarily composed of cellulose (30-45 wt.%), hemicellulose (25-35 wt.%) and lignin (21-35 wt%) along with minor amounts of alkali metals, proteins, and minerals. Cellulose is the polymerization product of cellulobiase linked with glucosidic linkages. It mainly consists of sub rings of D-glucopyranoses. This is formed by the interactions

between hydroxyl and aldehyde groups preset in D-glucose. It is both crystalline and amorphous with a degree of polymerization around 10,000. Hemicellulose, the second major biomass constituent, is a branched polymer of glucose, mannose, xylose, galactose, and arabinose. Unlike cellulose, it exhibits a very low degree of polymerization and hence decomposes at very low temperature (200-250°C), giving out more volatiles and less tar and char compared to cellulose (Caballero et al., 1996; Mohan et al., 2006). Lignin is a 3-dimensional amorphous polymer with phenylpropane units. It is formed by the polymerization of three-p-hydroxycinnamyl alcohol precursors – p-coumaryl, coniferyl, and sinnapyl alcohol (Caballero et al., 1996). It has a very complex structure with a very high degree of polymerization. Decomposition of lignin happens around 280-550°C, resulting in the production of mainly phenols due to cleavage of ether bonds and C-C linkages (Mohan et al., 2006). Structure of cellulose, hemicellulose and softwood lignin are shown in Figure 2.3 (Pandey, 1999).

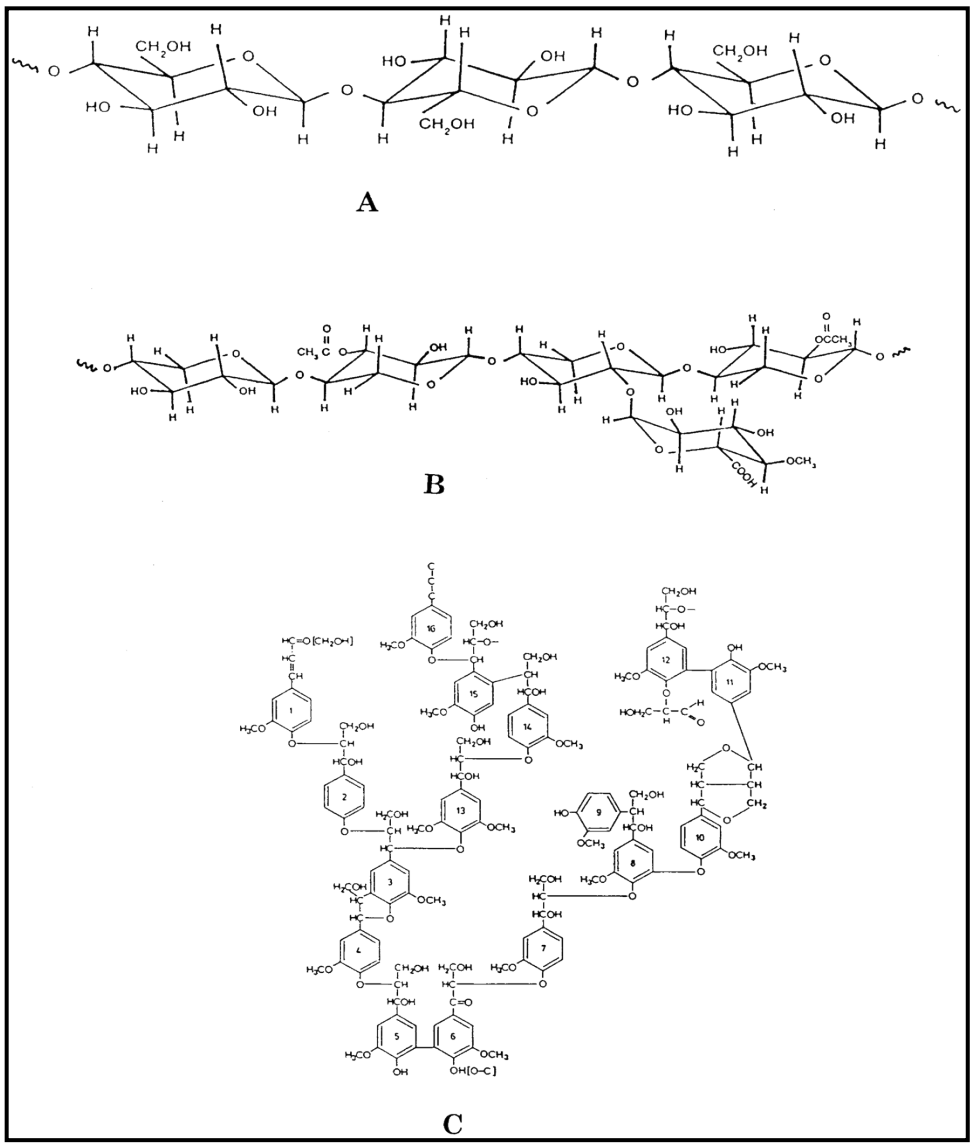

Figure 2.3: Structural representation of a) cellulose b) hemicellulose and c) softwood lignin

The structural and elemental composition of biomass changes with the biomass feedstock. Typical composition of biomass is carbon (~50 wt.%), hydrogen (~5 wt.%), and oxygen (~40 wt.%). The presence of high amounts of oxygen in the biomass causes serious problems during co-firing due to the absence of oxygen in coal. Also, biomass has very high moisture content, which has to be reduced before the biomass is used to recover energy through thermochemical processes (pyrolysis and gasification). High moisture content

results in high amount of char, the undesired product during pyrolysis (Acharjee et al., 2011). Moreover, biomass has to be reduced in size as all the techniques used to extract energy from biomass require only fine biomass input. The energy needed to grind biomass samples is quite high, and it also depends on the type of feedstock used (Mani et al., 2004). Mani et al. studied grinding energy required for size reduction of four different feedstocks(wheat, barley straws, corn stover and switchgrass) with three different screen sizes (3.2, 1.6 and 0.8 mm), and it was reported that among them switchgrass had the highest specific energy consumption (27.6 KWh/t) while corn stover had the lowest specific energy consumption (11.0 KWh/t) at 3.2 mm screen size (Mani et al., 2004). Hence, in recent days, biomass is pre-treated to improve the above-mentioned properties; this pre-treatment process is termed as "torrefaction".

2.3. Biomass Pre-treatment

Torrefaction is a process in which biomass is thermally treated at 200°-300°C in an inert atmosphere under low or high pressure (Medic et al., 2012). Torrefaction results in several physical and chemical changes in the biomass (Carter, 2012a). The process dries biomass and makes it irreversible non-hygroscopic. It also elevates the properties of biomass and transforms its energy into an easily transportable solid fuel (Ratte et al., 2011). Biomass has a very high O/C ratio as compared to coal, which accounts for its low calorific value. The torrefaction process helps in increasing the calorific value by eliminating the oxygen present in the biomass. The biggest advantage of this pre-treatment process is that it reduces the grinding energy to less than quarter of the energy required to grind fresh wood (Sadaka & Negi, 2009; Zheng et al., 2012). During torrefaction, the structure of biomass is completely altered and the resultant biomass is less fibrous in structure. Torrefaction is a

slow pyrolysis in which wood is heated at a slower rate which results in the release of certain compounds such as acetic acid, furfural, CO, CO_2 and water. These compounds correspond mainly to the decomposition product of hemicellulose. Additionally, acids such as acetic acid originating from the acetoxy group in the xylan side chain are removed during this pre-treatment process (Prins et al., 2006b). Torrefaction process is a two-step process in which the first step involves hemicellulose decomposition (250-260°C) and the second step involves partial cellulose decomposition along with certain structural changes in lignin and cellulose. Due to devolatilization and decomposition reactions taking place during torrefaction, there is a decrease in mass (~30 wt.%), but almost 90 % of initial energy content is preserved. This results in higher energy density in the torrefied biomass compared to raw biomass, which makes it more attractive during transportation. Yan et al. studied thermal behavior of loblolly pine in which he reported that the energy density of thermally pre-treated pine could be increased from 8-36% depending on the pre-treatment condition (Yan et al., 2009). The increase in energy density results in a subsequent decrease in the storage cost of large quantities of biomass required for biofuel production. The 30% of mass removed during torrefaction is vented out in the form of gases. Also, during torrefaction the extractable fraction increases in wood, and some of these heavy fractions with high boiling points stay in the wood while others vent out as vapors.

Torrefaction process can be done from 15 min to 3 h. Torrefaction temperature and time play an important role in improving the properties of biomass (Chen et al., 2011). Repellin et al. studied the influence of torrefaction temperature and time on certain physical properties of wood block such as calorific value and grindability. Increase in torrefaction temperature increased the calorific value significantly; however, at highest torrefaction

temperature (280°C), the calorific value increased by 40% along with 50% mass loss (Repellin et al., 2010). Similar studies have been done and are documented elsewhere (Arias et al., 2008; Chen et al., 2011; Medic et al., 2012; Wannapeera et al., 2011). Torrefaction also enhances fuel quality by producing less-oxygenated compounds through several thermochemical conversion techniques. As torrefied biomass has a lower O/C ratio, the liquid fuel produced from torrefied biomass pyrolysis has less holocellulose and more lignin residue. On the other hand, the pre-treatment process can alter the structure of biomass, changing the reaction pathways during pyrolysis and favoring the formation of certain bio-oil compounds (Meng et al., 2012). Few studies have reported an improvement in the quality of bio-oil obtained from fast pyrolysis of torrefied biomass compared to that of untreated biomass (Boateng & Mullen, 2013; Meng et al., 2012; Ren et al., 2013; Rousset et al., 2011; Srinivasan et al., 2012). Mullen et al. studied the quality of bio-oil derived from pyrolysis of torrefied biomass samples and reported that bio-oil produced from torrefied wood had low O/C ratio and high energy content (~27 MJ/kg) compared to the pyrolysis of non-treated biomass; however, the only drawback noticed was the bio-oil yield (Boateng & Mullen, 2013). It has also been proved that torrefied biomass can generate electricity with similar efficiency as coal (Rousset et al., 2011).

2.4. Biofuels

There are several techniques available to convert biomass into biofuels. However, they can be grouped into two main categories— biochemical and thermochemical conversion. Apart from these two major techniques, biomass can also be directly used for combustion process by co-firing it with coal to produce heat and energy. In this process, biomass is heated around 800-1100°C with excess air. Co-firing aids in reducing fossil CO_2

and other airborne emissions such as NO_X (Tillman, 2000). However, there are certain challenges associated with biomass co-firing such as ash deposition, corrosion and fuel conversion (Baxter, 2005). Higher concentration of potassium and other metals can be found in the ash from co-firing of some types of biomass (Sondreal et al., 2001). Also, an additional cost incentive for this retrofitting is required which results in higher market price of the electricity generated (De & Assadi, 2009). All these limitations pose a serious challenge in co-firing application. In biochemical conversion, biomass is converted into liquid fuels such as bioethanol, biomethanol and bio-butanol with the use of microorganisms. This conversion technique converts only holocellulose part of the biomass into fuels and also requires energy intensive pre-treatment processes to extract and purify the holocellulose.

Thermochemical technique involves conversion of biomass into fuels through thermal and chemical processes. The three main routes under thermochemical conversion are gasification, liquefaction and pyrolysis. Gasification is a process in which biomass is thermally decomposed at 850-1100°C under an inert environment resulting in syngas/producer gas which is composed of CO, CO_2, N_2, H_2 and CH_4 (San Miguel et al., 2012). Syngas can be used for various applications such as power generation from internal combustion engines, liquid fuel through Fischer-Tropsch reaction, and feedstock for various chemicals (Bridgwater, 2003). Hydrothermal liquefaction is a process in which biomass is heated at moderate to high temperature (250-550°C) and high pressure (2-5 MPa) in the presence of a solvent to produce liquid fuel called bio-oil (Akhtar & Amin, 2011). Pyrolysis is a thermal decomposition of biomass at a temperature around 400-700°C in the absence of oxygen. Products from pyrolysis process include vapors, gases and chars. Gases are

collected and rapidly quenched to produce liquid fuel, or bio-oil. This process is flexible to a wide variety of feedstock such as wood waste, switch grass, straw, perennial grass, pinewood, poultry litter, or peanut hulls (Greenhalf et al., 2013; Horne & Williams, 1996a; Jarvis et al., 2012; Mante & Agblevor, 2012; Westerhof et al., 2012). Among the various thermochemical conversion techniques, pyrolysis is highly attractive because of its flexibility and comparative high efficiency.

2.5. Pyrolysis

Thermal decomposition of biomass in the absence of oxygen is termed as pyrolysis. During pyrolysis, there is heat transfer to raise the temperature inside the feed, resulting in the initiation of primary pyrolysis. The hot volatiles produced from primary pyrolysis move towards cooler solids resulting in secondary reactions. Simultaneous primary and secondary pyrolysis takes place along with several other reactions such as water gas shift reaction, radical recombination, and dehydration. The overall process depends on various factors such as vapor residence time, temperature, and pressure. Pyrolysis can be classified into three types according to the vapor residence time as slow pyrolysis, fast pyrolysis and flash pyrolysis.

Slow Pyrolysis

Slow pyrolysis is a type of pyrolysis process in which the biomass is heated at a slower rate and with a longer vapor residence time (5 to 30 min), causing vapors to react with each other. This results in higher char yield and lower liquid product yield. However, with an increase in the pyrolysis temperature, the solid yield can be decreased, thereby increasing the liquid and gas yield (Williams & Besler, 1996).

Fast Pyrolysis

Fast pyrolysis is a rapid process wherein biomass is heated rapidly in the absence of oxygen with shorter residence time. Shorter residence time minimizes the secondary reactions and hence produces high liquid product yield and low solid yield (Czernik & Bridgwater, 2004). Typically fast pyrolysis process results in 60 -75 wt% liquid, 15-25 wt% char, and 10-20 wt% vapors (Bahng et al., 2009; Bridgwater, 2003; Mohan et al., 2006). Since fast pyrolysis takes place in a shorter time, heat and mass transfer process, phase transition phenomena, and chemical reaction kinetics play an important role (Bridgwater, 2012).

Flash Pyrolysis

Flash pyrolysis is similar to fast pyrolysis but has a higher heating rate than fast pyrolysis. In this technique, biomass is heated at a heating rate of 1000°C/s, with the reaction time being very short compared to slow and fast pyrolysis (Bahng et al., 2009). Typical operating conditions for all three pyrolysis types are given in Table 2.1 (Bahng et al., 2009).

Table 2.1: Typical Operating Parameters for various pyrolysis processes.

	Slow pyrolysis	Fast pyrolysis	Flash pyrolysis
Pyrolysis temperature (°C)	300-700	600-1000	800-1000
Heating rate (°C/s)	0.1-1	10-200	>1000
Particle size (mm)	5-5O	<1	<0.2

Solid residence time (s)	300-550	0.5-10	<0.5

2.6. Factors Affecting Pyrolysis Process

2.6.1. Reaction Temperature

As fast pyrolysis is a thermal decomposition process, reaction temperature plays an important role as it is necessary to bring the biomass particles to an optimum temperature and minimize their exposure to low temperatures that favor undesired product (Bridgwater, 2012; Bridgwater et al., 1999). The Optimum temperature for higher total product yield was found to be 500-520°C for woody biomass (Bridgwater et al., 1999). However, this temperature changes with respect to the feedstock used.

2.6.2. Heat Transfer and Heating Rate

Pyrolysis is an endothermic process and hence reaction temperature, which depends on the heating rate, plays a very important role. Heat transfer and mass transfer processes are the two main reactions taking place during pyrolysis process. The main changes that occur during pyrolysis are (Gerçel, 2002; Mohan et al., 2006):

1. Heat transfer to increase the temperature of solid biomass
2. Increase in temperature initiates the primary pyrolysis which results in volatiles and chars
3. Hot volatiles move towards the cooler region of solids resulting in heat transfer between hot volatiles and cooler unpyrolyzed solids.
4. Some of the volatiles are condensed in the cooler region resulting in few secondary reactions.

5. Reactions such as thermal decomposition, reforming, water gas shift also take place, which are mainly a function of residence time, temperature, and pressure.

Heating rate is the most essential feature for producing high yield of liquid product (bio-oil). High heating rates result in a shorter residence time, which reduces the yield of undesired product by minimizing secondary reactions. Low heating rates cause some resistance to heat and mass transfer inside the particle but increasing heating rates may overcome these resistances, resulting in higher conversion. However, increasing the heating rate more than 300°C/min does not significantly change the bio-oil production (Bridgwater & Peacocke, 2000).

2.6.3. Biomass Properties

Moisture content and particle size of biomass also affect the pyrolysis process. Biomass contains around 35 wt% water and this moisture gets settled in the bio-oil as water, thereby reducing its fuel property (Mohan et al., 2006). Hence, the acceptable level of moisture in biomass is ~ 10 wt.% (Bridgwater, 1999). It is necessary that biomass is reduced in size before it is processed into biofuels using several techniques (Bridgwater, 1999). Acceptable level of biomass particle size for pyrolysis process is up to 2 mm. However, it varies with respective to the type of reactor used (Ateş et al., 2004; Kang et al., 2006; Onay & Koçkar, 2006; Şensöz et al., 2000; Şensöz et al., 2006). Table 2.2 shows the acceptable particle size for different kinds of reactors (Bridgwater, 1999).

Table 2.2: Acceptable particle size with respect to reactor type

Reactor type	Acceptable particle size
Ablative	Large size feedstocks
Circulating fluid bed	Up to 6mm
Fluidized bed	< 2mm
Entrained flow	< 2mm

2.6.4. Type of Reactor

Several types of reactors can be used for carrying out fast pyrolysis process. Some of them are listed below. A wide variety of reactors have been used for pyrolysis process. Reactor configuration and mode of heat transfer influence the distribution of compounds in bio-oil to a significant extent. Following are some reactor types majorly used for pyrolysis process.

- **Auger Reactor**

  The main advantage of this system is that it does not require any carrier gas. Biomass is moved through an auger into an externally heated tube where it is mixed with hot sand. Hot sand is used as a heat transfer medium and helps in conduction of heat into the biomass. Such reactors are suitable for small scale pyrolysis activities. However, one of the main disadvantages is the wear and tear caused due to mechanical parts. Several studies have shown the production of bio-

oil using auger reactor (Garcia-Perez et al., 2007; Hassan et al., 2009; Ingram et al., 2007). Figure 2.4 represents the auger reactor system.

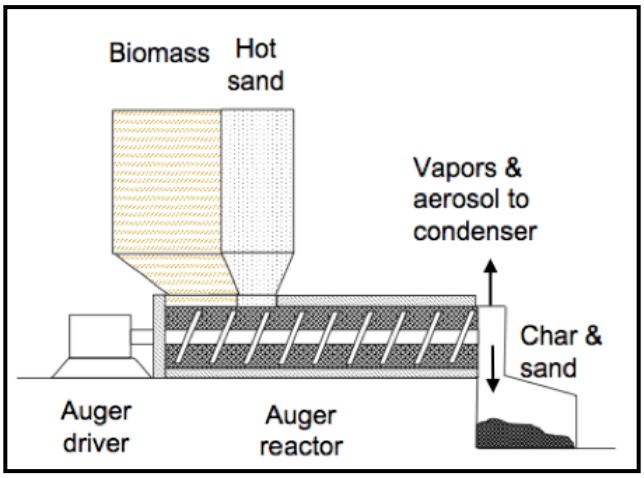

Figure 2.4: Schematic representation of auger reactor system (Robert C. Brown)

- **Bubbling Fluidized Bed Reactor**

This configuration requires a carrier gas for fluidization. However, certain advantages such as good temperature control, high heat transfer and short residence time make it more technologically efficient (Huber et al., 2006). The residence time of the vapors depends on the bed size and the flow rate of carrier gas. This configuration requires small biomass particles due to several heat transfer limitations within the biomass. A schematic representation of the reactor is given in Figure 2.5

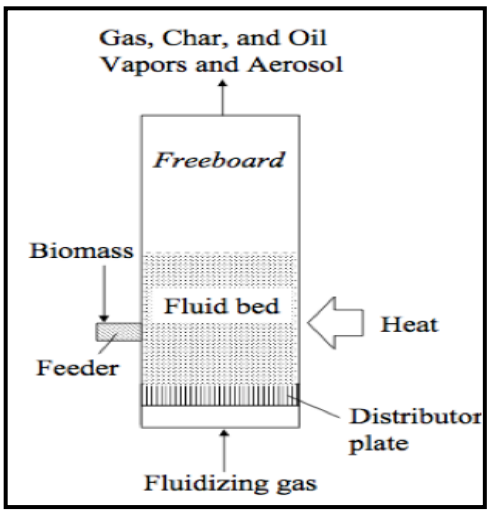

Figure 2.5: Schematic representation of bubbling fluidized bed reactor (Robert **C. Brown)**

- **Circulating Fluidized Bed Reactor**

A circulating fluidized bed reactor (Figure 2.6) operates with heat transfer modes as 80% conduction, 19% convection and 1% radiation (Bridgwater et al., 1999)**.** There is a greater char yield in the product due to high char abrasion from biomass. Therefore, post treatment of bio-oil is required to remove the char formed. Unlike the bubbling fluidized reactor, this reactor can handle large biomass particle (~6mm). However, this reactor configuration is more complex in structure compared to bubbling fluidized bed reactor.

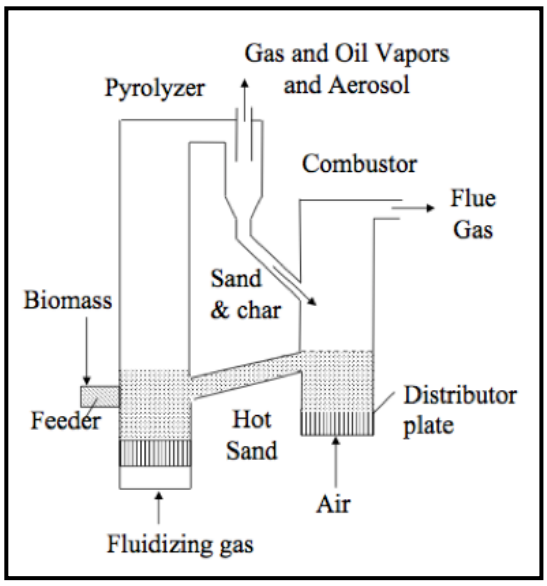

Figure 2.6: Schematic representation of circulating fluidized bed reactor

- **Ablative Pyrolyzer**

Biomass particle is pressed on a hot metal surface and moved which results in oil product through decomposition reaction (Figure 2.7) (Peacocke & Bridgwater, 1994). High pressure can be achieved through centrifugal or mechanical motion. There are a few advantages of using ablative pyrolyzer over conventional fluidized bed reactors (Bahng et al., 2009; Peacocke & Bridgwater, 1994; Peacocke et al., 1994)

1. Good heat transfer with high heating rates at small contact surface
2. Cost effective and energy efficient as no heating and cooling of fluidized gases is required
3. Biomass does not require any milling since heat is introduced as the particles come in direct contact with the surface

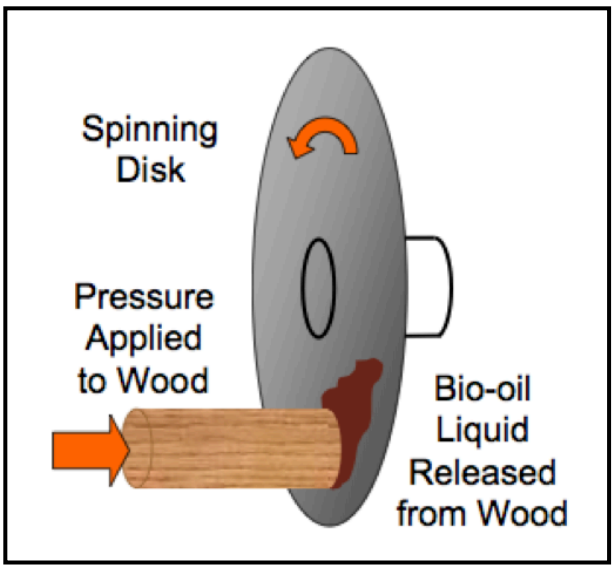

Figure 2.7: Schematic representation of ablative pyrolyzer

2.7. Bio-oil

The major product of fast pyrolysis is an immiscible dark brown liquid called pyrolysis oil or bio-oil. It is a complex mixture of water, carboxylic acids, esters, phenolics and other oxygenated compounds. Presence of several reactive species contributes to its unusual characteristics. Properties of bio-oil are different from that of conventional liquid fuels due to these unusual characteristics. Table 2.3 shows the comparison of the properties of pyrolysis oil with heavy fuels. It can be seen that major differences are in its water content, pH value and oxygen content. A detailed discussion of bio-oil properties is given in the next section.

Table 2.3: Properties of bio-oil and heavy fuel (Zhang et al., 2007)

Physical property	Bio-oil	Heavy fuel oil
Water content (wt. %)	15-30	0.1
pH	2.5	-
Specific gravity	1.2	0.94
Elemental composition (wt. %)		
C	54-58	85
H	5.5-7.0	11
O	35-40	1
N	0-0.2	0.3
Ash	0-0.2	0.1
HHV (MJ/kg)	16-19	40
Viscosity (at 50 °C) (cP)	40-100	180
Solids (wt%)	0.2-1	1

2.8. Properties of Bio-oil

2.8.1. Acidity

Some acidic compounds such as formic acid and acetic acid are released during pyrolysis of biomass mainly from the holocellulose (cellulose and hemicellulose) decomposition. Hence, bio-oil is acidic and its pH ranges from 2-3. This poses serious problems during storage and handling. According to Precision Polymer Engineering Ltd (PPE), the higher acidity of bio-fuels compared with conventional fuels increases the risk of leaks in equipment used for their storage.

2.8.2. Water Content

Water composes 15-35 wt.% of bio-oil. It is mainly formed from the dehydration process during pyrolysis. Water can also be formed through the dehydration of certain compounds during pyrolysis or secondary cracking of pyrolytic vapors. Although water helps in reducing the viscosity, presence of water results in low heating value and poor stability (Mohan et al., 2006). Also, water cannot be readily separated from bio-oil (Lu et al., 2009). Elliot et al. has studied the removal of water through azeotrophic distillation with toluene (Baker Eddie & Elliott Douglas, 1988).

2.8.3. Heating Value

Heating value is the energy released in the form of heat when the compound undergoes complete combustion in the presence of oxygen. Heating value is one of the important parameters of any fuel used in energy applications. The lower heating value (LHV) of bio-oil is about 14-18 MJ/kg. The higher heating value (HHV) of bio-oil is about 16-19 MJ/kg, which is half that of other traditional oil-based fuels such as gasoline, diesel, etc. The low heating value of bio-oil is mainly due to high water content in them. This makes them unfit for direct applications in internal combustion engines.

2.8.4. Density

The density of bio-oil is ~1.2 kg/L. Bio-oil contains almost 200 compounds, of which there are some higher molecular weight compounds such as syringols, guaiacols and sugar compounds. Presence of higher molecular weight results in higher density of bio-oil.

2.8.5. Viscosity

Bio-oil components lack thermodynamic equilibrium when they are formed; therefore with storage and temperature they tend to attain equilibrium, resulting in changes in certain properties such as viscosity and molecular weight. High viscosity of bio-oil with increase in storage time and temperature makes them unsuitable for transportation applications. Certain reactions such as polymerization, esterification, and etherification are significantly responsible for the rise in viscosity during storage (Diebold & Czernik, 1997). Addition of additives such as methanol was found to be an efficient method in stabilizing the viscosity of bio-oil in long-term storage and reducing the ageing rate at higher temperature (Boucher et al., 2000).

2.8.6. Oxygen Content

Typically bio-oil produced from pyrolysis process contains high oxygen which is 35-40 wt%. High oxygen and water content makes the bio-oil hydrophilic, which causes immiscibility with current hydrocarbon fuels.

2.9. Applications of Bio-oil

Bio-oil has various potential applications such as power generation, feedstock for several chemicals and also in transportation (Figure 2.8). A brief review of each application is given below.

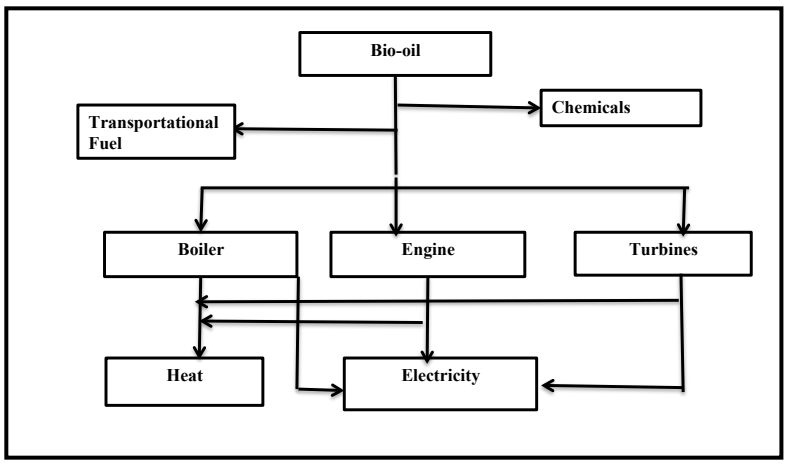

Figure 2.8: Applications of bio-oil

2.9.1. Power Generation

Bio-oil can be used to produce heat and power through combustion process. Combustion can take place in boilers/furnaces, turbines, and diesel engines. Among these equipment, boilers and furnaces have relatively low efficiency but can operate with a wide range of fuels. Therefore, bio-oil can be used for combustion purposes in boilers provided they have uniform characteristics and are economically feasible (Czernik & Bridgwater, 2004). For any type of equipment, the fuel properties play an important role in the overall performance. Examples of fuel property are:

- Ignition quality
- Viscosity
- Density
- Sulfur and heavy metal content
- Heating value

Bio-oil has a very high viscosity that must be lowered by incorporating some additives or by pre-heating the pipeline used to pump the bio-oil feed. Also, high solid content in the bio-oil can result in high particulate emissions during combustion although the emission of CO and NO_X are at acceptable levels. In addition, bio-oil has a very low ignition property and hence, bio-oil has to be blended with conventional hydrocarbon fuels for combustion purposes (Czernik & Bridgwater, 2004). Large-scale tests for co-firing bio-oil have been carried out in a coal station at Manitowac Public Utilities Power Station by co-firing pyrolysis liquid produced from Red Arrow Pyrolysis Plant at Wisconsin, 20 MWe boiler. A total of 360 h of operations with 5% thermal feed input from bio-oil resulted in 1MWe power output from pyrolysis liquid. They also reported that the plant observed no issues in emission levels, washing, or ash handling (Chiaramonti et al., 2007). Bio-oil co-firing with natural gas was also studied in a combustion campaign at a 350 MWe of natural gas fired power station in the Netherlands. They reported that this co-firing resulted in 4MWe of green electricity and that the bio-oil was converted into 25MWh of electricity. Coking and acid corrosion can be serious concerns with the use of bio-oil in diesel engines. Coking of the injector nozzle will disturb the entire combustion process by blocking the spray formation process (Solantausta et al., 1993).

2.9.2. Transportation Fuel

Bio-oil can be used as an alternate transportation fuel for gasoline and diesel by upgrading some of its properties such as high viscosity and high oxygen content. Wright reported in his techno-economic study that fuels such as naphtha and diesel can be produced from biomass pyrolysis at a product value of $3.09–2.11 per gallon (Wright et

al., 2010). Wright also estimated a capital cost of $911 and $585 million for building a first of its kind pyrolysis plant and upgrading biorefinery to produce product value of $6.55 and $3.41 gallons per gasoline equivalent (Wright et al., 2010). Various upgrading techniques are discussed in section 2.10.

2.9.3. Chemicals

A wide range of useful chemicals from specialties such as levoglucosan to commodities such as resins and fertilizers can be produced or extracted from bio-oil. However, extraction of these chemicals requires complex extraction techniques. Hence, techniques are available to extract chemicals either from the whole bio-oil or from the most easily separable fraction of the bio-oil. Since bio-oil has abundant functional groups such as carbonyl, carboxyl, esters, and phenols, several useful products can be produced from it. Dynamotive Corporation has produced a useful chemical, bio-lime, from pyrolysis oil which proves to be highly efficient in removing SO_X emissions from coal combustors (Czernik & Bridgwater, 2004). Chemicals such as urea or other $–NH_2$ containing materials can be formed by reacting bio-oil with ammonia (Czernik & Bridgwater, 2004). Bio-oil can also be used as a wood preservative, as it has terpenoid and phenolic compounds that act as insecticides and fungicides (Meier et al., 2008). In addition, this oil can be used for producing high value added chemicals for resins, additives and pharmaceuticals (Bridgwater, 2003).

2.10. Bio- Oil Upgrading

2.10.1. Hydrodeoxygenation (HDO)

Hydrodeoxygenation process occurs at extreme temperatures (230-500°C) and pressures (50-200 psi) in the presence of a heterogeneous catalyst to remove oxygen as water (Xiu & Shahbazi, 2012). Normally this process happens in two stages. In the first stage, which happens at lower temperatures, the bio-oil is stabilized, and in the second, higher temperature step, extensive deoxygenation occurs (Ardiyanti et al., 2011). Catalysts that are used for this process are generally sulfided catalysts such as NiCu, NiCo or NiMo supported on Al_2O_3 (Ardiyanti et al., 2012). Though this process is a possible upgrading technique, it does have several serious issues. This process is expensive, and it requires large quantities of hydrogen. The use of sulfided catalyst results in several problems, as it requires the addition of sulfur compounds such as H_2S in order to keep the catalyst active (Bui et al., 2011). Another important challenge is the coking and leeching of the catalyst, which eventually shorten its life (de Miguel Mercader et al., 2010; Weissman et al., 1992). Recently, several non-sulphided noble and non-noble metal catalysts have been explored for pyrolysis oil upgrading using HDO process. Non-sulfided catalyst includes ZSM-5 and non-sulfided Ni/SiO_2 (Horne & Williams, 1996b; Laurent & Delmon, 1994). Though noble metal catalysts are feasible catalyst for HDO process (Gutierrez et al., 2009; Horne & Williams, 1996b), their cost makes bio-oil upgrading economically non-feasible.

2.10.2 Catalytic Cracking

Catalytic cracking is an upgrading technique in which bio-oil is deoxygenated with the use of certain shape selective catalyst such as zeolite. In this process, the bio-oil

produced is generally heated to its vapor state and passed through a bed of catalyst where it reacts with the catalyst, resulting in a highly deoxygenated product through a series of dehydration, decarbonylation and decarboxylation reactions. Some of the shape selective catalysts that could be used for this technique are zeolite (HSM-5), H-Y, H-morderite, and silicilate (Adjaye & Bakhshi, 1995a; Adjaye & Bakhshi, 1995b). Catalytic cracking with HZM-5 catalyst does not require hydrogen and can take place at atmospheric pressure. The main challenge with this process is the deactivation of catalyst by coking. In some studies, the catalyst is regenerated and used after the upgrading process. However, continuous regeneration of catalyst resulted in its poor efficiency in producing aromatics; furthermore, after few runs the regenerated catalyst becomes totally deactivated with loss of acidic sites (Vitolo et al., 2001).

2.10.3. Catalytic Pyrolysis

This technique involves the integration of catalytic cracking along with pyrolysis process in a single step. There are several advantages in using the catalytic pyrolysis process, which include: production of more stable compounds like anhydrous sugars, production of fungible aromatics, and single step, cost effective chemistry. (French & Czernik, 2010). However, certain issues are also associated with the use of this upgrading technique such as an increase in water formation and high solid char residue, as well as a decrease in organic phase yield (Cheng et al., 2012). However, the quality of compounds produced from the organic phase is extremely valuable and hence studies have been focused on the selectivity of catalyst for increasing the production of certain chemicals or eliminating the formation of undesired compounds. Carlson et.al. developed a single step process to pyrolyze biomass in the presence of ZSM-5 catalyst to green gasoline, heating

oil, and other value added chemicals(Carlson et al., 2008). Main compounds from the single step process were naphthalene and toluene, which accounted for 25 % of chemicals present in gasoline fuel (Iliopoulou et al., 2007). Among several catalysts used for this purpose, shape selective zeolite proved to be highly efficient in effectively deoxygenating the pyrolytic vapors (Aho et al., 2007; Aho et al., 2008; Chen et al., 2003b; Lappas et al., 2002). Nowadays, the use of metal impregnated ZSM-5 is gaining attention for higher aromatic hydrocarbon production (Castaño et al., 2009; Thangalazhy-Gopakumar et al., 2012). A few studies were also focused on the utilization of mesoporous catalyst such as Al-MCM-41, aluminosilicates etc.(Adam et al., 2006; Antonakou et al., 2006). Scott et al. studied the catalytic pyrolysis behavior of polymers such as polystyrene, polyvinyl chloride, and polyethylene using activated carbon catalyst in a fluidized bed reactor (Scott et al., 1990). Several factors affect this upgrading technique such as catalyst type, catalyst to biomass ratio, catalyst acidity, heating rate, etc. High heating rate and high catalyst to biomass ratio are necessary for carrying the pyrolytic vapors into the catalyst pores and to prevent coking problems.

2.11. Reaction Mechanism of Pyrolysis

The three important components in biomass - namely cellulose, hemicellulose and lignin - follow individual behavior during pyrolysis (Demirbaş, 2000). Pyrolysis of cellulose is accompanied by gradual degradation, decomposition at lower temperature, and formation of levoglucosan at higher temperature. The first step in pyrolysis of cellulose involves the formation of glucose by breaking the glycosidic bonds .The second step involves the formation of glucosan by splitting one molecule of water. Piskorz et al. proposed a model for cellulose pyrolysis in which he reported that at higher temperature

(> 450°C) cellulose is converted into monomeric units with 2-4 carbon which then rearrange to form hydroxyacetaldyhe and levoglucosan (Piskorz et al., 1986). Later, they proposed a reaction mechanism named "waterloo model" for cellulose pyrolysis. Water loo model is a two-step process involving the production of cellulose with a lower degree of polymerization followed by simultaneous decarbonylation, dehydration, and depolymerization to form hydroxyacetaldehyde, acetol, glyoxal, and levoglucosan (Piskorz et al., 1989). The major product from pyrolysis of lignin is substituted phenols. The reason behind this is that the syringyl-propan units are not as linked to lignin as compared to the guaiacyl-propan and phenyl propan units; thus phenols are produced through secondary vapor cracking reactions. To get a better understanding of the reaction mechanism of pyrolysis, studies were done on model compounds representing different chemical classes present in bio-oil such as acids, esters, aldehydes and ketones. It was found from past studies that alcohols and ketones resulted in high aromatic hydrocarbon yield while acids and esters resulted in high gas, water and coke yield (Bridgwater, 2012). High coke yield is due to the extensive dehydration of high–oxygenated organic compounds present in the vapors and is a serious concern as it results in catalyst deactivation. In a few studies, constituents of biomass—cellulose and lignin- have been used as model compounds to understand the catalytic pyrolysis mechanism. Mihalcik et al, (Mihalcik et al., 2011) gave a three step pathway for deoxygenation of oxygenated organics: dehydration, decarboxylation and decarbonylation. Carlson et al. (Carlson et al., 2009) showed that the pyrolysis process involves a homogenous thermal decomposition reaction that results in small oxygenates which further undergo acid-catalyzed dehydration, decarboxylation and decarbonylation reactions to form olefins which later

combine to produce aromatics. More recently Huber et.al (Carlson et al., 2010) proposed a two-step mechanism for catalytic fast pyrolysis of glucose. The first step is the decomposition of glucose into small oxygenates (mainly anhydrous sugars) through retro-aldol, grob fragmentation, and dehydration reactions.

2.12. References

Acharjee, T.C., Coronella, C.J., Vasquez, V.R. 2011. Effect of thermal pretreatment on equilibrium moisture content of lignocellulosic biomass. *Bioresource Technology*, **102**(7), 4849-4854.

Adam, J., Antonakou, E., Lappas, A., Stöcker, M., Nilsen, M.H., Bouzga, A., Hustad, J.E., Øye, G. 2006. In situ catalytic upgrading of biomass derived fast pyrolysis vapours in a fixed bed reactor using mesoporous materials. *Microporous and Mesoporous Materials*, **96**(1–3), 93-101.

Adjaye, J.D., Bakhshi, N.N. 1995. Production of hydrocarbons by catalytic upgrading of a fast pyrolysis bio-oil. Part I: Conversion over various catalysts. *Fuel Processing Technology*, **45**(3), 161-183.

Adjaye, J.D., Bakhshi, N.N. 1995. Production of hydrocarbons by catalytic upgrading of a fast pyrolysis bio-oil. Part II: Comparative catalyst performance and reaction pathways. *Fuel Processing Technology*, **45**(3), 185-202.

Aho, A., Kumar, N., Eränen, K., Salmi, T., Hupa, M., Murzin, D.Y. 2007. Catalytic Pyrolysis of Biomass in a Fluidized Bed Reactor: Influence of the Acidity of H-Beta Zeolite. *Process Safety and Environmental Protection*, **85**(5), 473-480.

Aho, A., Kumar, N., Eränen, K., Salmi, T., Hupa, M., Murzin, D.Y. 2008. Catalytic pyrolysis of woody biomass in a fluidized bed reactor: Influence of the zeolite structure. *Fuel*, **87**(12), 2493-2501.

Akhtar, J., Amin, N.A.S. 2011. A review on process conditions for optimum bio-oil yield in hydrothermal liquefaction of biomass. *Renewable and Sustainable Energy Reviews*, **15**(3), 1615-1624.

Antolín, G., Irusta, R., Velasco, E., Carrasco, J., González, E., Ortíz, L. 1996. Biomass as an energy resource in Castilla y León (Spain). *Energy*, **21**(3), 165-172.

Antonakou, E., Lappas, A., Nilsen, M.H., Bouzga, A., Stöcker, M. 2006. Evaluation of various types of Al-MCM-41 materials as catalysts in biomass pyrolysis for the production of bio-fuels and chemicals. *Fuel*, **85**(14–15), 2202-2212.

Ardiyanti, A.R., Gutierrez, A., Honkela, M.L., Krause, A.O.I., Heeres, H.J. 2011. Hydrotreatment of wood-based pyrolysis oil using zirconia-supported mono- and bimetallic (Pt, Pd, Rh) catalysts. *Applied Catalysis A: General*, **407**(1–2), 56-66.

Ardiyanti, A.R., Khromova, S.A., Venderbosch, R.H., Yakovlev, V.A., Melián-Cabrera, I.V., Heeres, H.J. 2012. Catalytic hydrotreatment of fast pyrolysis oil using bimetallic Ni–Cu catalysts on various supports. *Applied Catalysis A: General*, **449**(0), 121-130.

Arias, B., Pevida, C., Fermoso, J., Plaza, M.G., Rubiera, F., Pis, J.J. 2008. Influence of torrefaction on the grindability and reactivity of woody biomass. *Fuel Processing Technology*, **89**(2), 169-175.

Ateş, F., Pütün, E., Pütün, A.E. 2004. Fast pyrolysis of sesame stalk: yields and structural analysis of bio-oil. *Journal of Analytical and Applied Pyrolysis*, **71**(2), 779-790.

Bahng, M.-K., Mukarakate, C., Robichaud, D.J., Nimlos, M.R. 2009. Current technologies for analysis of biomass thermochemical processing: A review. *Analytica Chimica Acta*, **651**(2), 117-138.

Baker Eddie, G., Elliott Douglas, C. 1988. Catalytic Hydrotreating of Biomass-Derived Oils. in: *Pyrolysis Oils from Biomass*, Vol. 376, American Chemical Society, pp. 228-240.

Balat, M. 2005. Use of biomass sources for energy in Turkey and a view to biomass potential. *Biomass and Bioenergy*, **29**(1), 32-41.

Balat, M., Balat, H. 2009. Recent trends in global production and utilization of bio-ethanol fuel. *Applied Energy*, **86**(11), 2273-2282.

Baxter, L. 2005. Biomass-coal co-combustion: opportunity for affordable renewable energy. *Fuel*, **84**(10), 1295-1302.

Boateng, A.A., Mullen, C.A. 2013. Fast pyrolysis of biomass thermally pretreated by torrefaction. *Journal of Analytical and Applied Pyrolysis*, **100**(0), 95-102.

Boucher, M.E., Chaala, A., Pakdel, H., Roy, C. 2000. Bio-oils obtained by vacuum pyrolysis of softwood bark as a liquid fuel for gas turbines. Part II: Stability and ageing of bio-oil and its blends with methanol and a pyrolytic aqueous phase. *Biomass and Bioenergy*, **19**(5), 351-361.

Bridgwater, A.V. 1999. Principles and practice of biomass fast pyrolysis processes for liquids. *Journal of Analytical and Applied Pyrolysis*, **51**(1–2), 3-22.

Bridgwater, A.V. 2003. Renewable fuels and chemicals by thermal processing of biomass. *Chemical Engineering Journal*, **91**(2–3), 87-102.

Bridgwater, A.V. 2012. Review of fast pyrolysis of biomass and product upgrading. *Biomass and Bioenergy*, **38**(0), 68-94.

Bridgwater, A.V., Meier, D., Radlein, D. 1999. An overview of fast pyrolysis of biomass. *Organic Geochemistry*, **30**(12), 1479-1493.

Bridgwater, A.V., Peacocke, G.V.C. 2000. Fast pyrolysis processes for biomass. *Renewable and Sustainable Energy Reviews*, **4**(1), 1-73.

Bui, V.N., Laurenti, D., Afanasiev, P., Geantet, C. 2011. Hydrodeoxygenation of guaiacol with CoMo catalysts. Part I: Promoting effect of cobalt on HDO selectivity and activity. *Applied Catalysis B: Environmental*, **101**(3–4), 239-245.

Caballero, J.A., Font, R., Marcilla, A. 1996. Kinetic study of the secondary thermal decomposition of Kraft lignin. *Journal of Analytical and Applied Pyrolysis*, **38**(1–2), 131-152.

Carlson, T., Tompsett, G., Conner, W., Huber, G. 2009. Aromatic Production from Catalytic Fast Pyrolysis of Biomass-Derived Feedstocks. *Topics in Catalysis*, **52**(3), 241-252.

Carlson, T.R., Jae, J., Lin, Y.-C., Tompsett, G.A., Huber, G.W. 2010. Catalytic fast pyrolysis of glucose with HZSM-5: The combined homogeneous and heterogeneous reactions. *Journal of Catalysis*, **270**(1), 110-124.

Carlson, T.R., Vispute, T.P., Huber, G.W. 2008. Green Gasoline by Catalytic Fast Pyrolysis of Solid Biomass Derived Compounds. *ChemSusChem*, **1**(5), 397-400.

Carter, C.L. 2012. Physicochemical Properties and Thermal Decomposition of Torrefied Woody Biomass and Energy Crop. in: *Biosystems Engineering*, Vol. Masters, Auburn University. Auburn, pp. 173.

Castaño, P., Gutiérrez, A., Villanueva, I., Pawelec, B., Bilbao, J., Arandes, J.M. 2009. Effect of the support acidity on the aromatic ring-opening of pyrolysis gasoline over Pt/HZSM-5 catalysts. *Catalysis Today*, **143**(1–2), 115-119.

Chen, G., Andries, J., Spliethoff, H. 2003. Catalytic pyrolysis of biomass for hydrogen rich fuel gas production. *Energy Conversion and Management*, **44**(14), 2289-2296.

Chen, W.-H., Hsu, H.-C., Lu, K.-M., Lee, W.-J., Lin, T.-C. 2011. Thermal pretreatment of wood (Lauan) block by torrefaction and its influence on the properties of the biomass. *Energy*, **36**(5), 3012-3021.

Cheng, Y.-T., Jae, J., Shi, J., Fan, W., Huber, G.W. 2012. Production of Renewable Aromatic Compounds by Catalytic Fast Pyrolysis of Lignocellulosic Biomass with Bifunctional Ga/ZSM-5 Catalysts. *Angewandte Chemie*, **124**(6), 1416-1419.

Chiaramonti, D., Oasmaa, A., Solantausta, Y. 2007. Power generation using fast pyrolysis liquids from biomass. *Renewable and Sustainable Energy Reviews*, **11**(6), 1056-1086.

Czernik, S., Bridgwater, A.V. 2004. Overview of Applications of Biomass Fast Pyrolysis Oil. *Energy & Fuels*, **18**(2), 590-598.

de Miguel Mercader, F., Groeneveld, M.J., Kersten, S.R.A., Way, N.W.J., Schaverien, C.J., Hogendoorn, J.A. 2010. Production of advanced biofuels: Co-processing of upgraded pyrolysis oil in standard refinery units. *Applied Catalysis B: Environmental*, **96**(1–2), 57-66.

De, S., Assadi, M. 2009. Impact of cofiring biomass with coal in power plants – A techno-economic assessment. *Biomass and Bioenergy*, **33**(2), 283-293.

Demirbas, M.F., Balat, M. 2006. Recent advances on the production and utilization trends of bio-fuels: A global perspective. *Energy Conversion and Management*, **47**(15–16), 2371-2381.

Diebold, J.P., Czernik, S. 1997. Additives To Lower and Stabilize the Viscosity of Pyrolysis Oils during Storage. *Energy & Fuels*, **11**(5), 1081-1091.

EIA. 2013. Annual Energy Outlook.

French, R., Czernik, S. 2010. Catalytic pyrolysis of biomass for biofuels production. *Fuel Processing Technology*, **91**(1), 25-32.

Garcia-Perez, M., Adams, T.T., Goodrum, J.W., Geller, D.P., Das, K.C. 2007. Production and Fuel Properties of Pine Chip Bio-oil/Biodiesel Blends. *Energy & Fuels*, **21**(4), 2363-2372.

Gerçel, H.F. 2002. The production and evaluation of bio-oils from the pyrolysis of sunflower-oil cake. *Biomass and Bioenergy*, **23**(4), 307-314.

Greenhalf, C.E., Nowakowski, D.J., Harms, A.B., Titiloye, J.O., Bridgwater, A.V. 2013. A comparative study of straw, perennial grasses and hardwoods in terms of fast pyrolysis products. *Fuel*, **108**(0), 216-230.

Gutierrez, A., Kaila, R.K., Honkela, M.L., Slioor, R., Krause, A.O.I. 2009. Hydrodeoxygenation of guaiacol on noble metal catalysts. *Catalysis Today*, **147**(3–4), 239-246.

Hassan, E.-b., Steele, P., Ingram, L. 2009. Characterization of Fast Pyrolysis Bio-oils Produced from Pretreated Pine Wood. *Applied Biochemistry and Biotechnology*, **154**(1), 3-13.

Horne, P.A., Williams, P.T. 1996. Influence of temperature on the products from the flash pyrolysis of biomass. *Fuel*, **75**(9), 1051-1059.

Horne, P.A., Williams, P.T. 1996. Reaction of oxygenated biomass pyrolysis model compounds over a ZSM-5 catalyst. *Renewable Energy*, **7**(2), 131-144.

Huber, G.W., Iborra, S., Corma, A. 2006. Synthesis of Transportation Fuels from Biomass: Chemistry, Catalysts, and Engineering. *Chemical Reviews*, **106**(9), 4044-4098.

Iliopoulou, E.F., Antonakou, E.V., Karakoulia, S.A., Vasalos, I.A., Lappas, A.A., Triantafyllidis, K.S. 2007. Catalytic conversion of biomass pyrolysis products by mesoporous materials: Effect of steam stability and acidity of Al-MCM-41 catalysts. *Chemical Engineering Journal*, **134**(1–3), 51-57.

Ingram, L., Mohan, D., Bricka, M., Steele, P., Strobel, D., Crocker, D., Mitchell, B., Mohammad, J., Cantrell, K., Pittman, C.U. 2007. Pyrolysis of Wood and Bark in an Auger Reactor: Physical Properties and Chemical Analysis of the Produced Bio-oils. *Energy & Fuels*, **22**(1), 614-625.

Jarvis, J.M., McKenna, A.M., Hilten, R.N., Das, K.C., Rodgers, R.P., Marshall, A.G. 2012. Characterization of Pine Pellet and Peanut Hull Pyrolysis Bio-oils by Negative-Ion Electrospray Ionization Fourier Transform Ion Cyclotron Resonance Mass Spectrometry. *Energy & Fuels*, **26**(6), 3810-3815.

Kamat, P.V. 2007. Meeting the Clean Energy Demand: Nanostructure Architectures for Solar Energy Conversion. *The Journal of Physical Chemistry C*, **111**(7), 2834-2860.

Kang, B.-S., Lee, K.H., Park, H.J., Park, Y.-K., Kim, J.-S. 2006. Fast pyrolysis of radiata pine in a bench scale plant with a fluidized bed: Influence of a char separation system and reaction conditions on the production of bio-oil. *Journal of Analytical and Applied Pyrolysis*, **76**(1–2), 32-37.

Lappas, A.A., Samolada, M.C., Iatridis, D.K., Voutetakis, S.S., Vasalos, I.A. 2002. Biomass pyrolysis in a circulating fluid bed reactor for the production of fuels and chemicals. *Fuel*, **81**(16), 2087-2095.

Laurent, E., Delmon, B. 1994. Influence of water in the deactivation of a sulfided NiMoγ-Al2O3 catalyst during hydrodeoxygenation. *Journal of Catalysis*, **146**(1), 281-291.

Lu, Q., Li, W.-Z., Zhu, X.-F. 2009. Overview of fuel properties of biomass fast pyrolysis oils. *Energy Conversion and Management*, **50**(5), 1376-1383.

Mani, S., Tabil, L.G., Sokhansanj, S. 2004. Grinding performance and physical properties of wheat and barley straws, corn stover and switchgrass. *Biomass and Bioenergy*, **27**(4), 339-352.

Mante, O.D., Agblevor, F.A. 2012. Storage stability of biocrude oils from fast pyrolysis of poultry litter. *Waste Management*, **32**(1), 67-76.

Medic, D., Darr, M., Shah, A., Potter, B., Zimmerman, J. 2012. Effects of torrefaction process parameters on biomass feedstock upgrading. *Fuel*, **91**(1), 147-154.

Meier, D., Andersons, B., Irbe, I., Chirkova, J., Faix, O. 2008. Preliminary Study on Fungicide and Sorption Effects of Fast Pyrolysis Liquids Used as Wood Preservative. in: *Progress in Thermochemical Biomass Conversion*, Blackwell Science Ltd, pp. 1550-1563.

Meng, J., Park, J., Tilotta, D., Park, S. 2012. The effect of torrefaction on the chemistry of fast-pyrolysis bio-oil. *Bioresource Technology*, **111**(0), 439-446.

Mihalcik, D.J., Mullen, C.A., Boateng, A.A. 2011. Screening acidic zeolites for catalytic fast pyrolysis of biomass and its components. *Journal of Analytical and Applied Pyrolysis*, **92**(1), 224-232.

Mohan, D., Pittman, C.U., Steele, P.H. 2006. Pyrolysis of Wood/Biomass for Bio-oil: A Critical Review. *Energy & Fuels*, **20**(3), 848-889.

Onay, O., Koçkar, O.M. 2006. Pyrolysis of rapeseed in a free fall reactor for production of bio-oil. *Fuel*, **85**(12–13), 1921-1928.

Pandey, K.K. 1999. A study of chemical structure of soft and hardwood and wood polymers by FTIR spectroscopy. *Journal of Applied Polymer Science*, **71**(12), 1969-1975.

Peacocke, G.V.C., Bridgwater, A.V. 1994. Ablative plate pyrolysis of biomass for liquids. *Biomass and Bioenergy*, **7**(1–6), 147-154.

Peacocke, G.V.C., Madrali, E.S., Li, C.Z., Güell, A.J., Wu, F., Kandiyoti, R., Bridgwater, A.V. 1994. Effect of reactor configuration on the yields and structures of pine-wood derived pyrolysis liquids: A comparison between ablative and wire-mesh pyrolysis. *Biomass and Bioenergy*, **7**(1–6), 155-167.

Piskorz, J., Radlein, D., Scott, D.S. 1986. On the mechanism of the rapid pyrolysis of cellulose. *Journal of Analytical and Applied Pyrolysis*, **9**(2), 121-137.

Piskorz, J., Radlein, D.S.A.G., Scott, D.S., Czernik, S. 1989. Pretreatment of wood and cellulose for production of sugars by fast pyrolysis. *Journal of Analytical and Applied Pyrolysis*, **16**(2), 127-142.

Prins, M.J., Ptasinski, K.J., Janssen, F.J.J.G. 2006. Torrefaction of wood: Part 2. Analysis of products. *Journal of Analytical and Applied Pyrolysis*, **77**(1), 35-40.

Ratte, J., Fardet, E., Mateos, D., Héry, J.S. 2011. Mathematical modelling of a continuous biomass torrefaction reactor: TORSPYD™ column. *Biomass and Bioenergy*, **35**(8), 3481-3495.

Ren, S., Lei, H., Wang, L., Bu, Q., Chen, S., Wu, J., Julson, J., Ruan, R. 2013. The effects of torrefaction on compositions of bio-oil and syngas from biomass pyrolysis by microwave heating. *Bioresource Technology*, **135**(0), 659-664.

Repellin, V., Govin, A., Rolland, M., Guyonnet, R. 2010. Energy requirement for fine grinding of torrefied wood. *Biomass and Bioenergy*, **34**(7), 923-930.

Robert C. Brown, J.H. Fast Pyrolysis and Bio-Oil Upgrading.

Rousset, P., Davrieux, F., Macedo, L., Perré, P. 2011. Characterisation of the torrefaction of beech wood using NIRS: Combined effects of temperature and duration. *Biomass and Bioenergy*, **35**(3), 1219-1226.

Sadaka, S., Negi, S. 2009. Improvements of biomass physical and thermochemical characteristics via torrefaction process. *Environmental Progress & Sustainable Energy*, **28**(3), 427-434.

San Miguel, G., Domínguez, M.P., Hernández, M., Sanz-Pérez, F. 2012. Characterization and potential applications of solid particles produced at a biomass gasification plant. *Biomass and Bioenergy*, **47**(0), 134-144.

Şensöz, S., Angın, D., Yorgun, S. 2000. Influence of particle size on the pyrolysis of rapeseed (Brassica napus L.): fuel properties of bio-oil. *Biomass and Bioenergy*, **19**(4), 271-279.

Şensöz, S., Demiral, İ., Ferdi Gerçel, H. 2006. Olive bagasse (Olea europea L.) pyrolysis. *Bioresource Technology*, **97**(3), 429-436.

Shafiee, S., Topal, E. 2009. When will fossil fuel reserves be diminished? *Energy Policy*, **37**(1), 181-189.

Solantausta, Y., Nylund, N.-O., Westerholm, M., Koljonen, T., Oasmaa, A. 1993. Wood-pyrolysis oil as fuel in a diesel-power plant. *Bioresource Technology*, **46**(1–2), 177-188.

Sondreal, E.A., Benson, S.A., Hurley, J.P., Mann, M.D., Pavlish, J.H., Swanson, M.L., Weber, G.F., Zygarlicke, C.J. 2001. Review of advances in combustion technology and biomass cofiring. *Fuel Processing Technology*, **71**(1–3), 7-38.

Srinivasan, V., Adhikari, S., Chattanathan, S.A., Park, S. 2012. Catalytic Pyrolysis of Torrefied Biomass for Hydrocarbons Production. *Energy & Fuels*, **26**(12), 7347-7353.

Thangalazhy-Gopakumar, S., Adhikari, S., Gupta, R.B. 2012. Catalytic Pyrolysis of Biomass over H+ZSM-5 under Hydrogen Pressure. *Energy & Fuels*, **26**(8), 5300-5306.

Tillman, D.A. 2000. Biomass cofiring: the technology, the experience, the combustion consequences. *Biomass and Bioenergy*, **19**(6), 365-384.

Vitolo, S., Bresci, B., Seggiani, M., Gallo, M.G. 2001. Catalytic upgrading of pyrolytic oils over HZSM-5 zeolite: behaviour of the catalyst when used in repeated upgrading–regenerating cycles. *Fuel*, **80**(1), 17-26.

Wannapeera, J., Fungtammasan, B., Worasuwannarak, N. 2011. Effects of temperature and holding time during torrefaction on the pyrolysis behaviors of woody biomass. *Journal of Analytical and Applied Pyrolysis*, **92**(1), 99-105.

Weissman, J.G., Lu, S., McElrath, B.M., Edwards, J.C. 1992. Deactivation of Hydrotreating Catalysts. in: *Studies in Surface Science and Catalysis*, (Eds.) J.S. Kevin, C.S. Emerson, Vol. Volume 73, Elsevier, pp. 377-384.

Westerhof, R.J.M., Brilman, D.W.F., Garcia-Perez, M., Wang, Z., Oudenhoven, S.R.G., Kersten, S.R.A. 2012. Stepwise Fast Pyrolysis of Pine Wood. *Energy & Fuels*, **26**(12), 7263-7273.

Williams, P.T., Besler, S. 1996. The influence of temperature and heating rate on the slow pyrolysis of biomass. *Renewable Energy*, **7**(3), 233-250.

Wright, M.M., Daugaard, D.E., Satrio, J.A., Brown, R.C. 2010. Techno-economic analysis of biomass fast pyrolysis to transportation fuels. *Fuel*, **89, Supplement 1**(0), S2-S10.

Xiu, S., Shahbazi, A. 2012. Bio-oil production and upgrading research: A review. *Renewable and Sustainable Energy Reviews*, **16**(7), 4406-4414.

Yan, W., Acharjee, T.C., Coronella, C.J., Vásquez, V.R. 2009. Thermal pretreatment of lignocellulosic biomass. *Environmental Progress & Sustainable Energy*, **28**(3), 435-440.

Zhang, Q., Chang, J., Wang, T., Xu, Y. 2007. Review of biomass pyrolysis oil properties and upgrading research. *Energy Conversion and Management*, **48**(1), 87-92.

Zheng, A., Zhao, Z., Chang, S., Huang, Z., He, F., Li, H. 2012. Effect of Torrefaction Temperature on Product Distribution from Two-Staged Pyrolysis of Biomass. *Energy & Fuels*, **26**(5), 2968-2974.

Chapter 3 - Catalytic Pyrolysis of Torrefied Biomass for Hydrocarbons Production

3.1. Abstract

A simple thermal pretreatment process called torrefaction has shown to be effective in improving the quality of pyrolysis-oil in terms of chemical composition. The main objective of this study was to integrate torrefaction with fast pyrolysis process to produce high quality of bio-oil. In this study, the effects of four pyrolysis temperatures (450, 500, 550 and 600^{o}C) and shape selective zeolite catalyst (H^{+}ZSM-5) on hydrocarbon yield were analyzed. Temperature and catalyst were found to be favorable for aromatic hydrocarbons from pyrolysis of torrefied biomass. The total carbon yield from catalytic pyrolysis of torrefied biomass was 1.45 times the total carbon yield from catalytic pyrolysis of untreated pine. Reaction mechanisms were proposed to understand the production of hydrocarbons from lignin and holocellulose derivatives.

3.2. Introduction

Biomass has a potential to alleviate the use of fossil based fuels because it is the only currently available carbon-based renewable source for liquid fuels production. In addition, biofuels including pyrolysis oil (bio-oil) can offer several environmental benefits such as low sulfur oxides (SO_x), nitrogen oxides (NO_x), and is almost carbon dioxide (CO_2) neutral unlike the existing fossil fuels.(Mohan et al., 2006).

Previous studies (Czernik & Bridgwater, 2004; Thangalazhy-Gopakumar et al., 2010) have shown that fast pyrolysis is an effective process to convert solid biomass to a liquid fuel, bio-oil, in short residence time. This fuel is dark brown liquid and a complex mixture of water, acids, oxygenated hydrocarbons, and solid char.(He et al., 2009). It has several potential applications such as power generation from gas turbines, internal combustion engines, and also as a feedstock for chemicals.(Chiaramonti et al., 2007; Fisk et al., 2009) However, bio-oil, in its present form, has to be upgraded to use it as a liquid transportation fuel. The high oxygen content (approximately 35 wt.% dry basis) imparts several negative attributes to the bio oil such as instability, low heating value, and also makes it immiscible with the current hydrocarbon fuels.(Zhang et al., 2007) Furthermore, bio-oil undergoes a chemical transformation during storage to attain thermodynamic equilibrium leading to changes in molecular weight distribution and viscosity of the oil. These disadvantages hinder bio-oil from becoming a feasible solution as an alternate liquid fuel. The oxygen content, viscosity and heating value are properties that have to be improved so as to attain a higher quality fuel. Therefore, an upgrading technique to improve the quality and stability of the liquid product has to be developed.

Two main upgrading techniques --cracking and hydrodeoxyenation-- have been studied for partial or complete deoxygenation of pyrolysis oil. Boil-oil cracking involves reacting biomass or pyrolytic vapors over certain shape selective catalysts to remove oxygen.(Corma et al., 2007; Fisk et al., 2009) (Mihalcik et al., 2011) Among all the catalysts, zeolite is particularly attractive because of its effectiveness in improving the aromatic yield by selective deoxygenation of pyrolysis vapors.(Carlson et al., 2009; Carlson et al., 2008) In this process, presence of catalyst enhances the aromatic yield due

to the rupture of C-C bonds associated with dehydration, decarbonylation and decarboxylation. Hydrodeoxygenation uses high pressure hydrogen in combination with desulphurization catalyst for the elimination of oxygen.(Fisk et al., 2009) An extensive review on both the techniques can be found in published documents elsewhere.(Elliott et al., 1991; Elliott & Hart, 2008; Xiu & Shahbazi, 2012).

Recently, a simple thermal pretreatment process, torrefaction, has applied to improve the properties of biomass. Torrefaction is a thermochemical process that occurs around 200-300°C in the absence of oxygen.(Sadaka & Negi, 2009) During torrefaction, biomass undergoes partial decomposition with the release of volatiles, which results in overall mass loss. Furthermore, the fibrous structure of the biomass is lost as a result of torrefaction mainly because of the decomposition of hemicellulose and depolymerization of cellulose. In addition, torrefaction results in a significant loss of oxygen from the biomass, which in return reduces the oxygen content, increasing the calorific value of pretreated biomass while decreasing the energy required for grinding. The grinding energy for untreated pine chips and forest residues could be as high as 237 kWh/t compared to 23 kWh/t for similar biomass when torrefied(Phanphanich & Mani, 2011). Nonetheless, torrefaction process requires some energy (approximately 100 kWh/t) for pine(Carter, 2012b) although the process changes from endothermic to exothermic when reaction temperature increases.(van der Stelt et al., 2011) From the numbers, it can be easily concluded that torrefaction followed by pyrolysis actually saves energy. It is also noteworthy mentioning that torrefaction process can be carried out just using thermal energy whereas grinding process requires electrical energy (which is usually expensive). While all advantages mentioned above are significant in the context of pyrolysis, the

latter one is particularly significant since the pyrolysis process requires very fine particles to increase liquid yield.(Shen et al., 2009).

Most of the previous studies have examined the effect of torrefaction temperature and reaction time on the physicochemical properties of biomass.(Felfli et al., 2005; Phanphanich & Mani, 2011; Pimchuai et al., 2010) A handful studies have focused on the influence of torrefied biomass on the quality of the liquid fuel.(Meng et al., 2012; Ren et al.; Uslu et al., 2008) However, none of them have focused on the combined effect of catalyst and pretreatment on the bio-oil quality. Therefore, the main objective of this paper was to study the effect of catalyst and torrefaction on hydrocarbons yield using fast pyrolysis process. Further, the influence of temperature and biomass to catalytic loading ratio on the various product yields was studied. The governing hypothesis is that the pretreated biomass (low in oxygen content) would produce more aromatic compounds as compared to raw biomass.

3.3. Experimental Setup

3.3.1. Biomass Preparation and Characterization

Pine wood chips were obtained from a local wood chipping plant in Opelika, Alabama. As a first step, those wood chips were dried in an oven at 75°C for 12 h and some of them were torrefied at 225°C for 30 min in a furnace. Both samples (raw and torrefied) were ground using hammer mill (New Holland Grinder Model 358) fitted with 1.2 mm screen. Proximate and ultimate analyses were performed for both samples. Proximate analysis included tests for moisture, ash, and volatile matter. Moisture, ash, and volatile matter were measured according to the ASTM E871, ASTM E1755 and ASTM E872 standards, respectively. Higher heating value (HHV) of biomass samples

was measured using an oxygen bomb calorimeter (IKA, Model C200). A CHNS analyzer (Perkin Elmer, Model CHNS/O 2400) was used to determine carbon, hydrogen, nitrogen of the samples.

3.3.2. Catalyst Preparation

ZSM-5 (Zeolyst, Inc. SiO_2/Al_2O_3 = 50, surface area = 425 m^2/g) was received in ammonium cation form and was calcined in air at 550°C for 2 h in a furnace to convert into H^+ZSM prior to use. For few experiments metal (cobalt, nickel, iron and manganese) impregnated zeolite was used as catalyst. The metals were impregnated using their ammonium nitrate or nitrate solutions: cobalt nitrate hexahydrate for cobalt, nickel nitrate for nickel, ferric nitrate nanohydrate for iron and manganese nitrate for manganese. As a first step, metal solutions were prepared in 20mL water in certain ratio so that the zeolite powder contained 5 wt.% of desired metals. The solution was dried at 120°C and calcined in air at 500°C for 3h. The dried catalyst was reduced by passing 5%H_2 and balance He gas in the rate of 35mL/min at 500°C for 2h. The biomass:metal impregnated catalyst was kept constant at 1:9 throughout the study.

3.3.3. Fast Pyrolysis- Pyroprobe

Fast pyrolysis experiments were carried out using a commercial pyrolyzer (CDS Analytical Inc., Model 5200). A Probe had a heating filament, which held the sample in a quartz tube and the heating rate of the filament was computer controlled. The reactant mixture (catalyst and biomass) was packed between quartz wool in a quartz tube (25 mm long with 1.9 mm internal diameter). Catalytic fast pyrolysis was carried at four different temperatures (450,500,550, and 600°C) and three different biomass:catalyst ratios (1:4, 1:9, and 1:14) for torrefied biomass. As a control, raw biomass was pyrolysed at 450°C

and 500°C with 1:9 biomass:catalyst ratio. Experiments were also carried out for both raw and torrefied biomass at 650°C to compare bio-oil produced from pyroprobe and fixed-bed reactor without catalyst. Experiments were carried out at three different temperatures (500, 550 and 600°C) using metal impregnation catalyst. Temperature specified for pyroprobe experiment is the filament temperature but the actual sample temperature in a pyroprobe is about 100-125^{o}C lower than the filament temperature. For catalytic fast pyrolysis experiments, zeolite catalyst was physically mixed with ground biomass samples in pre-selected ratios. The heating rate was kept constant at 2000°C/s throughout the study. The heating rate reported here is the filament-heating rate and the actual biomass-heating rate was found to be around 50°C/s (Thangalazhy-Gopakumar et al., 2011). Helium gas was used as the inert pyrolysis gas as well as the carrier gas for the GC/MS system. A known amount of (approximately 1 mg) reactant mixture was taken for each run. The vapor from pyrolysis was carried to a trap maintained at 40°C. The condensable vapor was adsorbed in the trap, and the non-condensable vapor was purged using the same He gas. The adsorbed gas was then desorbed by heating the trap to 300°C, and carried to GC/MS for analysis using ultrahigh purity (99.999%) He supplied from Airgas Inc. The vapor transfer line from pyroprobe to GC/MS was maintained at 300^{o}C. Bio-oil compounds were analyzed with an Agilent 7890 GC/5975 MS using a DB 1701 column. The GC front inlet temperature was kept at 250°C, and the GC oven was programmed with the following temperature regime: hold at 40°C for 2 min, heated to 250°C at 5°C/min, and hold at 250°C for 8 min. A split ratio of 50:1 was set for injection, and the gas flow rate was maintained at 1.25 mL/min. Compounds were identified using NIST (National Institute of Standards and Technology) mass spectral library. Compounds

which appeared consistently with high probability were selected and quantified. Quantification was done by injecting calibration standards into the GC/MS system. The slope of the calibration line was taken as the quantification factor in the calculation. Experiments were carried out in triplicates, and the average values are reported. Yield and selectivity in this chapter is calculated using the equation 3.1 and 3.2 respectively

$$Yield\ (\%) = \frac{weight\ of\ each\ compound\ in\ the\ output}{weight\ of\ biomass\ taken} \times 100$$ ---------- Equation 3.1

$$Selectivity\ (\%) = \frac{weight\ of\ desired\ product}{weight\ of\ total\ carbon\ in\ the\ product} \times 100$$ ---------- Equation 3.2

3.3.4. Pyrolysis – Fixed Bed Reactor

Fixed-bed experiment was conducted at 550°C assuming that the data from pyroprobe experiments can be compared. The reactor was made of stainless steel and was 18 inch long with 0.5 inch outer diameter and 0.385 inch inner diameter. The reactor was placed in a furnace (Thermo Scientific Model TF55035A-1) and, in each run, known amount of (approximately 5 g) of biomass sample was loaded in the reactor. A thermocouple was inserted inside the reactor to determine the heating rate for each experiment. Three condensers were placed in series for condensing vapor resulting from pyrolysis. Helium gas was used as a carrier gas for pyrolysis vapor, and maintained at 10 mL/min throughout the experiment. The non-condensable vapor was vented outside after the third condenser. Bio-oil and bio-char yields were measured after every run. The total yield of bio-oil was measured by summing up the liquid product yield from the 1st, 2nd and 3rd condensers. Bio-char was collected at the end of the run. Average values were reported from two replications. The bio-oil collected was observed to have two distinct phases and hence it was separated into tar and aqueous phase by centrifuging at 5°C and

1500 rpm for 15 min. The bio-oil was then separated into tar and aqueous phase by centrifuging at 5°C and 1500 rpm for 15 min. For chemical analysis, a representative sample was prepared by mixing known amount of bio-oil (~300 mg in the case of aqueous phase and ~150 mg in the case of tar phase) with 3 mL of methanol and was diluted to 10 mL with dichloromethane. A dilute sample was injected into the GC column for analysis using the same GC/MS conditions, as described earlier, except a split ratio, which was set at 5:1.

3.4. Results and Discussion

3.4.1 Biomass Characterization

Results from ultimate and proximate analyses of untreated and torrefied pine wood are given in Table 1. Small increase in the heating value was noticed for the torrefied pine. Also, there was a decrease in the oxygen and hydrogen content while the elemental carbon increased due to the pretreatment process. This can be due to the loss of hydroxyl group (~OH) as a result of torrefaction process.(Phanphanich & Mani, 2011; Prins et al., 2006a) An ANOVA analysis (95% confidence interval) showed that all the properties listed in Table 3.1 except for the ash content showed significant change with torrefaction.

Table 3.1: Physicochemical properties of raw and torrefied pine [a]

Sample	Ultimate analysis, wt.% (d.b)[a]				Proximate analysis, wt.% (d.b)[a]			HHV
	C	H	N	O	Ash	Volatile Matter	Fixed Carbon	(MJ/kg)
Pine	50.9±0.2	6.1±0.04	0.4±0.11	41.8±0.13	0.7±0.05	80.8±0.47	18.5±0.23	20.2±0.21
Torrefied Pine	53.6±0.77	5.7±0.09	0.7±0.01	39.0±0.42	0.8±0.01	76.4±0.27	22.8±0.18	21.1±0.10

[a]d.b = dry basis

3.4.2. Effect of Torrefaction

3.4.2a. Pyroprobe study

Effect of torrefaction on the product distribution from fast pyrolysis of biomass at 650°C is shown in Figure 3.1. The products were grouped into different categories such as aromatic hydrocarbons (AH), phenolics (PH), guaiacols (G), naphthalenes (Naph), furans (FN), and anhydrous sugars (AS) as shown in Table 3.2. The compositions of the products from the pyrolysis of torrefied biomass were significantly different from that of raw pine. The group phenolics included phenols and cresols. The amount of guaiacols produced was found to be slightly higher in the case of torrefied pine pyrolysis. However, phenolics yield remained almost constant from pyrolysis of raw and torrefied pine. Hydrocarbons, one of the important compounds in any liquid fuel, were found to be very minimal from the pyrolysis of raw pine, while it increased significantly when the torrefied pine was used. On the other hand, furans were significantly higher from the pyrolysis of raw pine.(Meng et al., 2012) These results indicated that the pretreatment favored the production of aromatic hydrocarbons in pyrolysis.

Table 3.2 : List of compounds identified from the MS library

Aromatic Hydrocarbons (AH)	**Phenolics (PH)**	**Guaiacols (G)**	**Naphthalene (Naph)**	**Anhydrous Sugars (AS)**	**Furans (F)**
Benzene	Phenol	Phenol, 2-methoxy-4-methyl-	Naphthalene	2-Cyclopenten-1-one	Furfural
Toluene	Phenol, 2-methyl-		Naphthalene, 1-methyl-		2-Furancarboxaldehyde, 5-methyl
Ethylbenzene	Phenol, 3-methyl-		Naphthalene, 2-methyl-		Furan-2-methyl
p-Xylene	Phenol, 2,3-dimethyl-		Naphthalene, 1-ethyl-		4-methyl furan
o-Xylene	Phenol, 2,4-dimethyl-		Naphthalene, 2,7-dimethyl-		benzofuran
Styrene			Naphthalene, 1,3-dimethyl-		
Benzene, 1-ethyl-2-methyl-			Naphthalene, 1,6,7-trimethyl-		
Benzene, 1,2,3-trimethyl-					
Indane					
Indene					
Biphenyl					

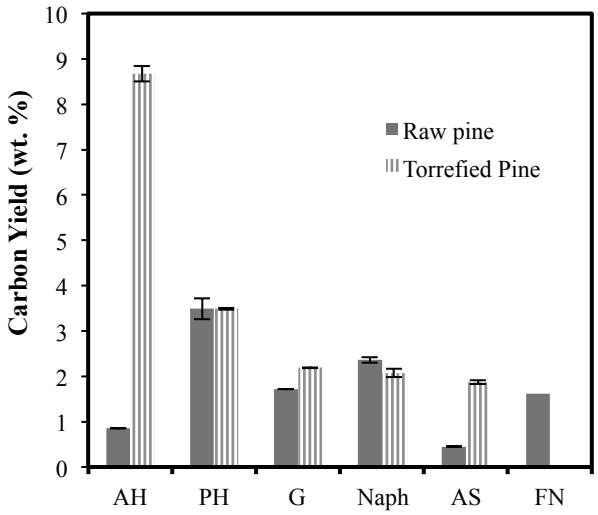

Figure 3.1: Product distribution from non-catalytic fast pyrolysis of torrefied and raw pine at 650^0C using a pyroprobe

3.3.2b Fixed Bed Reactor Study

Fast pyrolysis using fixed bed reactor resulted in less bio-oil yield from torrefied pine (30.28±0.86 wt.%) compared to raw pine (45.715±1.36 wt.%). On the other hand, char yield was high from torrefied pine (44.13±2.073 wt.%) than from raw pine (32.52±2.54 wt.%). The heating rate was found to be 1.96±0.80 °C/s for torrefied pine pyrolysis and 1.01±0.11°C/s for raw pine pyrolysis. The influence of pretreatment on the product distribution of tar and aqueous phase bio-oil from fast pyrolysis process is given in Figure 3.2. Compounds were distributed differently in tar phase and aqueous phase. Tar phase showed more of aromatic hydrocarbon compounds while, phenolics, guaiacols and naphthalenes were more in the aqueous phase bio-oil produced from pyrolysis of torrefied pine. Significant amount of aromatic hydrocarbons were observed in tar- and aqueous- phases of torrefied pine bio-oil.

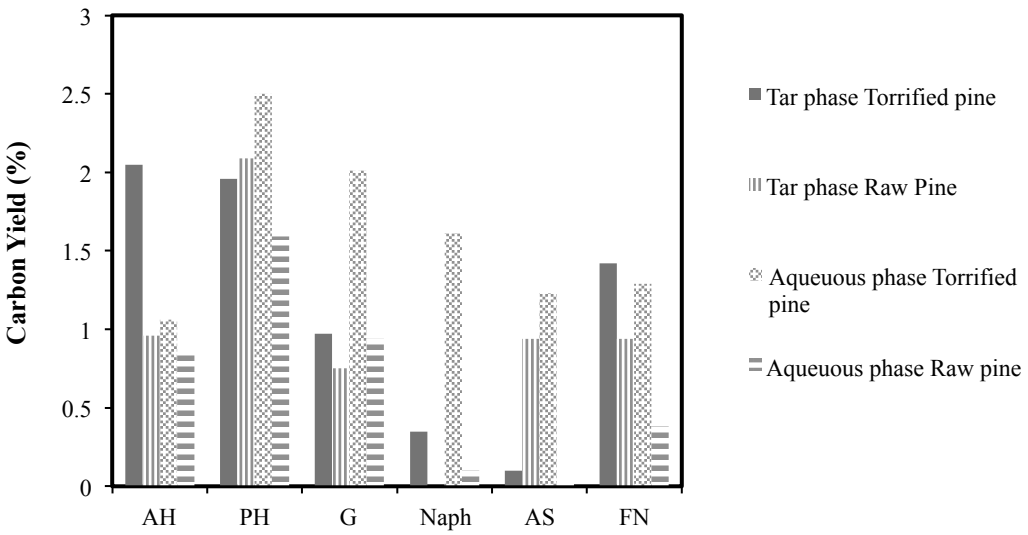

Figure 3.2: Product distribution from non-catalytic fast pyrolysis of torrefied and raw pine at 550^0C using a fixed bed reactor

Table 3.3 shows the product distribution of the pyrolysis products of raw and torrefied pine from pyroprobe and fixed bed reactor study. For the pyrolysis of raw pine, both pyroprobe and fixed bed reactor showed similar results but this was not the case in the pyrolysis of torrefied pine. From pyrolysis results of torrefied pine, it was noticed that more aromatic hydrocarbons were produced from pyroprobe than fixed bed reactor. Interestingly, furan compounds were produced more from pyrolysis of torrefied pine using fixed bed reactor. Pyroprobe also resulted in higher total carbon yield from the pyrolysis of torrefied pine. From these observations, it can be clearly seen that product distribution depends on the type of the reactor used. Fixed bed reactor and pyroprobe had several differences in terms of configuration and experimental parameters. Pyrolysis through fixed bed reactor was carried out at much lower heating rate and that could be a possibly reason for the difference in product distribution especially aromatic hydrocarbons.(Carlson et al., 2009) This is because at low heating rates the biomass is vaporized at low temperature levels itself and there is not much of a chance for other secondary degradations to occur.(Chen et al., 2003a)

Table 3.3 : Product distribution from fast pyrolysis of raw and torrefied pine from pyroprobe at 650°C and fixed bed reactor at 550°C

	Raw Pine(wt.% carbon)		Torrefied Pine(wt.% carbon)	
	Pyroprobe	Fixed bed reactor	Pyroprobe	Fixed bed reactor
Aromatic Hydrocarbon (AH)	0.76±0.23	1.52±0.12	8.64±1.36	3.11±0.51
Phenols (PH)	3.51±0.65	3.68±0.54	3.54±0.025	4.46±0.68
Guaiacols (G)	1.65±0.02	1.69±0.03	2.12±0.12	2.98±0.019
Naphthalene (Naph)	2.25±0.97	0.1±0.005	1.98±0.57	1.96±0.007

Anhydrous sugars (AS)	0.42±0.005	0.965±0.001	1.87±0.001	1.33±0.002
Furans (FN)	1.39±0.03	1.32±0.19	n.f[b]	2.71±0.09
Total Carbon Yield	9.98±0.12	8.45±0.21	18.15±0.98	16.55±1.4

[b]n.f = compounds not found

3.4.3. Catalytic Fast Pyrolysis

3.4.3a. Effect of Reaction Temperature

The effect of temperature on the total carbon yield for three different torrefied biomass:catalyst ratios namely, 1:4, 1:9 and 1:14 is shown in Figure 3.3. It can be seen that the increase in reaction temperature from 450°C to 550°C increases the total carbon yield significantly for all three biomass to catalyst ratios. At high biomass to catalyst ratio (1:14), there is a slight drop in the carbon yield with further increase in temperature from 550° to 600°C. Catalytic fast pyrolysis of raw pine resulted in ~14 (wt %) of total carbon at 450^{o}C and biomass:catalyst ratio of 1:9 (not shown in Figure 3.3). The carbon distribution on each group is given in Table 3.4.

Table 3.4 : Product distribution from catalytic fast pyrolysis of raw pine at 450°C with 1:9 biomass to catalyst ratio

	Raw Pine	Torrefied Pine
	Average (wt% carbon)	Average (wt% carbon)
Aromatic Hydrocarbon (AH)	5.66±0.23	10.2±1.36
Phenols (PH)	3.51±0.65	1.08±0.025
Guaiacols (G)	1.65±0.02	1.07±0.12
Naphthalene (Naph)	2.25±0.97	5.66±0.31

Anhydrous sugars (AS)	0.42±0.005	n.f[b]
Furans (FN)	1.39±0.03	2.31±0.11
Total Carbon Yield	14.88±1.12	20.32±1.26

[b]n.f = compounds not found

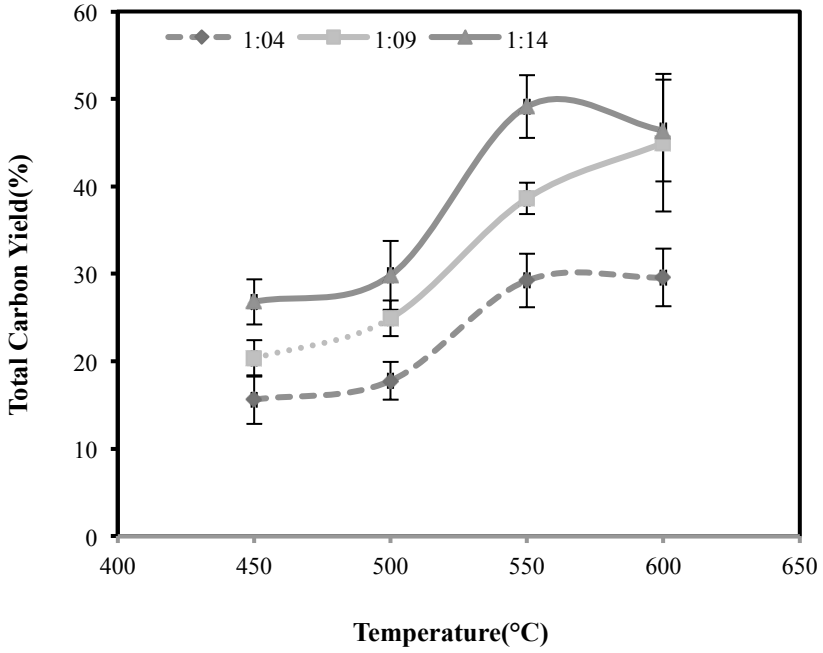

Figure 3.3: Effect of temperature on total carbon yield for different torrefied biomass to catalyst ratio

The product distribution with temperature for 1:9 biomass:catalyst ratio is shown in Figure 3.4. The three main components of biomass, cellulose, hemicellulose and lignin, decompose at various temperatures and produce different compounds. Thermal decomposition of holocellulose gives furan derivatives and few low molecular weight compounds such as formic acid, acetol.(Patwardhan et al., 2011) However, low molecular weight compounds were not observed in this study. The yield of furan derivatives is high

at low temperature probably because of the primary degradation and decrease with increase in temperature due to its weak thermal stability which results in the secondary vapor phase degradations.(Branca et al., 2003) Phenols and guaiacols are mainly derived from the decomposition of lignin.(Murwanashyaka et al., 2001) From the figure, it can be seen that the phenols increases while guaiacols decreases with temperature. Similar trend was observed from the pyrolysis results with 1:4 and 1:14 biomass to catalyst ratios. This could be due to the demethoxylation reactions of guaiacols at high temperatures to give phenols.

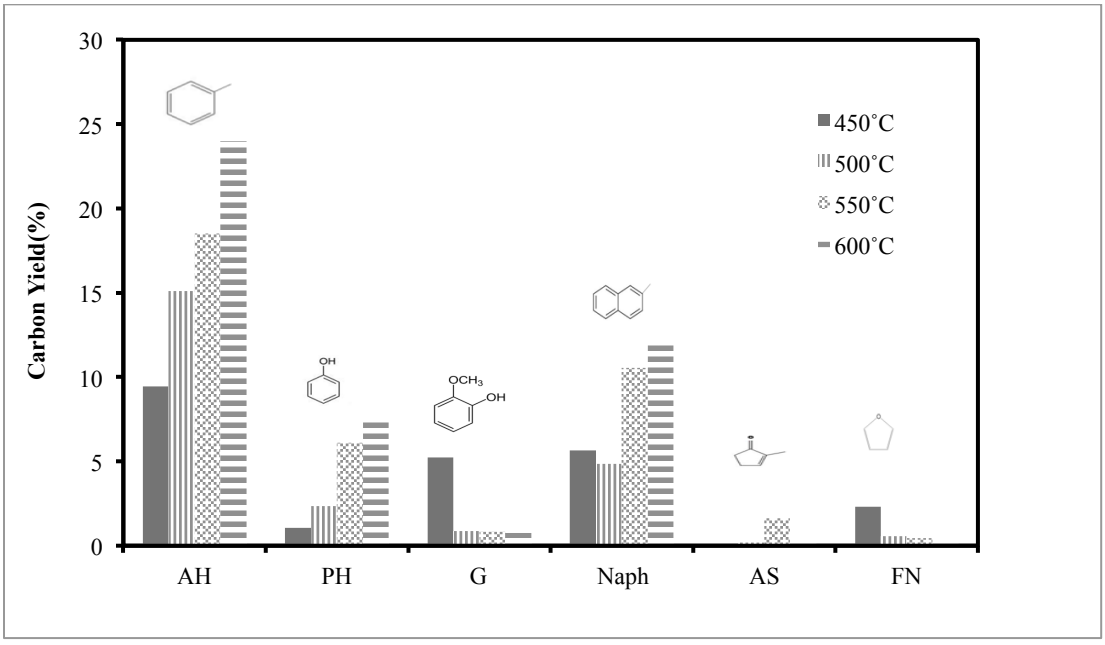

Figure 3.4: Effect of temperature on product distribution of catalytic fast pyrolysis of torrefied pine with 1:9 biomass to catalyst ratio

Aromatics selectivity as a function of temperature is given in Figure 3.5. Selectivity of benzene increased with temperature while selectivity of p-xylene decreased with temperature. As the temperature increased from 450°C to 550°C, the selectivity of

naphthalenes slightly increased. Further increase in temperature to 600°C resulted in the decrease of its selectivity. Similar trend was noticed from the pyrolysis results obtained with 1:4 and 1:14 biomass to catalyst ratios.

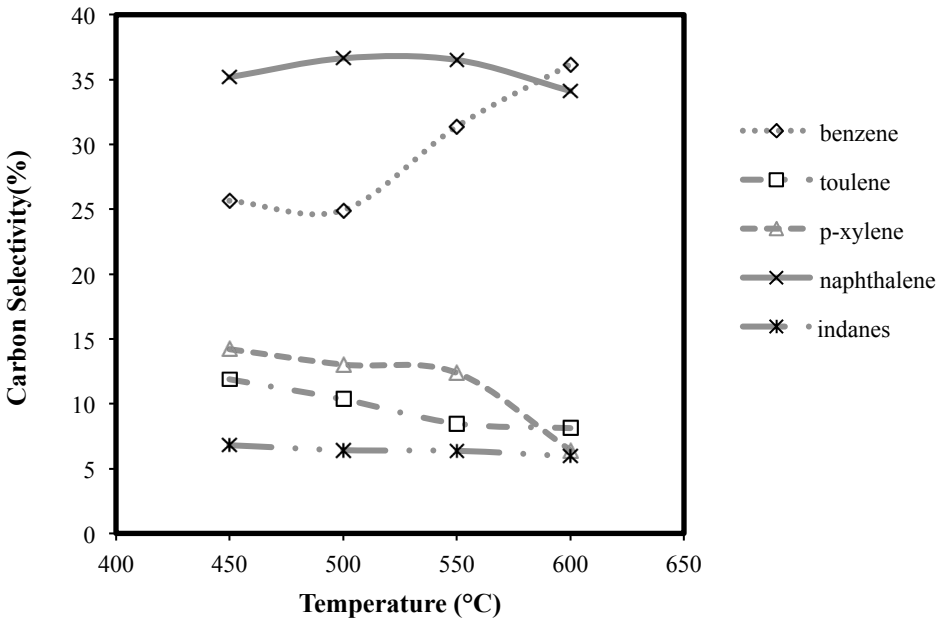

Figure 3.5: Effect of temperature on the aromatic selectivity for the catalytic fast pyrolysis of torrefied pine with 1:9 biomass to catalyst ratio

3.4.3b. Effect of Catalyst to Biomass Ratio

Figure 3.6 shows the effect of biomass to catalyst ratio on the product composition at 600°C. Aromatic hydrocarbons were most affected by catalyst to biomass ratio and, significantly increased with biomass to catalyst ratio. Among the aromatic hydrocarbons, benzene, toluene, and styrene were primary compounds, and few alkyl substituted aromatics such as benzene-1-ethyl-2-methyl, benzene 1, 2, 3 trimethyl, and

benzene 1, 2, 3, 4 tetra methyl were also seen in traces. Naphthalene compounds also followed the same trend with increase in biomass to catalyst ratio. This can be due to the size selectivity of zeolite catalyst as the kinetic diameter of naphthalene (6Å) is very similar to ZSM-5 pore size (~6.2Å).(Carlson et al., 2009) It was also observed that the thermally stable oxygenates mainly furans and its derivatives were formed at low catalyst to biomass ratio. Similar behavior was also observed during the catalytic fast pyrolysis of glucose.(Carlson et al., 2008) The oxygenated compounds can diffuse into the pores of the H^+ZSM-5 catalyst, and can result in aromatics through decarbonylation, dehydration, and oligomerization reactions.(Carlson et al., 2010) Aromatic selectivity as a function of biomass to catalyst ratio is shown in Figure 3.7. Increasing the biomass to catalyst ratio increased the selectivity of toluene and p-xylene to a little extent while the selectivity of benzene and its derivatives decreased. Decrease in naphthalene selectivity was also noticed with increase in biomass to catalyst ratio.

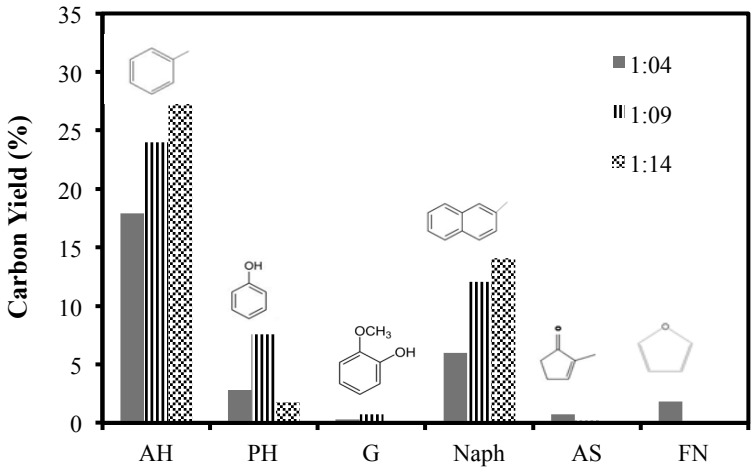

Figure 3.6: Product distribution for the catalytic pyrolysis of torrefied biomass at 600°C with different biomass to catalyst ratio

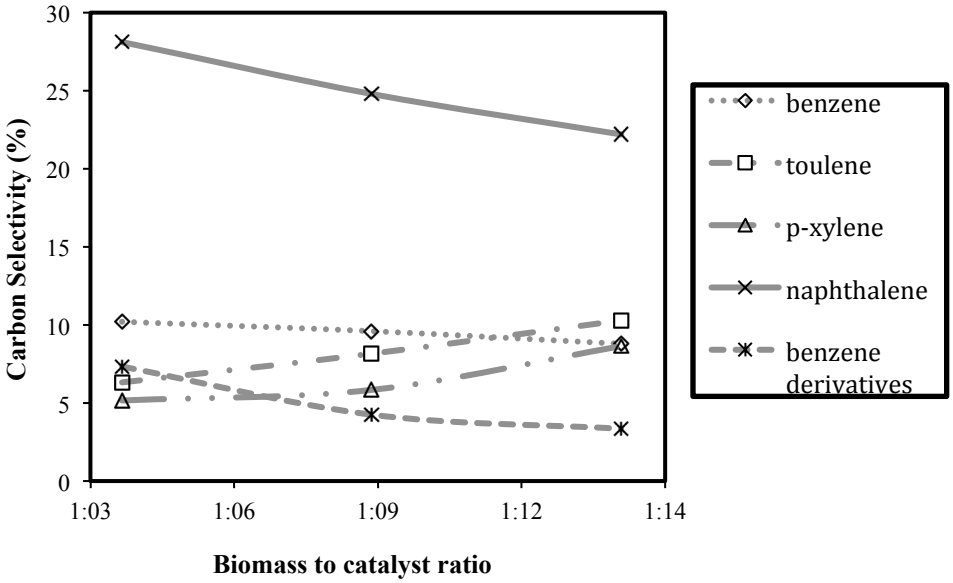

Figure 3.7: Aromatic selectivity as a function of torrefied biomass to catalyst ratio at 600°C

3.4.4. Reaction Mechanism

As discussed above, more lignin and less holocellulose derivatives were observed in the bio-oil as a result of pretreatment. Lignin derivatives included guaiacol and phenolic compounds, and guaiacols were seen in significant amount at lower temperatures. However, as the temperature increased, the guaiacols decreased while phenols and aromatic hydrocarbons increased. This indicated that guaiacols can possibly be an intermediate in the formation of phenols and hydrocarbons. In order to verify this, catalytic pyrolysis of guaiacol was carried out at 600°C with 1:9 guaiacol to catalyst ratio. From pyrolysis, it was seen that aromatic hydrocarbon which included benzene, toluene, p-xylene, benzene tri- and di- methyl and indenes constituted for 26.27 wt.% (mass basis). Interestingly, phenols were not produced in significant amount and they accounted only for 2.18 wt.% (mass basis). Naphthalenes were also noticed in traces from pyrolysis of guaiacol. All these results indicated that the primary products from pyrolysis of guaicaol are aromatic hydrocarbons and not phenols. This was contradictory to the results reported in another literature(Nimmanwudipong et al., 2011) where the primary product from pyrolysis of guaiacols with HY-ZSM catalyst was phenols and not aromatic hydrocarbons. Hence phenolics in our study could have resulted directly from the decomposition of ether bonds in lignin. Also, catalytic pyrolysis of phenol (600°C with 1:9 phenol to catalyst ratio) was carried out to see if phenol was transformed into hydrocarbons. Results showed that pyrolysis of phenol produced only phenol derivatives such as methyl phenols, di-methyl phenols and not aromatic hydrocarbon. Hence, it was clear that major source of aromatic hydrocarbons were guaiacols and not phenolics. Guaiacols have less structural stability and hence can undergo degradation and

demethylation to form more stable catechols. Further dehydration of catechols can result in phenols. However, primary reaction in our study is the conversion of guaiacol into cresols through Friedel –Craft transalkylation reaction and further conversion of cresols into aromatic hydrocarbons through dehydration reaction (Figure 3.8). In order to validate that cresols transforms into aromatics, catalytic pyrolysis of p-cresol at 600°C was performed. Results of this experiment showed that aromatic hydrocarbons contributed to about 54.08 % (mass basis) of the products.

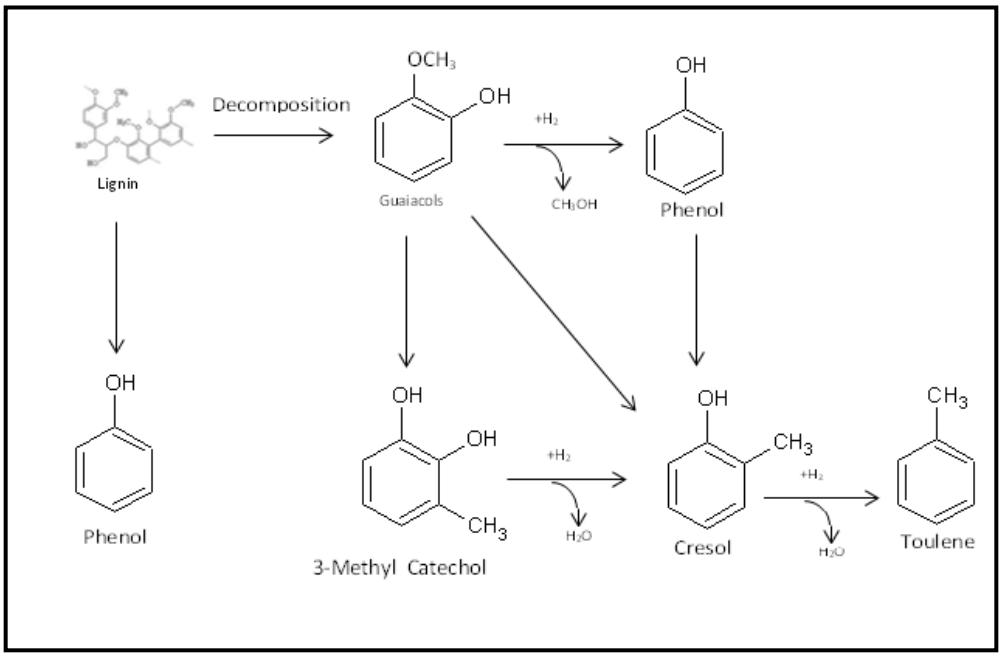

Figure 3.8: Reaction mechanism of the decomposition of lignin

Holocellulose derivatives included mainly furans and its derivatives. From the results it was observed that furans were noticed in significant amount at low temperature and low biomass to catalyst ratio. Hence, at higher temperature and higher catalyst to biomass ratio furan can be converted to several different products. Furans could be a possible intermediate in the production of aromatics. Hence, catalytic pyrolysis of furan

was carried out at 600°C with 1:9 biomass to catalyst ratio. This resulted in 29.64 wt.% aromatic hydrocarbons, 4.90 wt.% naphthalenes, and also phenols and guaiacols of about 3.62 wt.%. These results showed that furan undergo series of decarbonylation and oligomerization reactions to form aromatic hydrocarbons(Cheng & Huber, 2011). Loss of carbonyl from furan results in allenes which can further undergo oligomerization reactions to form aromatics and olefins (Figure 3.9).

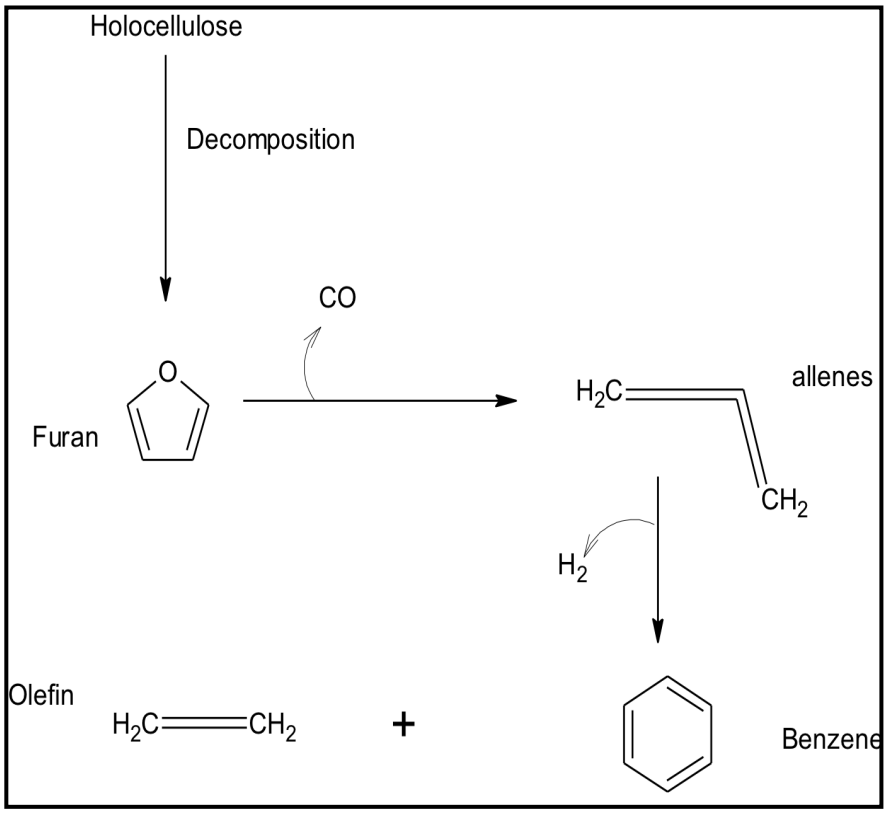

Figure 3.9: Reaction mechanism of the decomposition of hemicellulose

3.4.5. Metal impregnated Catalytic Pyrolysis

Figure 3.10 shows the total carbon yield from pyrolysis of raw pine using different metal impregnated catalyst at three different temperatures. It can be seen from

the graph that among the four metal impregnated catalyst, manganese showed a linear increase in the total carbon with temperature while iron showed a steady decrease with temperature. Use of cobalt impregnated ZSM-5 showed a sudden decrease in total carbon yield when the temperature was raised from 500 to 550°C followed by a steep increase with further raise in temperature. The maximum yield (44.96 wt.%) was observed by cobalt at 600°C. Effect of metal impregnated catalyst and temperature on the product distribution from pyrolysis of raw biomass is shown in Figure 3.11. Similar to total carbon yield, aromatic hydrocarbons were also produced highest (33.78 wt.%) when cobalt impregnated zeolite was used. Furans and anhydrous sugars were found in traces with the use of all four metals impregnated catalyst. Naphthalenes were found only with the use of cobalt and phenols were found to be relatively high only at least temperature (500°C) with the use of all catalyst except for iron. Overall, it can be observed that among the four metals impregnated, cobalt showed positive effect in promoting aromatic hydrocarbon yield. Figure 3.12 compares the product distribution from catalytic pyrolysis of raw biomass using zeolite catalyst with and without metal impregnation. From the figure it can be observed that both cobalt and iron impregnated zeolite resulted in almost 13% and 9% more aromatics respectively compared to that from zeolite without metal impregnation. Use of Ni-ZSM-5 resulted in aromatics similar to that of ZSM-5 catalyst. However, zeolite catalyst without any metal impregnation resulted in 9% more aromatics compared to manganese impregnated zeolite indicating that manganese is not a good metal for enhancing catalytic cracking processes.

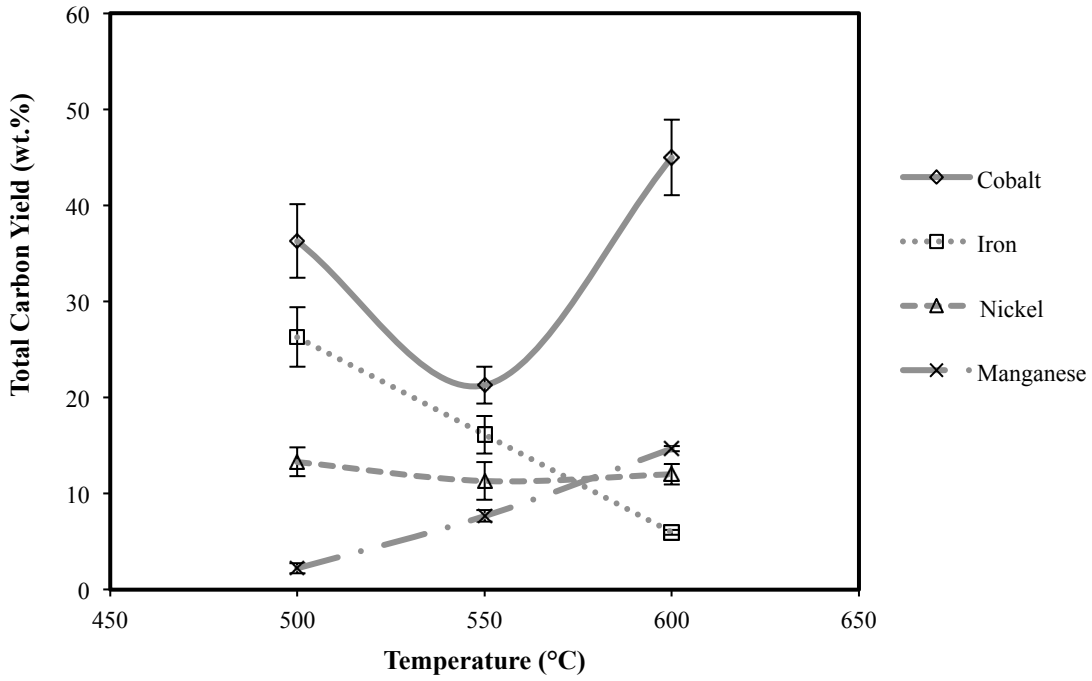

Figure 3.10: Total carbon yield from pyrolysis of raw pine using various metal impregnated catalyst at three different temperatures with 1:9 biomass to catalyst ratio

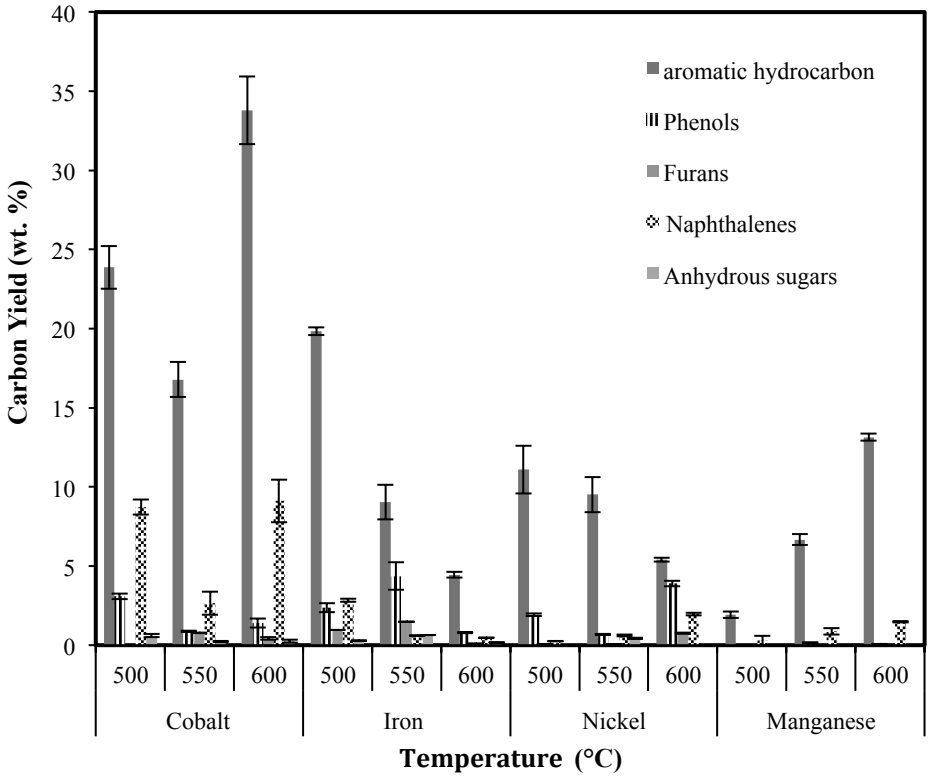

Figure 3.11: Effect of metal impregnated catalyst and temperature on the product distribution from pyrolysis of raw biomass

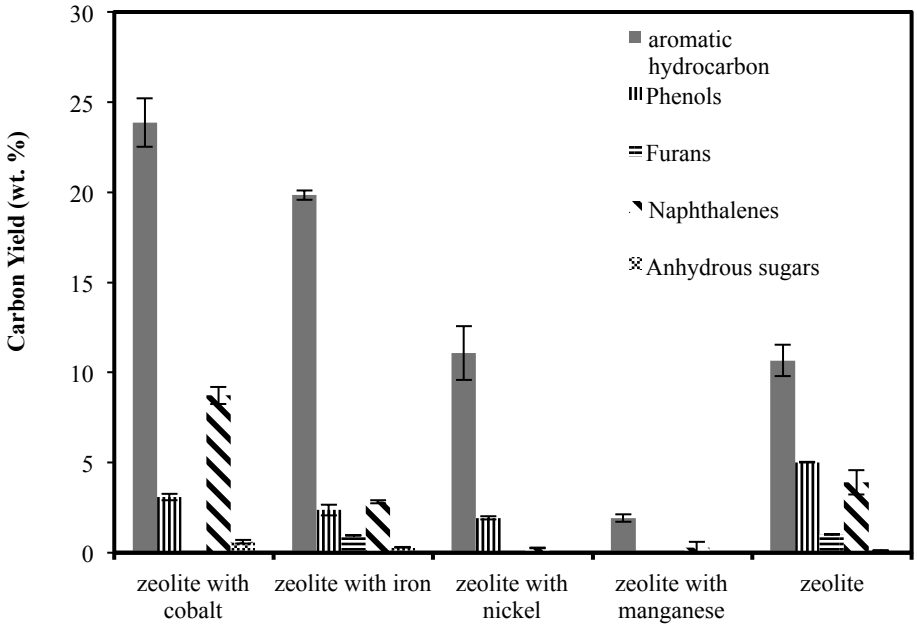

Figure 3.12: Comparison of product distribution from pyrolysis of raw biomass using zeolite catalyst with and without metal impregnation at 500°C

3.5. Conclusion

Simple pretreatment process, torrefaction, has shown to be effective in improving the quality of bio-oil produced from catalytic fast pyrolysis. Torrefaction had significant impact in the physicochemical properties of the biomass, which included increase in heating value and reduction in oxygen content. Torrefaction also resulted in more of lignin derivatives –guaiacols, phenols and less of holocellulose derivatives mainly, furans. Interestingly, guaiacols and furans were proposed to be possible intermediates in the formation of aromatics. Aromatic hydrocarbons were significantly produced as a result of torrefaction, and temperature and catalyst enhanced their production. Presence of catalyst resulted in the formation of naphthalenes due to its size selectivity. All these

results indicated that the combined effect of pretreatment and shape selective catalyst (H^+ZSM-5) resulted in highly de-oxygenated liquid product.

3.6. References

Branca, C., Giudicianni, P., Di Blasi, C. 2003. GC/MS characterization of liquids generated from low-temperature pyrolysis of wood. *Industrial & Engineering Chemistry Research*, **42**(14), 3190-3202.

Carlson, T., Tompsett, G., Conner, W., Huber, G. 2009. Aromatic production from catalytic fast pyrolysis of biomass-derived feedstocks. *Topics in Catalysis*, **52**(3), 241-252.

Carlson, T.R., Jae, J., Lin, Y.-C., Tompsett, G.A., Huber, G.W. 2010. Catalytic fast pyrolysis of glucose with HZSM-5: The combined homogeneous and heterogeneous reactions. *Journal of Catalysis*, **270**(1), 110-124.

Carlson, T.R., Vispute, T.P., Huber, G.W. 2008. Green gasoline by catalytic fast pyrolysis of solid biomass derived compounds. *ChemSusChem*, **1**(5), 397-400.

Carter, C.L. 2012. Physicochemical Properties and Thermal Decomposition of Torrefied Woody Biomass and Energy Crop, Auburn University.

Chen, G., Andries, J., Luo, Z., Spliethoff, H. 2003. Biomass pyrolysis/gasification for product gas production: the overall investigation of parametric effects. *Energy Conversion and Management*, **44**(11), 1875-1884.

Cheng, Y.-T., Huber, G.W. 2011. Chemistry of furan conversion into aromatics and olefins over HZSM-5: a model biomass conversion reaction. *ACS Catalysis*, **1**(6), 611-628.

Chiaramonti, D., Oasmaa, A., Solantausta, Y. 2007. Power generation using fast pyrolysis liquids from biomass. *Renewable and Sustainable Energy Reviews*, **11**(6), 1056-1086.

Corma, A., Huber, G.W., Sauvanaud, L., O'Connor, P. 2007. Processing biomass-derived oxygenates in the oil refinery: Catalytic cracking (FCC) reaction pathways and role of catalyst. *Journal of Catalysis*, **247**(2), 307-327.

Czernik, S., Bridgwater, A.V. 2004. Overview of applications of biomass fast pyrolysis oil. *Energy & Fuels*, **18**(2), 590-598.

Elliott, D.C., Beckman, D., Bridgwater, A.V., Diebold, J.P., Gevert, S.B., Solantausta, Y. 1991. Developments in direct thermochemical liquefaction of biomass: 1983-1990. *Energy & Fuels*, **5**(3), 399-410.

Elliott, D.C., Hart, T.R. 2008. Catalytic hydroprocessing of chemical models for bio-oil. *Energy & Fuels*, **23**(2), 631-637.

Felfli, F.F., Luengo, C.A., Suárez, J.A., Beatón, P.A. 2005. Wood briquette torrefaction. *Energy for Sustainable Development*, **9**(3), 19-22.

Fisk, C.A., Morgan, T., Ji, Y., Crocker, M., Crofcheck, C., Lewis, S.A. 2009. Bio-oil upgrading over platinum catalysts using in situ generated hydrogen. *Applied Catalysis A: General*, **358**(2), 150-156.

He, R., Ye, X.P., Harte, F., English, B. 2009. Effects of high-pressure homogenization on physicochemical properties and storage stability of switchgrass bio-oil. *Fuel Processing Technology*, **90**(3), 415-421.

Meng, J., Park, J., Tilotta, D., Park, S. 2012. The effect of torrefaction on the chemistry of fast-pyrolysis bio-oil. *Bioresource Technology*, **111**(0), 439-446.

Mihalcik, D.J., Mullen, C.A., Boateng, A.A. 2011. Screening acidic zeolites for catalytic fast pyrolysis of biomass and its components. *Journal of Analytical and Applied Pyrolysis*, **92**(1), 224-232.

Mohan, D., Pittman, C.U., Steele, P.H. 2006. Pyrolysis of wood/biomass for bio-oil: a critical review. *Energy & Fuels*, **20**(3), 848-889.

Murwanashyaka, J.N., Pakdel, H., Roy, C. 2001. Step-wise and one-step vacuum pyrolysis of birch-derived biomass to monitor the evolution of phenols. *Journal of Analytical and Applied Pyrolysis*, **60**(2), 219-231.

Nimmanwudipong, T., Runnebaum, R., Block, D., Gates, B. 2011. Catalytic reactions of guaiacol: reaction network and evidence of oxygen removal in reactions with hydrogen. *Catalysis Letters*, **141**(6), 779-783.

Patwardhan, P.R., Brown, R.C., Shanks, B.H. 2011. Product distribution from the fast pyrolysis of hemicellulose. *ChemSusChem*, **4**(5), 636-643.

Phanphanich, M., Mani, S. 2011. Impact of torrefaction on the grindability and fuel characteristics of forest biomass. *Bioresource Technology*, **102**(2), 1246-1253.

Pimchuai, A., Dutta, A., Basu, P. 2010. Torrefaction of agriculture residue to enhance combustible properties†. *Energy & Fuels*, **24**(9), 4638-4645.

Prins, M.J., Ptasinski, K.J., Janssen, F.J.J.G. 2006. More efficient biomass gasification via torrefaction. *Energy*, **31**(15), 3458-3470.

Ren, S., Lei, H., Wang, L., Bu, Q., Chen, S., Wu, J., Julson, J., Ruan, R. The effects of torrefaction on compositions of bio-oil and syngas from biomass pyrolysis by microwave heating. *Bioresource Technology*(0).

Sadaka, S., Negi, S. 2009. Improvements of biomass physical and thermochemical characteristics via torrefaction process. *Environmental Progress & Sustainable Energy*, **28**(3), 427-434.

Shen, J., Wang, X.-S., Garcia-Perez, M., Mourant, D., Rhodes, M.J., Li, C.-Z. 2009. Effects of particle size on the fast pyrolysis of oil mallee woody biomass. *Fuel*, **88**(10), 1810-1817.

Thangalazhy-Gopakumar, S., Adhikari, S., Ravindran, H., Gupta, R.B., Fasina, O., Tu, M., Fernando, S.D. 2010. Physiochemical properties of bio-oil produced at various temperatures from pine wood using an auger reactor. *Bioresource Technology*, **101**(21), 8389-8395.

Uslu, A., Faaij, A.P.C., Bergman, P.C.A. 2008. Pre-treatment technologies, and their effect on international bioenergy supply chain logistics. Techno-economic evaluation of torrefaction, fast pyrolysis and pelletisation. *Energy*, **33**(8), 1206-1223.

van der Stelt, M.J.C., Gerhauser, H., Kiel, J.H.A., Ptasinski, K.J. 2011. Biomass upgrading by torrefaction for the production of biofuels: A review. *Biomass and Bioenergy*, **35**(9), 3748-3762.

Xiu, S., Shahbazi, A. 2012. Bio-oil production and upgrading research: A review. *Renewable and Sustainable Energy Reviews*, **16**(7), 4406-4414.

Zhang, Q., Chang, J., Wang, T., Xu, Y. 2007. Review of biomass pyrolysis oil properties and upgrading research. *Energy Conversion and Management*, **48**(1), 87-92.

Chapter 4 - Catalytic Pyrolysis of Raw and Thermally Treated Cellulose using Different Acidic Zeolites

4.1. Abstract

Fast pyrolysis of biomass using zeolite catalyst has shown to be effective in improving aromatic production. This study focuses on aromatic production through catalytic pyrolysis of major biomass constituent i.e., cellulose. Furthermore, cellulose was torrefied to understand torrefaction's effect on pyrolysis products. The influence of SiO_2/Al_2O_3 ratios of zeolite (ZSM-5) catalyst on aromatics production during pyrolysis of raw and torrefied cellulose was investigated. Results showed that the catalyst acidity played a pivotal role in eliminating anhydrous sugars and other oxygenated compounds while producing more aromatics. The maximum aromatics yield (~25 wt.%) was obtained when ZSM-5 with the highest acidity (SiO_2/Al_2O_3 =30) was used while the lowest yield (7.99 wt.%) was obtained when the least acidic catalyst was used (SiO_2/Al_2O_3 =280). Also, torrefaction process showed to have positive effect on the aromatic production from pyrolysis. No aromatics were produced from the pyrolysis of raw cellulose in the absence of catalyst whereas significant amount of aromatic compounds were produced from both catalytic and non-catalytic pyrolysis of torrefied cellulose. Aromatics produced from catalytic pyrolysis of torrefied cellulose were 5% more than that produced from raw cellulose at the highest temperature and catalyst acidity (SiO_2/Al_2O_3 =30).

4.2. Introduction

Biomass is considered as an excellent alternate energy source to help in meeting the world's fast growing energy demand. Renewable energy constitutes about 17% of the total U.S. energy consumption, and liquid biofuels accounts for almost 5% of the renewable energy (EIA, 2013). Among different thermochemical and biochemical processes to convert biomass into biofuels, fast pyrolysis seems to be promising due to its high liquid yield. Although bio-oil can be used for production of transportation fuels, chemicals, and energy, bio-oil has certain properties that make it a poor fuel (Bridgwater, 1999). High water content in bio-oil results in low heating value which in turn results in poor thermal and chemical stability (Lu et al., 2009). Moreover, its poor ignition and combustion properties makes it difficult to be even co-fired with coal or other conventional resources (Tillman, 2000). Inspite of several differences in its properties compared to the conventional fuels, it is considered to be a material that can be potentially used along with fossil derived fuels to produce several useful products. However, in order to be used as an alternate transportation fuel, the high oxygen content (~35 wt. %) in bio-oil has to be reduced.

A number of studies are being focused on different upgrading techniques to improve the quality and stability of pyrolysis oil using different catalysts with or without the presence of high-pressure hydrogen (Adjaye & Bakhshi, 1995b; Sharma & Bakhshi, 1993; Zhang et al., 2007). Upgrading techniques focus on reduction or complete removal of oxygen present in the fuel, which otherwise makes it immiscible with current hydrocarbon fuel. At present, elimination of oxygen in biomass to some extent by thermal pre-treatment process termed as "torrefaction" is gaining some attention. Torrefaction is a mild pyrolysis

process that takes place at 200-300°C in the absence of oxygen accompanied by changes in physical and chemical properties of the feedstock. Hemicellulose degradation, which occurs during torrefaction can be considered a two-step process where light chain molecules mainly sugars are formed initially followed by their catalytic degradation resulting in the release of CO and CO_2 (Prins et al., 2006b). In addition, few acid compounds are also removed which leads to acid catalyzed dehydration reactions to form formaldehyde, furfural and other aldehydes (Tjeerdsma et al., 1998). There is a decrease in oxygen and hydrogen content that causes relative increase of carbon. Also, due to the removal of hemicellulose during torrefaction, there is a reduction in mass by 20 to 30% but almost 90% of the initial energy content is preserved and hence the energy density of torrefied biomass is higher and is closer to that of coal used for combustion purposes (Phanphanich & Mani, 2011; van der Stelt et al., 2011; Zwart et al., 2006). Above all, torrefaction reduces the grinding energy which is potentially beneficial since fast pyrolysis process requires fine particles to produce high bio-oil yield (Shen et al., 2009).

However, before understanding the reaction mechanism of biomass and torrefied biomass pyrolysis, it is essential to study the pyrolytic behavior of the polysaccharides present in biomass extensively. Hemicellulose, cellulose and lignin are the three main constituents of biomass and consist of approximately 25-35 wt.%, 40-50 wt.%, and 21-35 wt.%, respectively. Cellulose is a linear polymer of glucose with β-1,4 linkages, which makes cellulose less flexible compared to hemicellulose (Mohan et al., 2006). It is both crystalline and amorphous with degree of polymerization around 10,000. Pyrolysis behavior of cellulose has been studied in several past investigations and few kinetic models have also

been developed. One such model was a three-reaction model in which the "active cellulose" (levoglucosan) formed by an "initiation reaction" undergoes parallel first order reactions to give char, volatiles and gaseous products (Bradbury et al., 1979).

Several past studies have discussed fast pyrolysis of biomass constituents, especially cellulose (Antal & Varhegyi, 1995; Carlson et al., 2010; Piskorz et al., 1986; Raveendran et al., 1996; Yang et al., 2007). Only limited studies are available on the fast pyrolysis of torrefied biomass. However, none of them have focused on the catalytic pyrolysis of torrefied cellulose. Therefore, the purpose of this study is to understand the influence of torrefaction, pyrolysis temperature and catalyst acidity on the fast pyrolysis products of cellulose.

4.3. Experimental Setup

4.3.1. Cellulose Torrefaction

Pure cellulose with a mean particle size between 50-350 microns used in this study was purchased from Sigma Aldrich. The cellulose sample was then thermally pre-treated (torrefied) at 225˚C for 30 minutes in a tubular furnace (Thermo Scientific model TF55035A-1) and vapors were purged using nitrogen stream flowing in at 20 mL/min. During torrefaction process, about 10 g of raw cellulose was taken in a stainless steel reactor (ID =0.35 in, OD =0.5 in and 18 inch long) and the torrefied cellulose was weighed after the pre-treatment process. Ultimate analysis was performed for both raw and torrefied cellulose using a CHNS analyzer (Perkin-Elmer, model CHNS/O 2400 II) to measure carbon, hydrogen, nitrogen and sulfur content. Moisture content of raw and torrefied cellulose was determined using ASTM standard (ASTM E871). Higher heating

value of raw and torrefied cellulose was measured using an oxygen bomb calorimeter (IKA, model C 200). FTIR analysis was done to study the structure of raw and torrefied cellulose using a PerkinElmer Spectrum model 400 (Perkin Elmer Co., Waltham, MA). For each sample, the spectrum was collected within 10s by applying a vertical load on the sample. All scans were done at room temperature which was ~22°C.

4.3.2. Fast Pyrolysis

Fast pyrolysis experiments were carried out using a commercial pyrolyzer (CDS Analytical Inc., model 5200). A Probe had a heating filament, which held the sample in a quartz tube and the heating rate of the filament was computer controlled. A reactant mixture (catalyst and cellulose) was packed between quartz wool in a quartz tube (25 mm long with 1.9 mm internal diameter). Catalytic fast pyrolysis was carried at three different temperatures (500, 550, and 600 °C) with four zeolite catalyst of different acidity (SiO_2/Al_2O_3 – 30, 50, 80 and 280) for both torrefied and raw cellulose. Catalyst to cellulose ratio was 1:4 and was kept constant for all the experiments. Temperature specified in pyroprobe experiments is the filament temperature but the actual sample temperature in a pyroprobe can be 100−125 °C lower than the filament temperature. Four types of ZSM-5 catalyst (Zeolyst, Inc.) were received in ammonium cation form and were calcined in air at 550 °C for 2 h in a furnace to convert into H^+ZSM prior to use. Mean particle size, silica to alumina ratio, and surface area of the four zeolites are given in Table4.1. Zeolite catalyst was physically mixed with cellulose or torrefied cellulose samples in 1:4 ratio. The biomass heating rate was kept constant at 2000 °C/s throughout the study. The heating rate reported here is the filament-heating rate and the actual

biomass-heating rate was found to be around 50°C/s (Thangalazhy-Gopakumar et al., 2011). Helium gas was used as an inert pyrolysis gas as well as the carrier gas for the GC/MS system. A known amount of (approximately 1-3 mg) reactant mixture was taken for each run. The vapor from pyrolysis was carried to a trap maintained at 40 °C. The condensable vapor was adsorbed in the trap whereas non condensable vapor was purged using helium gas. The adsorbed compounds was then desorbed by heating the trap to 300 °C, and carried to GC/MS for analysis using ultrahigh purity (99.999%) helium purchased from Airgas Inc. The vapor transfer line from pyroprobe to GC/MS was maintained at 300 °C. Bio-oil compounds were analyzed with an Agilent 7890 GC/5975 MS using a DB 1701 column. The GC front inlet temperature was kept at 250 °C, and the GC oven was programmed with the following temperature regime: hold at 40 °C for 2 min, heated to 250 °C at 5 °C/min, and hold at 250 °C for 8 min. A split ratio of 50:1 was set for injection, and the gas flow rate was maintained at 1.25 mL/min. Compounds were identified using NIST (National Institute of Standards and Technology) mass spectral library. Compounds that appeared consistently with high probability were selected and quantified. Quantification was done by injecting calibration standards into the GC/MS system. The slope of the calibration line was taken as the quantification factor in the calculation. Experiments were carried out in triplicates, and the average values are reported. The results are reported as carbon yield, which is calculated using Equation 4.1. In the case of torrefied biomass, it is the weight of torrefied biomass and carbon fraction of the torrefied biomass. The overall carbon yield takes account of carbon lost during torrefaction as well.

$$Carbon\ yield\ (wt.\%) = \frac{weight\ of\ each\ compound \times mass\ fraction\ of\ carbon\ in\ each\ compound}{weight\ of\ biomass \times mass\ fraction\ of\ carbon\ in\ biomass} \times 100$$ --- (Equation 4.1)

Table 4.1: Properties of different acidic zeolites

Silica to alumina ratio	Particle size (μm)	Surface area (m^2/g)
30	81.14	400
50	87.32	425
80	87.58	425
280	89.16	400

4.4. Results

4.4.1. Effect of Torrefaction

Effect of torrefaction on the mass, energy, and its chemical composition is presented in Figure 4.1. From the figure it can be seen that almost 80% of the mass (dry basis) and ~ 97% of the original energy are retained in cellulose after the pre-treatment process. This 20% mass loss could be attributed to volatile compounds from partial decomposition of cellulose during torrefaction. However, there was no significant change in the elemental composition of torrefied cellulose. From the figure, it is evident that there is only a slight increase in the carbon content along with a slight decrease in oxygen content. This could be due to the pre-treatment process conditions (225°C for 30 min) as it plays a major role in altering the physicochemical properties of biomass during torrefaction (Liaw et al., 2013; van der Stelt et al., 2011).

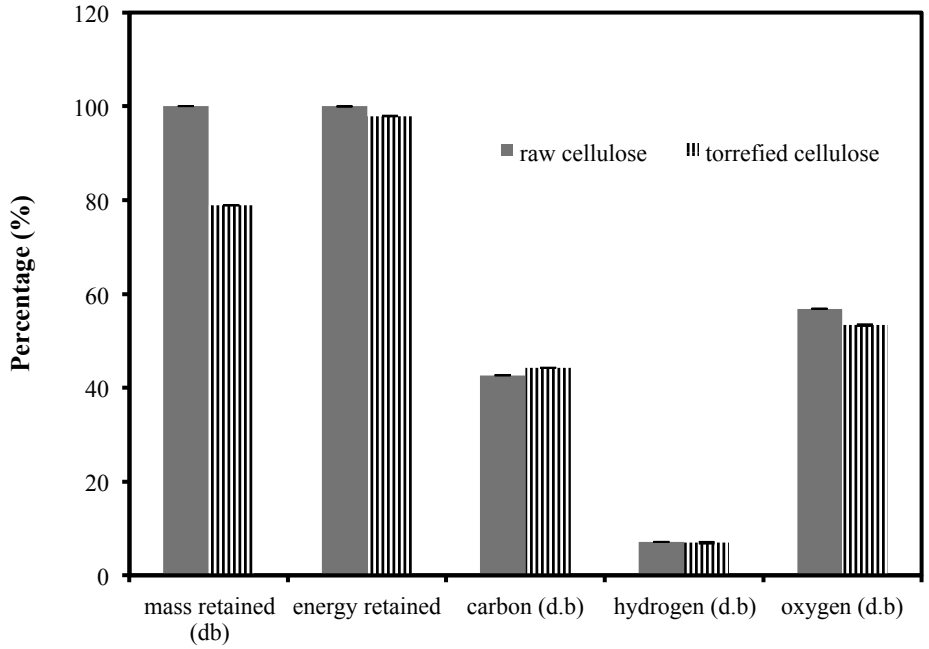

Figure 4.1: Effect of torrefaction on the mass, energy, carbon, hydrogen and oxygen content of the cellulose

4.4.2. Effect of Torrefaction: Carbon Yield

Products from GC/MS were grouped into four distinct groups- aromatics, phenols, furans and anhydrous sugars. The major compounds in each of these groups are shown in Figure 4.2. Figure 4.3 shows the effect of torrefaction on the product distribution from fast pyrolysis of cellulose at 600°C. It can be observed that no phenolics were observed from fast pyrolysis of both raw and torrefied cellulose. Anhydrous sugar, mainly levoglucosan, was found to be a major product (~ 14 wt%) from fast pyrolysis of cellulose while it was very minimal (~ 0.5 wt%) from the pyrolysis of torrefied cellulose. Moreover, pyrolysis of torrefied cellulose resulted in more of aromatics (~ 10 wt %), which was completely absent from raw cellulose (R.C) pyrolysis. Hence, it can be

assumed that thermal pre-treatment modifies the structure of cellulose by weakening the C-O-C and glycosidic bonds resulting in more aromatics during pyrolysis. In order to verify this, an FTIR study was performed for raw and torrefied cellulose (Figure 4.4). The spectra collected from raw and torrefied cellulose were similar with few differences listed below.

1. Peak at 1068 cm^{-1} ("a" in figure) corresponding to C-O-C group were found to decline for torrefied cellulose indicating the weakening of hemiacetyl bonds (Park et al., 2013; Via et al., 2013).
2. C-O-C stretching peak at ~1180cm^{-1} ("b" in figure) was found to be absent in torrefied cellulose (Soares et al., 2001; Via et al., 2013)
3. Interestingly, peak corresponding to aliphatic C-H bonds at 1360cm^{-1} ("c" in figure) and weak carbonyl stretch at ~1730 cm^{-1} ("d" in figure) grew for torrefied cellulose (Soares et al., 2001; Via et al., 2013).

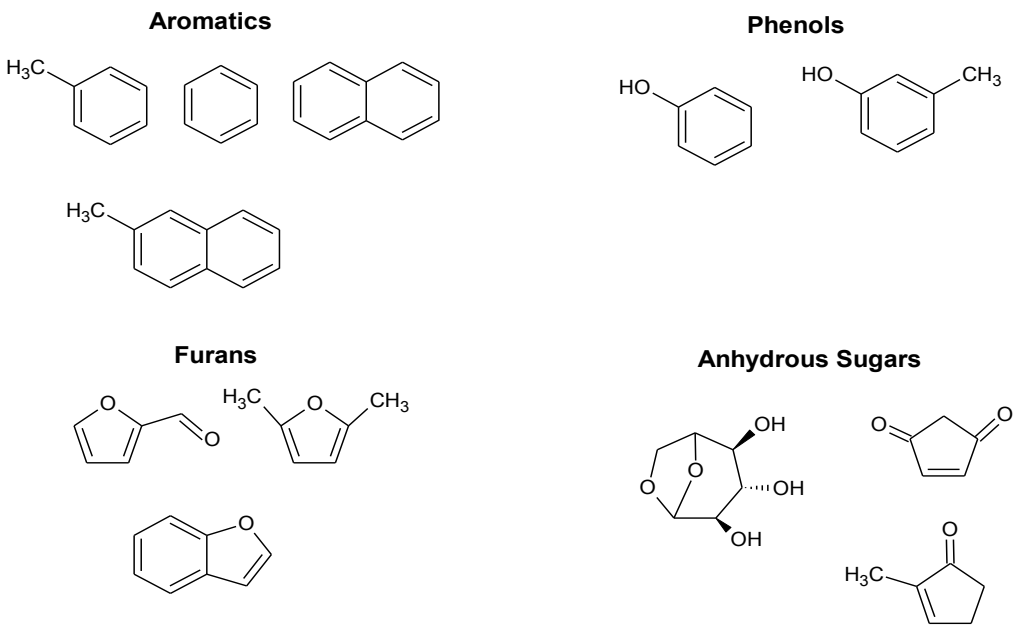

Figure 4.2: Major products of catalytic pyrolysis of raw and torrefied cellulose collected from GC/MS library

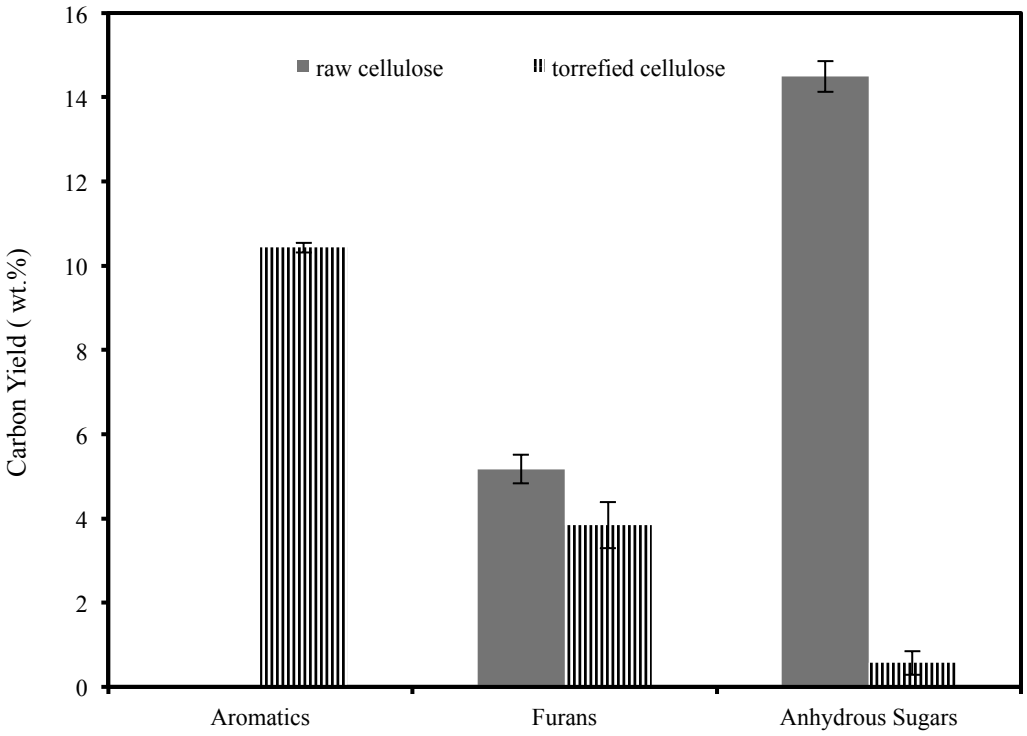

Figure 4.3: Effect of torrefaction on the product distribution from the non-catalytic fast pyrolysis of cellulose at 600°C

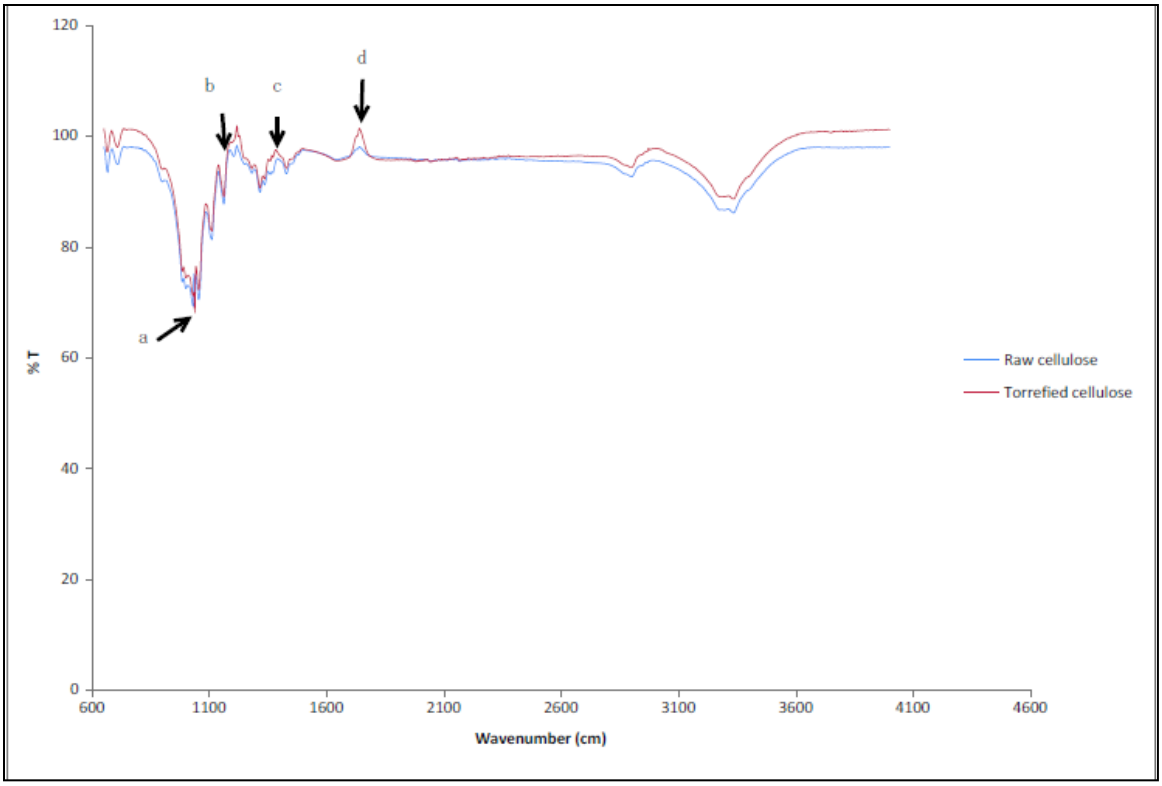

Figure 4.4: FTIR spectra for raw and torrefied cellulose

4.4.3. Catalytic Pyrolysis of Raw and Torrefied Cellulose

The effect of pyrolysis temperature on total carbon yield from the catalytic pyrolysis of raw cellulose with four different acidic zeolites is given in Figure 4.5. It can be observed that there is a substantial increase in total carbon yield initially as the temperature increases from 500˚C to 550˚C, however, after that it either remains constant or shows a slight drop with further increase in temperature from 550˚C to 600˚C. Also, this trend is same for all four zeolite catalyst. Cellulose degrades at around 250-350˚C to produce primarily anhydrous sugars like levoglucosan (Mohan et al., 2006). These compounds in the presence of catalyst can undergo series of reactions to get converted or broken down into several other carbon compounds. Although the reaction temperature

enhances this conversion process, after reaching an optimum temperature, which in our study was found to be 550°C, there will not be any major increase in carbon yield with further raise in temperature and this is clearly evident from our result.

The effect of temperature on total carbon yield from the catalytic pyrolysis of torrefied cellulose (T.C) is given in Figure 4.6. From the figure it can be observed that there is a significant increase in the total carbon yield as temperature increases from 500° to 550°C. Maximum yield (~39.5%) was obtained at 550°C with the use of ZSM-5 catalyst of the highest acidity (SiO_2/Al_2O_3= 30). With further increase in temperature from 550° to 600°C, the carbon yield remains constant when more acidic catalyst (SiO_2/Al_2O_3=30 and 50) were used and showed a sudden drop when low acidic catalyst (SiO_2/Al_2O_3 = 80 and 280) were used. The lowest yield (~ 5.9 %) was produced at 600°C with the use of the least acidic ZSM-5 catalyst (Si/Al_20_3=280). It can also be seen that the catalytic pyrolysis of raw cellulose produced more total carbon yield (~16.94 %) compared to that of torrefied cellulose even with the use of the least acidic ZSM-5 catalyst. Statistical analysis (Tukey's test) was performed to study the significant differences between temperatures and catalyst acidity on the total carbon yield from pyrolysis of raw and torrefied cellulose. From the results it was seen that for pyrolysis of raw cellulose, temperature had a significant effect only when the most acidic zeolite was used and it did not have any significant effect with the use of any other acidic zeolite. When the most acidic zeolite was used, the total carbon yield at high temperatures (550 and 600 °C) was significantly different from the yield at lowest temperature (500 °C). However, no significant difference was seen between the yields at 550 and 600 °C. This observation was the same for torrefied cellulose pyrolysis using the highest acidic zeolite.

In addition to this, when low acidic zeolites (SiO_2/Al_2O_3= 80 or 280) were used, it was observed that the total carbon yield at temperatures 500 and 550 °C was significantly different from the yield at 600 °C for torrefied cellulose pyrolysis. In case of raw cellulose pyrolysis, catalyst acidity had significant effect only at high temperatures (550 and 600 °C). At 550° C, the total carbon yield obtained with the use of the highest acidic zeolite was significantly different from all the other acidic zeolites. Among the total carbon yield obtained using other acidic zeolites, only the yield obtained with the use of zeolite with SiO_2/Al_2O_3= 50 and 80 were not significantly different. However, at 600°C, the total carbon yields obtained from all acidic zeolites were significantly different from one another. This was the same for catalytic pyrolysis of torrefied cellulose. Nonetheless, pyrolysis of torrefied cellulose at 500°C, the total carbon yields obtained using all acidic zeolites were significantly different from each other with an exception of zeolite with SiO_2/Al_2O_3= 50 and SiO_2/Al_2O_3= 80.

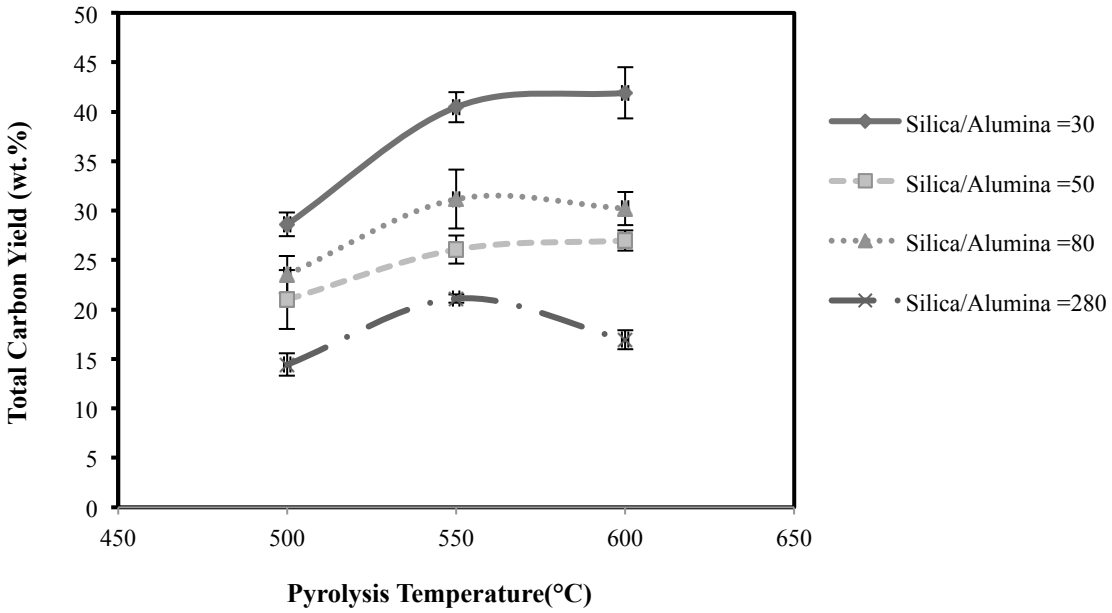

Figure 4.5: Effect of pyrolysis temperature on total carbon yield from the catalytic pyrolysis of raw cellulose with three different acidic zeolites (catalyst to feed ratio – 1:4)

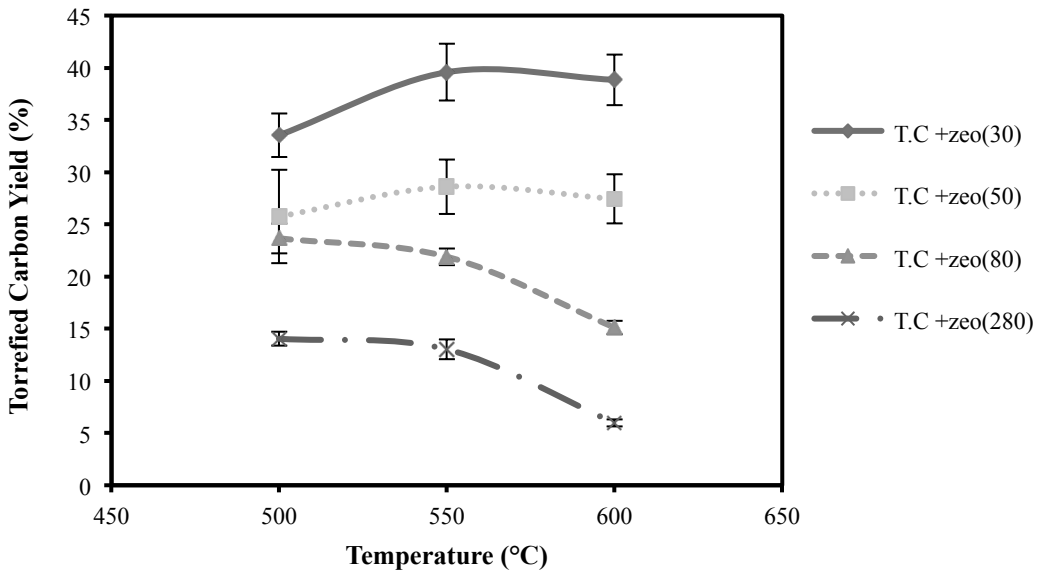

Figure 4.6: Effect of pyrolysis temperature on total carbon yield from catalytic pyrolysis of torrefied cellulose

Figure 4.7 shows the combined effect of pyrolysis temperature and catalyst acidity on the product distribution of catalytic pyrolysis of raw cellulose. Raw cellulose pyrolysis gave predominantly high yield of aromatics (~25 wt.%) with the use of most acidic zeolite (SiO_2/Al_2O_3=30) compared to less acidic zeolites (SiO_2/Al_2O_3= 80, 280). Use of zeolite with SiO_2/Al_20_3=50 also produced more aromatics which accounted for ~ 20 wt% carbon. Also, aromatics yield increased with temperature in all cases (SiO_2/Al_20_3=30, 50, 80 and 280), however, prominent increase was seen only from 500°C to 550°C. Furans and its derivatives were found to be less with the use of the most acidic ZSM-5 catalyst (SiO_2/Al_20_3=30). This could be due to the fact that more acidic catalyst exhibits good cracking ability(Mihalcik et al., 2011). In addition, presence of catalyst helped in minimizing anhydrous sugar yield from pyrolysis of raw cellulose. Results

from Tukey test showed that for raw cellulose pyrolysis, except with the use of most and least acidic zeolites, other two acidic zeolites showed a significant difference on the aromatic yield with temperature. With the use of acidic zeolite of SiO_2/Al_2O_3= 50 and SiO_2/Al_2O_3= 80, the yield at 500°C was significantly different from the yield at 550 and 600 °C. However, no significant difference was observed between the yield at 550 and 600°C. Results from Tukey test for the effect of catalyst acidity on aromatic yield showed that at the lowest temperature, the yield obtained with the use of high acidity zeolite (SiO_2/Al_2O_3= 30 and SiO_2/Al_2O_3= 50) was significantly different from the yield obtained with the use of low acidic zeolite (SiO_2/Al_2O_3= 80 and SiO_2/Al_2O_3= 280). At high temperatures (550 and 600°C), the yields obtained with the use of zeolite with SiO_2/Al_2O_3= 30, SiO_2/Al_2O_3= 50, and SiO_2/Al_2O_3= 80 were significantly different only from the yield obtained with the use of least acidic zeolite.

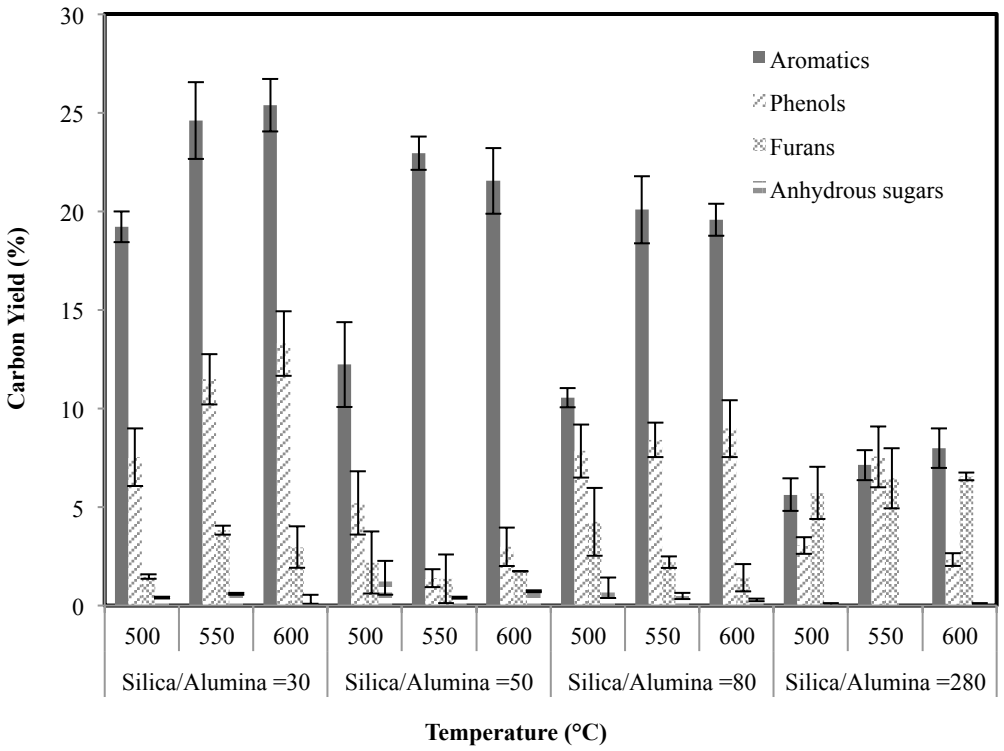

Figure 4.7: Effect of pyrolysis temperature and catalyst acidity on the product distribution from catalytic pyrolysis of raw cellulose

Effect of temperature and catalyst acidity on product distribution from the catalytic pyrolysis of torrefied cellulose is given in Figure 4.8. It can be seen from the figure that both temperature and ZSM-5 acidity had a positive effect on aromatic yield from the catalytic pyrolysis of torrefied cellulose. Aromatics, which included substituted benzene and naphthalene, were produced more at highest temperature and catalyst acidity (maximum yield = 30.91 wt% at 600°C with ZSM-5 (SiO_2/Al_2O_3 = 30)). This yield was substantially more than that produced from the catalytic pyrolysis of raw cellulose (~25 wt%) at the same conditions. However, other groups such as phenols and furans were found relatively more from the catalytic pyrolysis of raw cellulose than torrefied cellulose

at all three temperatures and four ZSM-5 acidity. Hence, it could be interpreted that along with the effect of catalyst acidity, the thermal pre-treatment process also enhances the hydrocarbon production. Results from Tukey's test showed that the use of high acidic zeolite (SiO_2/Al_2O_3= 30 and SiO_2/Al_2O_3= 50) at 500°C resulted in the aromatic yield significantly different from 550 and 600°C, however, the yield at 550 and 600°C is not significantly different from each other. The use of low acidic zeolite (SiO_2/Al_2O_3= 80 and SiO_2/Al_2O_3= 280) at 600°C resulted in aromatic yield significantly different from 500 and 550°C, however, the yield at 500 and 550°C is not significantly different from each other. However, aromatic yield with four acidic zeolites were significantly different from each other at all temperatures.

Although, the results show the torrefaction process promotes the carbon yield from pyrolysis, it should be noted that there is some carbon loss associated with the mass loss during torrefaction process. Hence, taking the carbon loss into account, Figure 4.9 shows the effect of torrefaction on the overall carbon yield from pyrolysis of cellulose. It can be observed that in almost all cases torrefied cellulose resulted in more overall carbon yield. The highest yield (~21%) was found from torrefied cellulose pyrolysis at 550°C with the use the highest acidic zeolite (SiO_2/Al_2O_3= 30) and it was 5% more than raw cellulose pyrolysis.

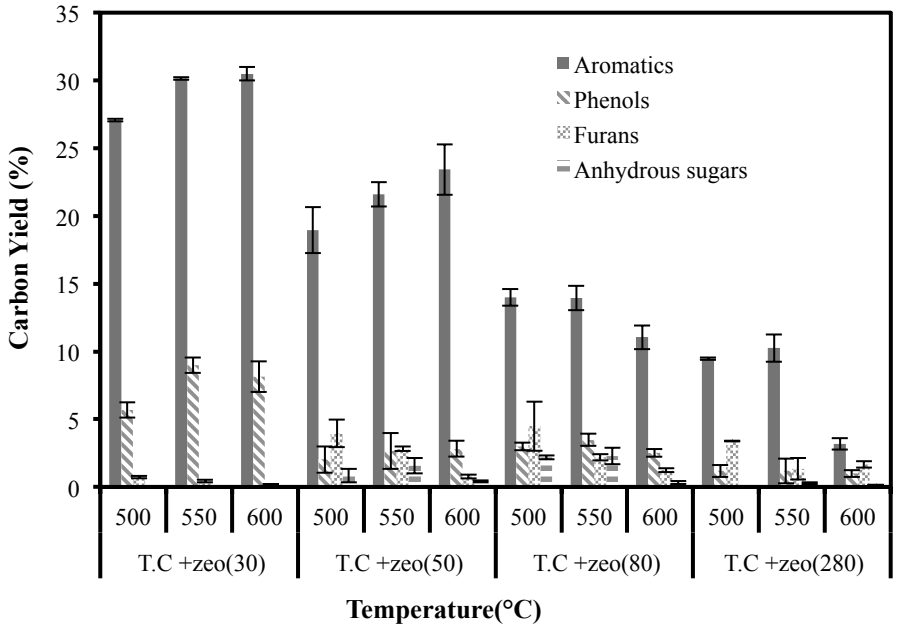

Figure 4.8: Effect of pyrolysis temperature and catalyst acidity on the product distribution from catalytic pyrolysis of torrefied cellulose

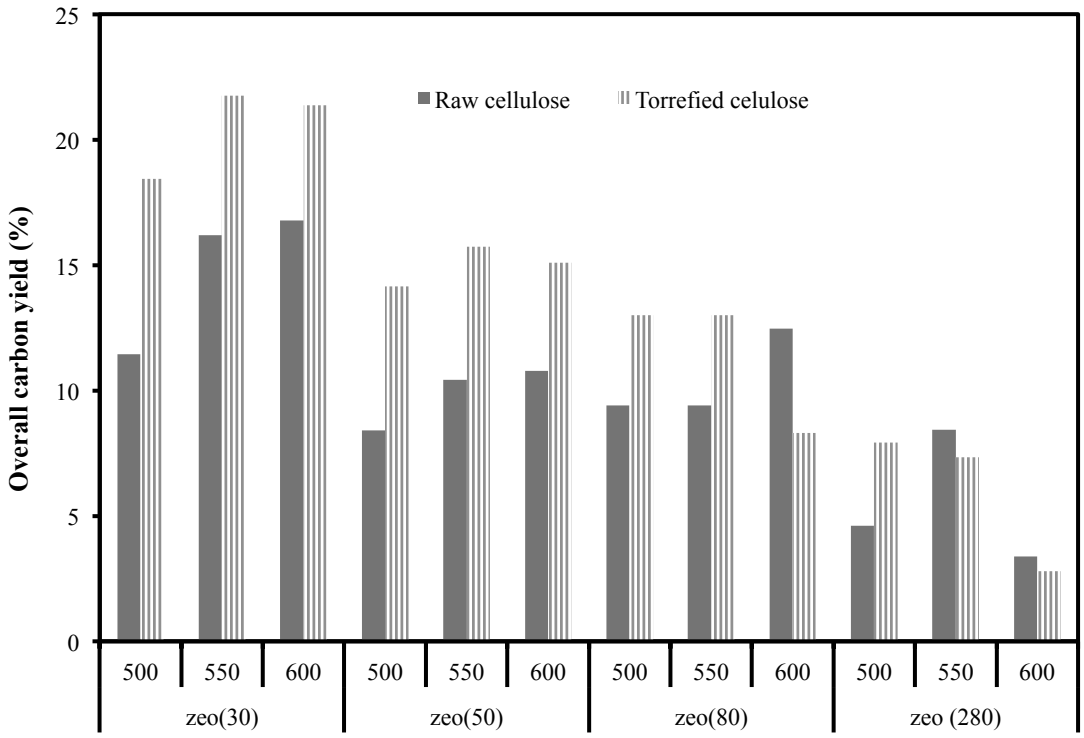

Figure 4.9: Effect of torrefaction on the average overall carbon yield from pyrolysis of cellulose

4.5. Discussion

4.5.1. Catalyst Chemistry and Acidity

Several researchers (Carlson et al., 2009; Carlson et al., 2010; Mihalcik et al., 2011) have proposed various reaction mechanisms on the catalytic conversion of carbohydrates into aromatics or hydrocarbon pool. Mihalcik et al. (Mihalcik et al., 2011) gave a three step pathway for deoxygenation of oxygenated organics – dehydration, decarboxylation and decarbonylation. In addition, the study also concluded that since pyrolysis of cellulose with ZSM-5 resulted in more of CO_2, dehydration and decarboxylation reactions were more active. Carlson et al. (Carlson et al., 2009)

concluded that pyrolysis process involves homogenous thermal decomposition reaction that results in small oxygenates which further undergoes acid catalyzed dehydration, decarboxylation and decarbonylation reactions to form olefins which later combines to produce aromatics. In another study of Huber and his co-workers (Carlson et al., 2010), a two-step mechanism for catalytic fast pyrolysis of glucose was proposed. In the first step glucose is decomposed into small oxygenates (mainly anhydrous sugars) through retro-aldol, grob fragmentation and dehydration reactions followed by the conversion of dehydrated products to aromatics in the catalyst pore in the second step. Results from our current study also show that primary product from non-catalytic pyrolysis of raw cellulose is levoglucosan and this anhydrous sugar is completely eliminated when catalyst is used. Hence, catalyst provides a platform for selectively converting the anhydrous sugars into aromatic hydrocarbons. Also, the products from catalytic pyrolysis of cellulose show that aromatics yield increases as the catalyst acidity decreases. Maximum yield (~25%) was found with the use of catalyst having highest acidity (SiO_2/Al_2O_3=30) at 600°C. Therefore, it could be concluded that high catalyst acidity or low SiO_2/Al_2O_3 ratio increases the ability of catalyst to perform cracking reactions in case of raw cellulose pyrolysis. An overall mechanism that can be drawn from all the above mechanisms and our results is that pyrolysis of raw cellulose results in small oxygenates – primarily levoglucosan and few furans. Presence of catalyst enables the selective elimination or conversion of these oxygenates into aromatics through dehydration, decarboxylation and decarbonylation reactions. Although, several studies have been carried out for catalytic pyrolysis of raw cellulose, no research work has reported the effect of catalyst chemistry on torrefied cellulose pyrolysis.

4.5.2. Reaction Mechanism

Figure 4.10 shows the reaction mechanism for the pyrolysis of raw and torrefied cellulose. The reaction mechanism of raw cellulose shown in Figure 4.10 is documented elsewhere (Lu et al., 2011) According to Lu et al. (Lu et al., 2011) during pyrolysis of raw cellulose the glycosidic bonds, which forms the backbone of cellulose weakens resulting in several reducing sugars. Anhydrous sugar mainly levoglucosan is formed through a series of protonation and deprotonation reactions. A reaction mechanism for pyrolysis of torrefied cellulose was proposed based on our observation. As previously discussed, more aromatics and very less anhydrous sugars were produced from pyrolysis of torrefied cellulose. This indicated that torrefaction could cause changes in cellulose structure. From the FTIR study, it was concluded that torrefaction results in weakening of several bonds such as C-O-C, C-O-H and CH_2-OH. Therefore, it can be hypothesized that during torrefaction, certain bonds in the cellulose weakens along with glycosidic bond breakage that results in an open chain structure. However, these open chain structures might be created during pyrolysis as well. Torrefaction changes cellulose structure (depolymerization, decrystalization, condensation) and it is possible that these changes in torrefaction could push "ring-opening" during pyrolysis, comparing to the pyrolysis with non-torrefied cellulose. During pyrolysis, the open chain structure undergoes several dehydration, decarbonylation and aromatization reactions to form oelifind, BTX (benzene, toluene and xylene) and furans as primary products.

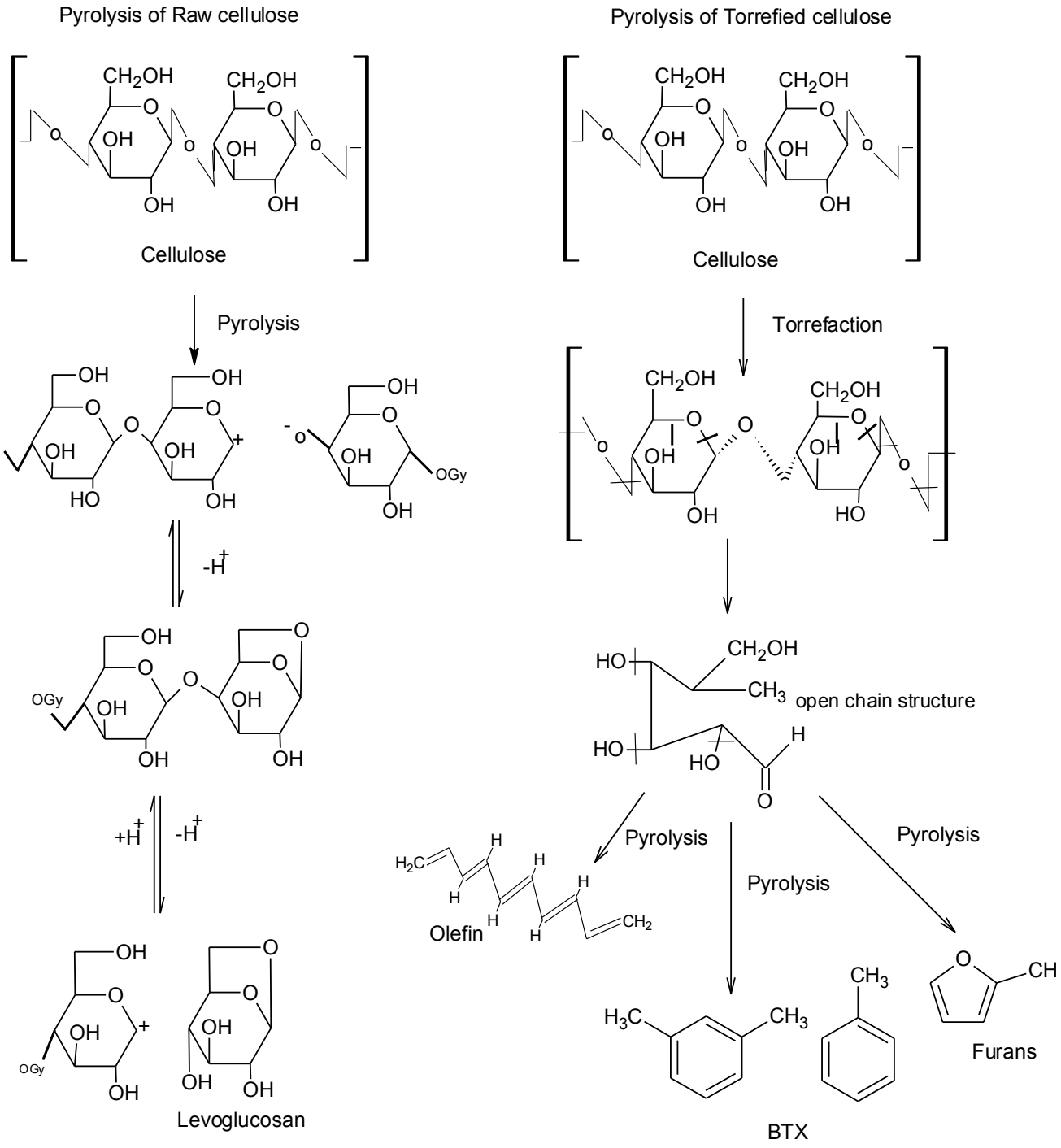

Figure 4.10: Proposed reaction mechanism for non catalytic pyrolysis of raw and torrefied cellulose

4.6. Conclusion

Catalytic fast pyrolysis was carried out on raw and torrefied cellulose with zeolite catalyst of varying acidity. It was concluded from the results that catalyst acidity, pyrolysis temperature and torrefaction enhanced the production of aromatics from fast pyrolysis of cellulose. It was observed that anhydrous sugars (levoglucosan) which accounted for ~14 wt% from the pyrolysis of raw cellulose were found very minimal from the pyrolysis of torrefied cellulose. Similarly, aromatics was ~ 10 wt.% from pyrolysis of torrefied cellulose while it was completely absent from pyrolysis of raw cellulose which indicated that torrefaction resulted in several significant structural changes in cellulose. From FTIR study, it was hypothesized that as a result of torrefaction, certain bonds in cellulose weakens resulting in an open chain structure which undergoes dehydration, decarbonylation and aromatization reactions to produce aromatics as primary products. Results from catalytic pyrolysis of raw and torrefied cellulose showed that catalyst acidity played a pivotal role in eliminating oxygenates and promoting the aromatic production. Maximum yield of aromatics was obtained when ZSM-5 with highest acidity (SiO_2/Al_2O_3=30) was used for both torrefied and raw cellulose. For catalytic pyrolysis of torrefied and raw cellulose, the total carbon yield increased with increase in temperature until 550°C after which it either remained constant or showed a slight drop. A reaction mechanism was proposed for torrefied cellulose pyrolysis. Production of aromatics from pyrolysis of torrefied cellulose indicated that torrefaction caused several significant structural changes in cellulose. It was concluded that as a result of torrefaction, certain bonds in cellulose weakens resulting in an open

chain structure which undergoes dehydration, decarbonylation and aromatization reactions to produce aromatics as primary products.

4.7. References

Adjaye, J.D., Bakhshi, N.N. 1995. Production of hydrocarbons by catalytic upgrading of a fast pyrolysis bio-oil. Part II: Comparative catalyst performance and reaction pathways. *Fuel Processing Technology*, **45**(3), 185-202.

Antal, M.J., Jr., Varhegyi, G. 1995. Cellulose Pyrolysis Kinetics: The Current State of Knowledge. *Industrial & Engineering Chemistry Research*, **34**(3), 703-717.

Bradbury, A.G.W., Sakai, Y., Shafizadeh, F. 1979. A kinetic model for pyrolysis of cellulose. *Journal of Applied Polymer Science*, **23**(11), 3271-3280.

Bridgwater, A.V. 1999. Principles and practice of biomass fast pyrolysis processes for liquids. *Journal of Analytical and Applied Pyrolysis*, **51**(1–2), 3-22.

Carlson, T., Tompsett, G., Conner, W., Huber, G. 2009. Aromatic Production from Catalytic Fast Pyrolysis of Biomass-Derived Feedstocks. *Topics in Catalysis*, **52**(3), 241-252.

Carlson, T.R., Jae, J., Lin, Y.-C., Tompsett, G.A., Huber, G.W. 2010. Catalytic fast pyrolysis of glucose with HZSM-5: The combined homogeneous and heterogeneous reactions. *Journal of Catalysis*, **270**(1), 110-124.

EIA. 2013. Annual Energy Outlook.

Liaw, S.-S., Zhou, S., Wu, H., Garcia-Perez, M. 2013. Effect of pretreatment temperature on the yield and properties of bio-oils obtained from the auger pyrolysis of Douglas fir wood. *Fuel*, **103**(0), 672-682.

Lu, Q., Li, W.-Z., Zhu, X.-F. 2009. Overview of fuel properties of biomass fast pyrolysis oils. *Energy Conversion and Management*, **50**(5), 1376-1383.

Lu, Q., Yang, X.-c., Dong, C.-q., Zhang, Z.-f., Zhang, X.-m., Zhu, X.-f. 2011. Influence of pyrolysis temperature and time on the cellulose fast pyrolysis products: Analytical Py-GC/MS study. *Journal of Analytical and Applied Pyrolysis*, **92**(2), 430-438.

Mihalcik, D.J., Mullen, C.A., Boateng, A.A. 2011. Screening acidic zeolites for catalytic fast pyrolysis of biomass and its components. *Journal of Analytical and Applied Pyrolysis*, **92**(1), 224-232.

Mohan, D., Pittman, C.U., Steele, P.H. 2006. Pyrolysis of Wood/Biomass for Bio-oil: A Critical Review. *Energy & Fuels*, **20**(3), 848-889.

Park, J., Meng, J., Lim, K.H., Rojas, O.J., Park, S. 2013. Transformation of lignocellulosic biomass during torrefaction. *Journal of Analytical and Applied Pyrolysis*, **100**(0), 199-206.

Phanphanich, M., Mani, S. 2011. Impact of torrefaction on the grindability and fuel characteristics of forest biomass. *Bioresource Technology*, **102**(2), 1246-1253.

Piskorz, J., Radlein, D., Scott, D.S. 1986. On the mechanism of the rapid pyrolysis of cellulose. *Journal of Analytical and Applied Pyrolysis*, **9**(2), 121-137.

Prins, M.J., Ptasinski, K.J., Janssen, F.J.J.G. 2006. Torrefaction of wood: Part 2. Analysis of products. *Journal of Analytical and Applied Pyrolysis*, **77**(1), 35-40.

Raveendran, K., Ganesh, A., Khilar, K.C. 1996. Pyrolysis characteristics of biomass and biomass components. *Fuel*, **75**(8), 987-998.

Sharma, R.K., Bakhshi, N.N. 1993. Catalytic upgrading of pyrolysis oil. *Energy & Fuels*, **7**(2), 306-314.

Shen, J., Wang, X.-S., Garcia-Perez, M., Mourant, D., Rhodes, M.J., Li, C.-Z. 2009. Effects of particle size on the fast pyrolysis of oil mallee woody biomass. *Fuel*, **88**(10), 1810-1817.

Soares, S., Ricardo, N.M.P.S., Jones, S., Heatley, F. 2001. High temperature thermal degradation of cellulose in air studied using FTIR and 1H and 13C solid-state NMR. *European Polymer Journal*, **37**(4), 737-745.

Tillman, D.A. 2000. Biomass cofiring: the technology, the experience, the combustion consequences. *Biomass and Bioenergy*, **19**(6), 365-384.

Tjeerdsma, B., Boonstra, M., Pizzi, A., Tekely, P., Militz, H. 1998. Characterisation of thermally modified wood: molecular reasons for wood performance improvement. *European Journal of Wood and Wood Products*, **56**(3), 149-153.

van der Stelt, M.J.C., Gerhauser, H., Kiel, J.H.A., Ptasinski, K.J. 2011. Biomass upgrading by torrefaction for the production of biofuels: A review. *Biomass and Bioenergy*, **35**(9), 3748-3762.

Via, B.K., Adhikari, S., Taylor, S. 2013. Modeling for proximate analysis and heating value of torrefied biomass with vibration spectroscopy. *Bioresource Technology*, **133**(0), 1-8.

Yang, H., Yan, R., Chen, H., Lee, D.H., Zheng, C. 2007. Characteristics of hemicellulose, cellulose and lignin pyrolysis. *Fuel*, **86**(12–13), 1781-1788.

Zhang, Q., Chang, J., Wang, T., Xu, Y. 2007. Review of biomass pyrolysis oil properties and upgrading research. *Energy Conversion and Management*, **48**(1), 87-92.

Zwart, R.W.R., Boerrigter, H., van der Drift, A. 2006. The Impact of Biomass Pretreatment on the Feasibility of Overseas Biomass Conversion to Fischer−Tropsch Products. *Energy & Fuels*, **20**(5), 2192-2197.

Chapter 5- Catalytic Pyrolysis of Raw and Thermally Treated Lignin using Different Acidic Zeolites

5.1. Abstract

In this study, the effect of three pyrolysis temperatures (500, 550 and 600°C) and shape selective zeolite catalyst with varying acidity on aromatic hydrocarbon yield from pyrolysis of raw and torrefied lignin was analyzed. Catalyst acidity was found to be highly favorable for aromatic hydrocarbon production in the case of raw and torrefied lignin pyrolysis. High aromatic hydrocarbon yield (~27 wt.% C) was produced from pyrolysis of torrefied lignin with the most acidic zeolite catalyst (SiO_2/Al_2O_3= 30) at 600°C. With the use of the most acidic zeolite catalyst (SiO_2/Al_2O_3 = 30) at the highest pyroprobe temperature (600°C), total carbon yield from catalytic pyrolysis of torrefied lignin was 1.2 times the yield from catalytic pyrolysis of raw lignin. A Fourier transform infrared spectroscopy study showed that torrefied lignin had more condensed guaiacyl lignin linkages which could be the primary reason for the relatively higher aromatic yield.

5.2. Introduction

Increasing energy demand along with dwindling fossil fuel reservoirs has necessitated the use of renewable energy as an alternate energy source. Among

renewable energy sources, biomass has been a promising source for clean transportation energy, and fast pyrolysis has been recognized as an efficient way to produce a high yield of liquid product known as bio-oil (Bridgwater, 1999). Biomass is a carbon based material and is composed of organic molecules containing hydrogen, oxygen, nitrogen, and inorganics such as alkali and alkaline earth minerals. Typical composition of biomass is carbon (~50 wt. %), hydrogen (~5 wt.%), and oxygen (~40 wt.%)
(Vassilev et al., 2010). Conventional fuels such as gasoline and diesel are long chain hydrocarbon molecules that lack oxygen. Hence, in order to make fuels produced from biomass compatible with these hydrocarbon fuels, it is necessary to deoxygenate fuel or its source (biomass). A number of studies have focused on two main upgrading techniques: hydrodeoxygenation and catalytic pyrolysis for deoxygenating bio-oil (Branca et al., 2012; French & Czernik, 2010; Lu et al., 2010; Mante et al., 2013). Past studies evaluated the effect of catalyst properties such as type, pore size, acidity, and biomass to catalyst ratio on product yield and distribution (Carlson et al., 2008; Jeon et al., 2013; Joshi & Lawal, 2012; Mihalcik et al., 2011; Mochizuki et al., 2013; Widyaningrum et al., 2012). In addition to these upgrading techniques, which enhance the deoxygenation of bio-oil, a pre-treatment process known as torrefaction is gaining a lot of attention since it focuses on eliminating oxygen from biomass itself before it is thermally converted. During torrefaction, biomass is heated at 200-300°C in an inert environment. As a result of this thermal pre-treatment, oxygen content is reduced in the biomass by selective decomposition of hemicellulose. Also, water molecule present in the biomass is also removed during torrefaction making it hydrophobic. Many researchers have studied the effect of torrefaction parameters such as torrefaction temperature and

residence time on the product composition from the pyrolysis process (Boateng & Mullen, 2013; Meng et al., 2012; Ren et al., 2013; Zheng et al., 2012; Zheng et al., 2013). However, very limited studies have focused on the effect of torrefaction on individual biomass constituent pyrolysis.

The three main constituents of biomass are cellulose, lignin and hemicellulose. Lignin is the second-most abundant component in lignocellulosic biomass. It is formed by the polymerization of three-p-hydroxycinnamyl alcohol precursors: p-coumaryl, coniferyl and sinnapyl alcohol. This polymerization results in three types of lignin units: p-hydroxyl phenyl, guaiacyl, and syringyl lignin (Caballero et al., 1996). Various techniques have been developed to extract lignin from biomass; namely, steam explosion, Kraft pulping, and addition of chemicals, organosolvents, and enzymes. However, among these, the lignin separated through organosolv pulping is most attractive as the process uses sulfur free chemicals (de Wild et al., 2012). The structure of lignin is complicated with five different linkages: β-O-4, α-O-4, 5-5, β-5 and β-β linkage. Its structure remains complicated even after torrefaction process as it decomposes at a very high temperature compared to cellulose and hemicellulose. Effect of torrefaction on biomass structure is documented elsewhere (Ibrahim et al.; Via et al., 2013). Therefore, the objective of this work was to study the effect of torrefaction, catalyst acidity, and temperature on pyrolysis behavior of lignin.

5.3. Experimental Setup

5.3.1. Lignin Torrefaction

The pure organosolv lignin with a geometric mean diameter of 76.12 μm used in this study was obtained from Lignol Energy Corp (Burnaby, Canada). It was then thermally

pre-treated (torrefied) at 225˚C for 30 minutes in a furnace (Thermo Scientific model TF55035A-1). A fixed bed reactor setup was used for this purpose. The reactor was made of stainless steel and was 18 in long, 0.5 in OD, and 0.35 in ID. About 10 g of raw lignin was taken for torrefaction, and the weight of torrefied lignin was measured after the pre-treatment process. Helium gas with ~ 20 mL/min flow rate was used as purge gas to remove the vapors formed during the reaction. The carrier gas and vapors generated during torrefaction were vented out in the fume hood. Chemical characterization was done for both raw and torrefied lignin samples using a CHNS analyzer (Perkin-Elmer, model CHNS/O 2400) to measure carbon, hydrogen, nitrogen, and sulfur contents. An FTIR analysis to study the structure of raw and torrefied lignin was done using a PerkinElmer Spectrum model 400 (Perkin Elmer Co., Waltham, MA). For each sample, the spectrum was collected within 10s by applying a vertical load on the sample. All scans were done at room temperature, which was ~22°C. Physical characterization, which included moisture content and ash content, was determined for both the samples using ASTM E871, E1775 respectively. Higher heating value for raw and torrefied lignin was measured using an oxygen bomb calorimeter (IKA, model C 200).

5.3.2. Fast Pyrolysis

Fast pyrolysis experiments were carried out using a commercial pyrolyzer (CDS Analytical Inc., model 5200). A Probe had a heating filament, which held the sample in a quartz tube and the heating rate on the heating filament was computer controlled. The reactant mixture (catalyst and lignin) was packed between quartz wool in a quartz tube (25 mm long with 1.9 mm ID). Catalytic fast pyrolysis was carried out at three different temperatures (500, 550, and 600 °C) with zeolite catalyst having different acidities

(SiO_2/Al_2O_3 – 30, 50, 80 and 280) for both torrefied and raw lignin. The catalyst to feed ratio was 1:4 and was constant for all the experiments. The temperature specified for the pyroprobe experiment is the filament temperature, but the actual sample temperature in a pyroprobe is about 100−125 °C lower than the filament temperature. Four types of ZSM-5 (Zeolyst, Inc.) were received in ammonium cation form and were calcined in air at 550 °C for 2 h in a furnace for conversion into H^+ZSM prior to use. Mean particle size, silica to alumina ratio, and surface area of the four zeolites are given in Table 5.1. Each zeolite catalyst was physically mixed with raw and torrefied lignin samples in a 1:4 ratio. The biomass heating rate was kept constant at 2000 °C/s throughout the study. The heating rate reported here is the filament-heating rate and the actual biomass-heating rate was found to be around 50°C/s (Thangalazhy-Gopakumar et al., 2011). Helium gas was used as the inert pyrolysis gas as well as the carrier gas for the GC/MS system. A known amount (approximately 1-3 mg) of reactant mixture was taken for each run. The vapor from pyrolysis was carried to a trap maintained at 40°C. The condensable vapor was adsorbed in the trap, and the noncondensable vapor was purged using the same He gas. The adsorbed gas was then desorbed by heating the trap to 300°C, and carried to GC/MS for analysis using ultrahigh purity (99.999%) He supplied from Airgas, Inc. The vapor transfer line from pyroprobe to GC/MS was maintained at 300°C. Bio-oil compounds were analyzed with an Agilent 7890 GC/5975 MS using a DB 1701 column. The GC front inlet temperature was kept at 250°C, and the GC oven was programmed with the following temperature regime: hold at 40 °C for 2 min, heat to 250°C at 5 °C/min, and hold at 250°C for 8 min. A split ratio of 50:1 was set for injection, and the gas flow rate was maintained at 1.25 mL/min. Compounds were identified using NIST (National

Institute of Standards and Technology) mass spectral library. Compounds that appeared consistently with high probability were selected and quantified. Quantification was done by injecting calibration standards into the GC/MS system. The slope of the calibration line was taken as the quantification factor in the calculation. Experiments were carried out in triplicates, and the average values are reported. The results are reported as carbon yield, which is calculated using Equation 5.1. In the case of torrefied biomass, it is the weight of torrefied biomass and carbon fraction of the torrefied biomass. The overall carbon yield takes into account carbon lost during torrefaction as well.

$$Carbon\ yield\ (wt.\%) = \frac{Weight\ of\ each\ compound \times mass\ fraction\ of\ carbon\ in\ each\ compound}{Weight\ of\ biomass \times mass\ fraction\ of\ carbon\ in\ biomass} \times 100 \text{--Equation 5.1}$$

Table 5.1: Properties of different acidic zeolites

Silica to alumina ratio	Mean particle size (μm)	Surface area (m^2/g)
30	81.14	400
50	87.32	425
80	87.58	425
280	89.16	400

5.4. Results and Discussion

5.4.1 Effect of Torrefaction: Mass and Ultimate Analyses

Effect of torrefaction on mass retained, and carbon, hydrogen, and oxygen composition of lignin (dry basis) is shown in Figure 5.1. It can be seen that about 90% of mass is retained as a result of the torrefaction process. This 10% mass loss could be due to a few volatiles - mainly oxygenates - during torrefaction. It can also be noted that almost 95 % of energy in lignin is retained after the torrefaction process. Also, from the elemental composition, it was found that torrefaction did not cause any prominent

increase in the percentage composition of carbon. This explains that torrefaction does not have a predominant effect on the elemental composition of lignin, as the decomposition rate of lignin is very low below 300°C. Ash content measured was 0.305 ± 0.06 (%) and 0.9 ± 0.14 (%) for raw and torrefied lignin.

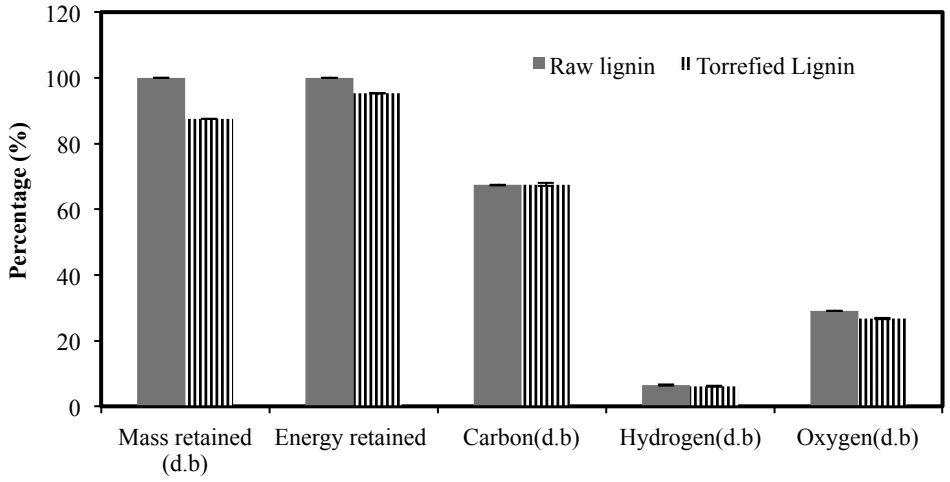

Figure 5.1: Effect of torrefaction on the mass, carbon, hydrogen and oxygen content of lignin

5.4.2. Non-Catalytic Pyrolysis of Raw and Torrefied Lignin

Products from GC/MS library were grouped into three main groups; namely, aromatics (aromatic hydrocarbons), phenols, and guaiacols. Major compounds in each group are given in Table 5.1. Product distribution from non-catalytic pyrolysis of raw and torrefied lignin at 600°C is shown in Figure 5.2.

Results are reported as carbon yield, which is calculated using equation 5.1. Aromatic hydrocarbons, major compound for our study, were found to be produced from pyrolysis of both raw and torrefied lignin. However, their yield was greater from pyrolysis of

torrefied lignin. Another interesting observation was that the primary product from pyrolysis of raw lignin was guaiacols, and they were found to be comparatively minimal from pyrolysis of torrefied lignin. Also, the major product from pyrolysis of torrefied lignin was phenols, which were relatively lower in the pyrolysis of raw lignin. This indicated that torrefaction could result in possible structural changes in lignin that could be the reason behind lower guaiacols and higher phenols in the pyrolysis product.

Table 5.2: Major Compounds reported from GC/MS library

Aromatics	**Phenols**	**Guaiacols**
Benzene	Phenols	Phenol -2-methoxy-4-methyl
Toluene	Phenol-2-methyl	Phenol-2-methoxy
Xylene	Phenol-4-methyl	Phenol -2-methoxy-4-ethyl
Styrene	Phenol 2,3-dimethyl	
Indane		
Indene		
2-Methyl Indene		
Naphthalene		
Naphthalene-1-methyl		
Naphthalene-2,6-dimethyl		

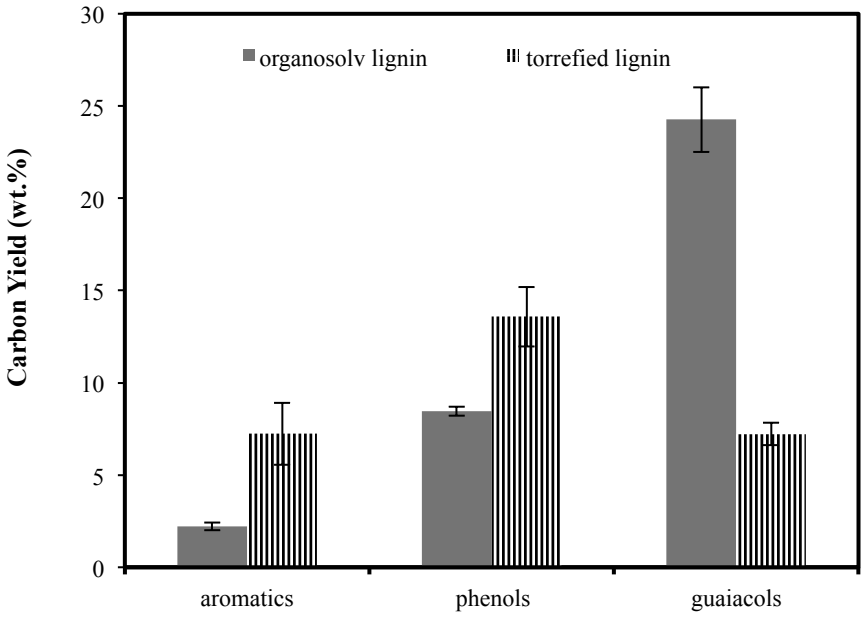

Figure 5.2: Product distribution from non-catalytic pyrolysis of raw and torrefied lignin at 600°C

5.4.3. FTIR Study

To study structural changes in lignin during torrefaction, an FTIR study was done for both raw and torrefied lignin, and the following structural signals were found (Figure 5.3): conjugated C-O bonds (~1600 cm^{-1}), existence of C-O or C-H group (1050 and 1440 cm^{-1}), aromatic and aliphatic hydroxyl group (3000 and 1060 cm^{-1}), C-H due to aromatic structure (900 cm^{-1}) (Alriols et al., 2010; El Hage et al., 2009)

It can be seen that the spectral profiles and intensities of the bands were quite similar for both the samples, which indicates that the core lignin structure did not change much during the torrefaction process. However, certain significant differences were found between torrefied and raw lignin as given below. This was in correspondence with the results reported by Nakano and Meshitsuka (Nakano & Meshitsuka, 1992).

1. Band at 1275 cm^{-1} (“a” in figure) corresponds to aromatic skeletal vibration along with C-O stretched. This band is stronger for torrefied lignin, indicating that the thermal pre-treatment increases the aromatic fraction
2. Band at 1660 cm^{-1} (“b” in figure) indicates that torrefied lignin had relatively more condensed guaiacyl unit than etherified ones. Hence, as a result of torrefaction, the ether bonds, which correspond to the β-O-4 linkage, are cleaved and condensation of lignin happens by linking carbon directly through 5-5 linkages. This is supported by the compositional data from pyrolysis of torrefied lignin where the product from pyrolysis resulted in minimal guaiacols and more phenols.

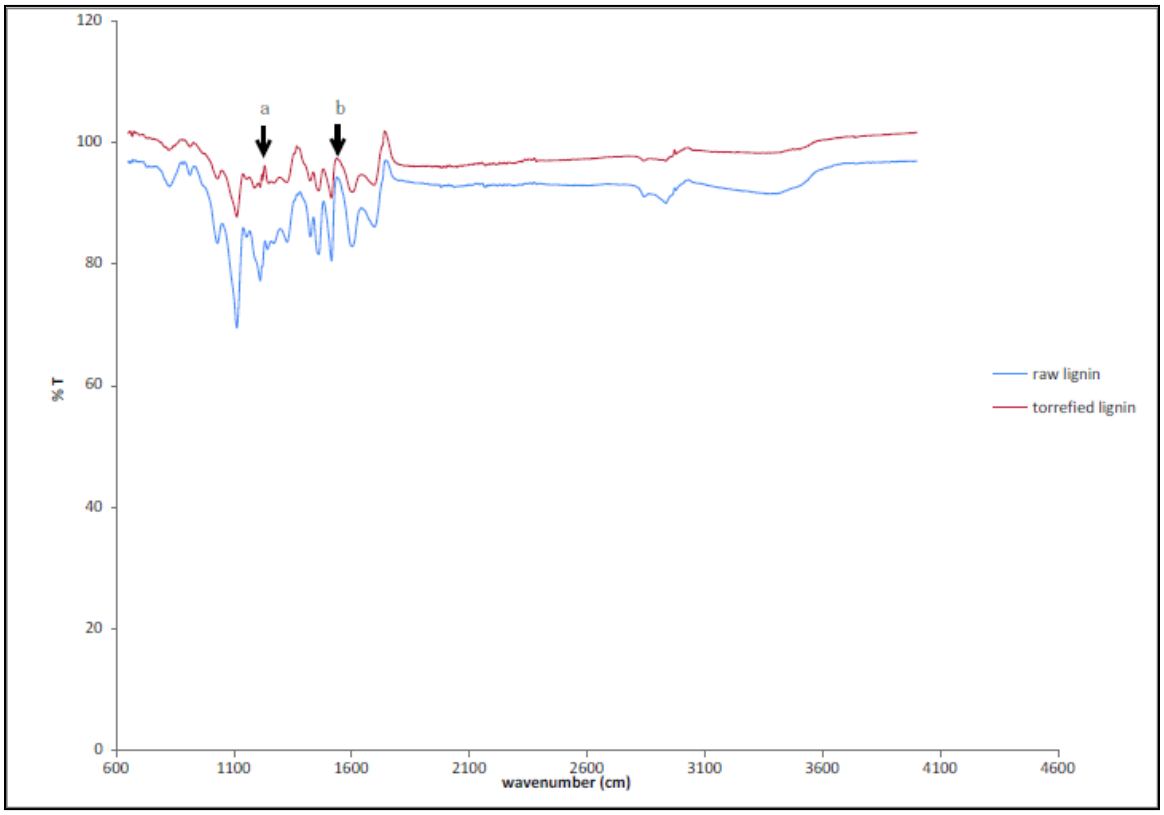

Figure 5.3: FTIR spectra of raw and torrefied organosolv lignin

5.4.4. Catalytic Pyrolysis

5.4.4a Raw Lignin: Effect of pyrolysis Temperature and Catalyst Acidity

The effect of temperature on total carbon yield from the pyrolysis of raw lignin (RL) with zeolite catalyst of different acidity is shown in Figure 5.4. It can be seen that the total carbon yield, which was the sum of carbon yields from aromatics, phenols and guaiacols, increased with pyrolysis temperature. However, this increase was predominant only when the pyrolysis temperature was increased from 500 to 550°C, after which the total carbon yield showed a slight increase when a high acidity catalyst (SiO_2/Al_2O_3= 30 and 50) was used and remained constant when a low acidity catalyst (SiO_2/Al_2O_3 =80) was used. A statistical test (Tukey's test) was performed to understand whether or not there are any significant differences (significance level (ά) = 0.05) on the mean value of total carbon yield with the use of catalyst with varying acidity and pyrolysis temperature. From the results, it was found that the total carbon yield from catalytic pyrolysis of raw lignin using the most acidic zeolite (SiO_2/Al_2O_3= 30) is significantly different than the other acidic zeolites (SiO_2/Al_2O_3= 50,80,280) at all three pyrolysis temperatures. However, it was also observed that the total carbon yield obtained with the use of less acidic zeolites (SiO_2/Al_2O_3= 80 and 280) are not significantly different from each other. Surprisingly, it was observed that pyrolysis temperature did not play any significant role on the total carbon yield. Effect of catalyst acidity and temperature on the product distribution from catalytic pyrolysis of raw lignin is shown in Figure 5.5. Presence of catalyst resulted in a significant amount of aromatic hydrocarbons from pyrolysis of raw lignin. Moreover, it also enhanced the decrease in guaiacols production, which was the primary product from the non-catalytic pyrolysis of raw lignin. This indicated that the presence of the catalyst promoted the direct deoxygenation of methoxy phenols to

aromatic hydrocarbons. Also, during pyrolysis of lignin, intense depolymerization of aliphatic linkers takes place resulting in the production of olefins, which can be converted to aromatic hydrocarbons through aromatization reaction (Mullen & Boateng, 2010). It can also be observed that as catalyst acidity increases, the production of aromatic hydrocarbons also increases. This trend was the same at all three pyrolysis temperatures. Statistical analysis (Tukey's test) results indicated that the use of more acidic zeolites (SiO_2/Al_2O_3= 30 and 50) did not have any significant difference between themselves, but they were significantly different from aromatics produced using less acidic zeolites (SiO_2/Al_2O_3= 80 and 280) at all pyrolysis temperatures except 600°C. At the highest pyrolysis temperature (600°C), aromatic yields obtained with the use of zeolites of SiO_2/Al_2O_3= 50 and 80 were not significantly different. From Figure 5.5 it can also be observed that when a low acidity catalyst was used (SiO_2/Al_2O_3= 80 and 280), aromatic hydrocarbons showed an increase with pyrolysis temperature until 550°C, after which a further increase in temperature to 600°C resulted in a drop in the carbon yield from aromatic hydrocarbons. However, when a high acidity catalyst was used (SiO_2/Al_2O_3= 30 and 50), aromatic hydrocarbons increased with increase in temperature. At low temperatures, guaiacols were found only with the use of low acidic zeolite catalyst (SiO_2/Al_2O_3 =80 and 280). This indicates that ZSM-5 with a relatively higher acidity is more efficient in cleaving methoxy group and aromatic C-O bonds in the lignin polymer. Interestingly, phenols were found to be predominant with the use of the least acidic catalyst (SiO_2/Al_2O_3= 280). Among phenolic compounds, dimethyl phenol showed an increase when the least acidic zeolite was used. Similar to the total carbon yield,

statistical analysis indicated that pyrolysis temperature did not play any significant role in enhancing promoting aromatic yield.

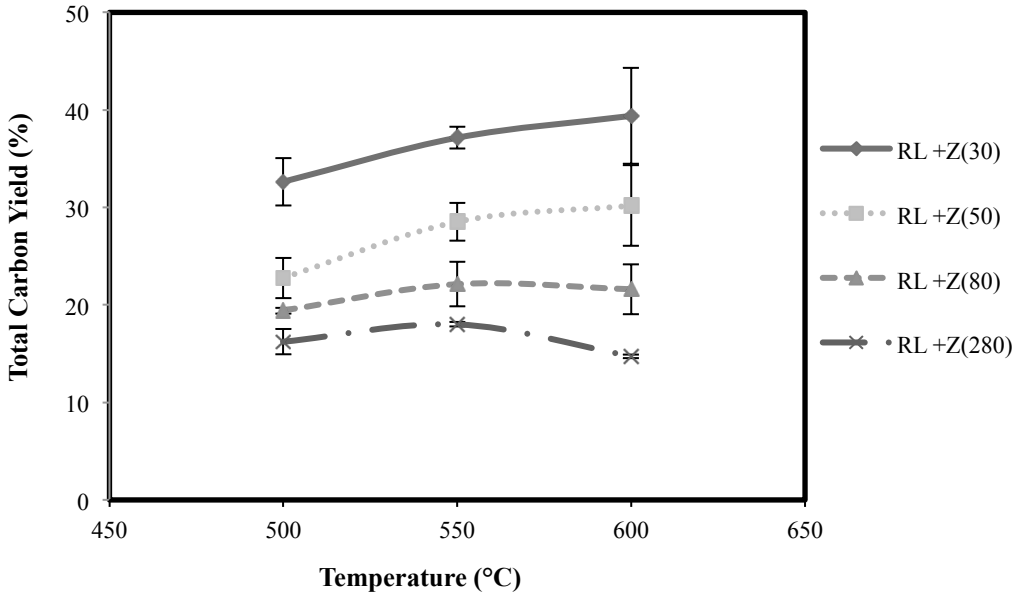

Figure 5.4: Effect of temperature on the carbon yield from catalytic pyrolysis of raw lignin with 1:4 biomass to catalyst ratio

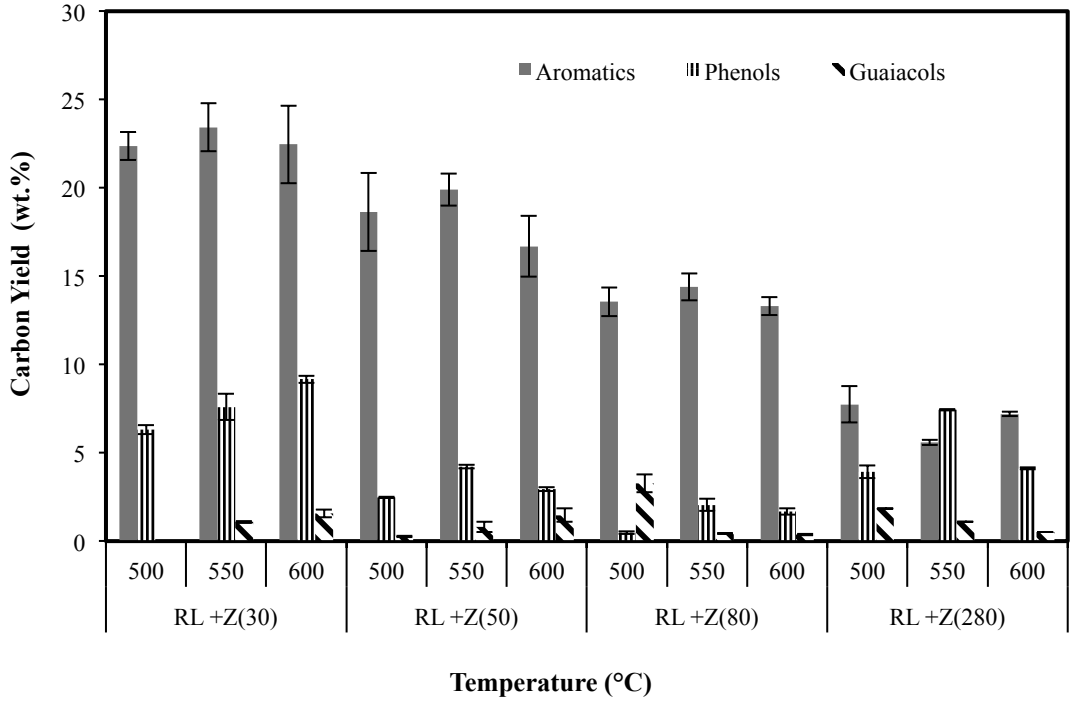

Figure 5.5: Effect of catalyst acidity and pyrolysis temperature on the product distribution of raw lignin pyrolysis

5.4.4b. Torrefied Lignin: Effect of Temperature and Catalyst Acidity

The effect of torrefaction on the total carbon yield from catalytic pyrolysis of torrefied lignin (TL) with zeolite catalyst with varying acidity is shown in Figure 5.6. The total carbon yield increased with increase in temperature only with the use of the most acidic zeolite (SiO_2/Al_2O_3= 30). When low acidity zeolites (SiO_2/Al_2O_3= 80 and 280) were used, the total carbon yield showed an initial drop with increase in temperature from 500 to 550°C. A further increase in temperature from 550 to 600°C showed an increase in the total carbon yield. From statistical analysis (Tukey's test), it was seen that only with the use of the most acidic zeolite (SiO_2/Al_2O_3= 30) resulted in significantly

different total carbon yield at all three pyrolysis temperatures. With the use of the least acidic catalyst (SiO_2/Al_2O_3= 280), the yield at 550°C was different from the yield at 600°C; however, no significant difference was observed between the yields at 500 and 600 °C and between the yields at 500 and 550°C. Also, it was found that at the lowest pyrolysis temperature, use of more acidic zeolites (SiO_2/Al_2O_3= 30 and 50) resulted in total carbon yields significantly different from the yields with the use of low acidic zeolites (SiO_2/Al_2O_3= 80 and 280). However, at the highest temperature, yields obtained with the use of all acidic zeolites were different from each other. Figure 5.7 shows the effect of catalyst acidity and pyrolysis temperature on the product distribution from pyrolysis of torrefied lignin. Similar to the catalytic pyrolysis of raw lignin, catalytic pyrolysis of torrefied lignin also resulted in aromatic hydrocarbon as a primary product. Moreover, their yield increased with increase in catalyst acidity during pyrolysis at all the three pyrolysis temperatures. Simple phenols were significantly produced only with the use of the high acidity catalyst (SiO_2/Al_2O_3= 30) through the partial decomposition of lignin polymer. Aromatic hydrocarbons showed an initial sudden drop when the pyrolysis temperature increased from 500 to 550°C; however, the yield was high (~27 wt.% carbon) at the highest pyrolysis temperature (600°C). Among the aromatics, BTX (benzene, toluene and xylene) were the main compounds that showed a decrease when the temperature was increased to 550°C. This trend was same with the use of all zeolites except for zeolite with SiO_2/Al_2O_3= 50. Guaicols were found to be completely absent with the use of high acidity zeolite (SiO_2/Al_2O_3= 30 and 50), and they were found in traces when a relatively lower acidic catalyst was used. Elimination of guaiacols production could be due to the structural changes of torrefied lignin coupled with the

deoxygenation efficiency of zeolite catalyst. Overall, it can be concluded that the Bronsted acid sites of zeolite catalyst that determine its acidity favor the cleavage of methoxyl unit in guaiacols by donating protons and thereby resulting in either aromatic hydrocarbons or phenols. From statistical analysis, it was found that with the use of more acidic zeolites (SiO_2/Al_2O_3= 30 and 50), aromatic yields at 500 and 550°C were significantly different from the yields at 600°C. No significant difference was observed between the yields at 500 and 550°C. However, when a zeolite with SiO_2/Al_2O_3= 80 was used, the yield at 550°C was significantly different from that at 500 and 600°C. No significant difference was observed between the yields at 500 and 600°C. Also, it was observed that the aromatic yield with the use of the more acidic zeolites (SiO_2/Al_2O_3= 30 and 50) was significantly different from the yield with the use of the less acidic zeolites (SiO_2/Al_2O_3= 80 and 280) at all temperatures except 600°C. At the highest pyrolysis temperature (600°C), the yields obtained with the use of the acidic zeolites were significantly different from each other.

It is essential to understand that although torrefaction promotes the carbon yield from pyrolysis, there is always some carbon lost during torrefaction due to mass loss. Therefore, the effect of torrefaction on the overall carbon efficiency (liquid phase) of pyrolysis process is shown in Figure 5.8. It can be seen that in almost all cases, torrefaction did show promising improvement on the overall carbon yield from the pyrolysis process. Also, this increase is greater when a low acidity zeolite (SiO_2/Al_2O_3= 80 and 280) is used. This indicates that a high acidity zeolite promotes the carbon yield from pyrolysis of torrefied and raw lignin whereas the use of a low acidity zeolite enhances the overall carbon only from pyrolysis of torrefied lignin. When the zeolite with

SiO_2/Al_2O_3= 80 was used, torrefied lignin pyrolysis at 550°C resulted in 10% more overall carbon yield than that of raw lignin pyrolysis.

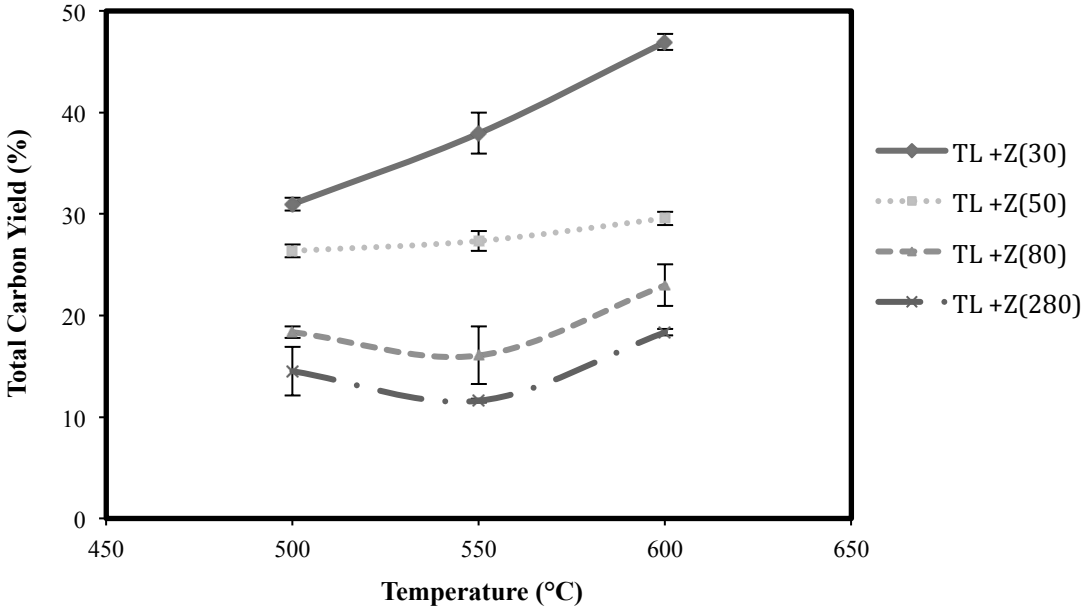

Figure 5.6: Effect of temperature on the carbon yield from catalytic pyrolysis of torrefied lignin with 1:4 biomass to catalyst ratio

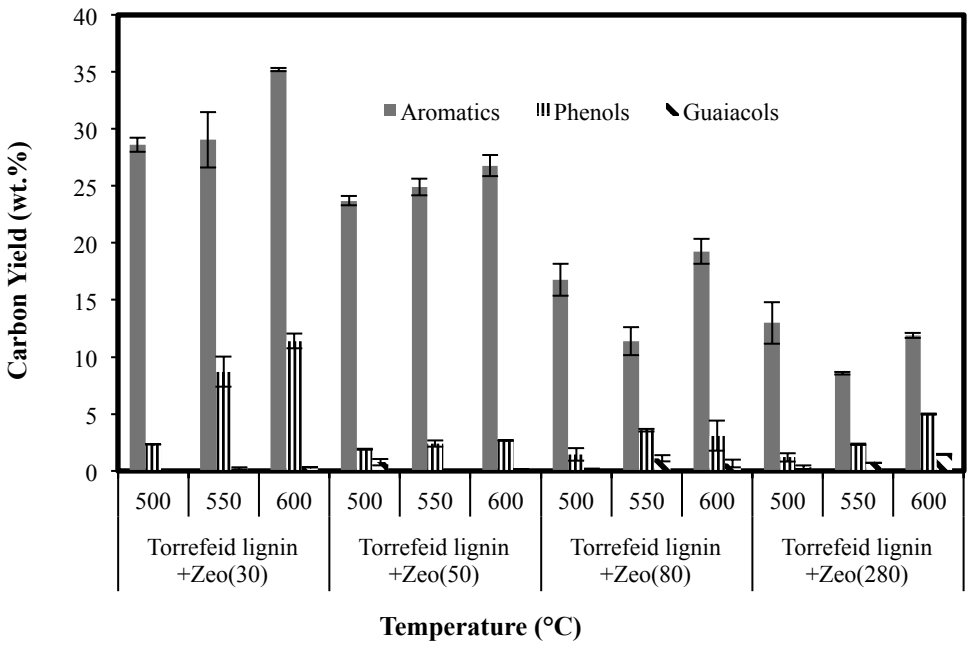

Figure 5.7: Effect of catalyst acidity and pyrolysis temperature on the product distribution of torrefied lignin pyrolysis

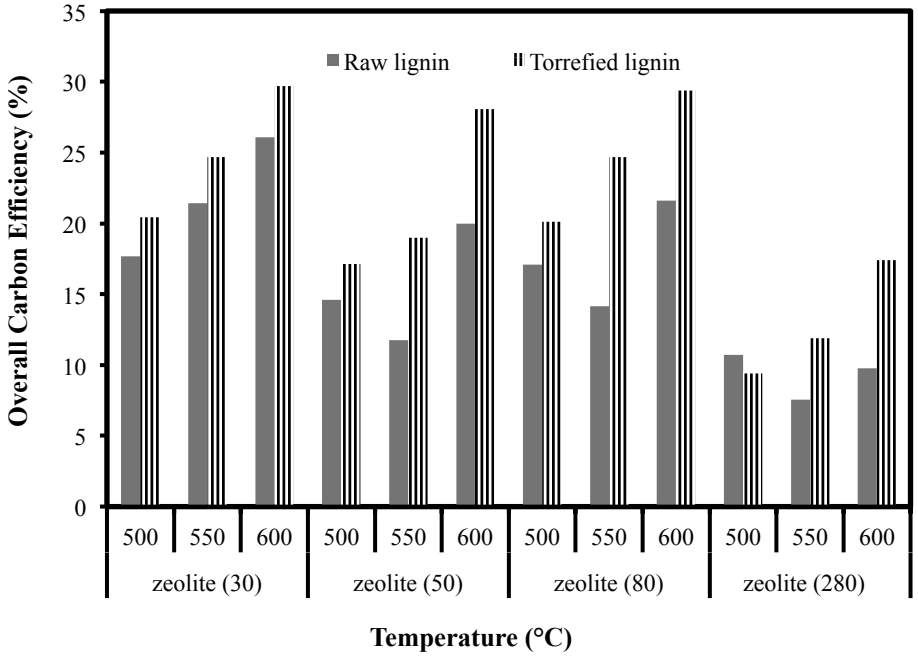

Figure 5.8: Effect of torrefaction on the average overall carbon yield from pyrolysis of lignin

5.5. Conclusion

Catalytic fast pyrolysis was carried out on torrefied and raw lignin with zeolite catalyst of varying acidity (SiO_2/Al_2O_3= 30,50,80 and 280). From the results, it was concluded that catalyst acidity and torrefaction significantly enhanced the production of aromatics from fast pyrolysis of lignin. It was observed that the major product from non-catalytic pyrolysis of raw lignin was guaiacols ~24 wt%; these guaiacols were produced in relatively smaller amounts during the pyrolysis of torrefied lignin (~7 wt.%). An FTIR study showed that more condensed guaiacyl linkages were seen due to torrefaction, which resulted in fewer guaiacols and more phenols during pyrolysis. Aromatics were produced from pyrolysis of both raw and torrefied lignin in the absence of the catalyst. Results from catalytic pyrolysis of raw and torrefied lignin showed that catalyst acidity

played a pivotal role in eliminating oxygenates and promoting aromatic production. More aromatics were formed when the ZSM-5 with the highest acidity (SiO_2/Al_20_3=30) was used for both torrefied and raw lignin. In spite of carbon loss during torrefaction, pyrolysis of torrefied lignin resulted in a higher overall carbon yield than that of pyrolysis of raw lignin.

5.6. References

Alriols, M.G., García, A., Llano-ponte, R., Labidi, J. 2010. Combined organosolv and ultrafiltration lignocellulosic biorefinery process. *Chemical Engineering Journal*, **157**(1), 113-120.

Boateng, A.A., Mullen, C.A. 2013. Fast pyrolysis of biomass thermally pretreated by torrefaction. *Journal of Analytical and Applied Pyrolysis*, **100**(0), 95-102.

Branca, C., Di Blasi, C., Galgano, A. 2012. Catalyst Screening for the Production of Furfural from Corncob Pyrolysis. *Energy & Fuels*, **26**(3), 1520-1530.

Bridgwater, A.V. 1999. Principles and practice of biomass fast pyrolysis processes for liquids. *Journal of Analytical and Applied Pyrolysis*, **51**(1–2), 3-22.

Caballero, J.A., Font, R., Marcilla, A. 1996. Kinetic study of the secondary thermal decomposition of Kraft lignin. *Journal of Analytical and Applied Pyrolysis*, **38**(1–2), 131-152.

Carlson, T.R., Vispute, T.P., Huber, G.W. 2008. Green gasoline by catalytic fast pyrolysis of solid biomass derived compounds. *ChemSusChem*, **1**(5), 397-400.

de Wild, P.J., Huijgen, W.J.J., Heeres, H.J. 2012. Pyrolysis of wheat straw-derived organosolv lignin. *Journal of Analytical and Applied Pyrolysis*, **93**(0), 95-103.

El Hage, R., Brosse, N., Chrusciel, L., Sanchez, C., Sannigrahi, P., Ragauskas, A. 2009. Characterization of milled wood lignin and ethanol organosolv lignin from miscanthus. *Polymer Degradation and Stability*, **94**(10), 1632-1638.

French, R., Czernik, S. 2010. Catalytic pyrolysis of biomass for biofuels production. *Fuel Processing Technology*, **91**(1), 25-32.

Ibrahim, R.H.H., Darvell, L.I., Jones, J.M., Williams, A. Physicochemical characterisation of torrefied biomass. *Journal of Analytical and Applied Pyrolysis*(0).

Jeon, M.-J., Jeon, J.-K., Suh, D.J., Park, S.H., Sa, Y.J., Joo, S.H., Park, Y.-K. 2013. Catalytic pyrolysis of biomass components over mesoporous catalysts using Py-GC/MS. *Catalysis Today*, **204**(0), 170-178.

Joshi, N., Lawal, A. 2012. Hydrodeoxygenation of pyrolysis oil in a microreactor. *Chemical Engineering Science*, **74**(0), 1-8.

Lu, Q., Li, W.-Z., Zhu, X.-F. 2009. Overview of fuel properties of biomass fast pyrolysis oils. *Energy Conversion and Management*, **50**(5), 1376-1383.

Lu, Q., Yang, X.-c., Dong, C.-q., Zhang, Z.-f., Zhang, X.-m., Zhu, X.-f. 2011. Influence of pyrolysis temperature and time on the cellulose fast pyrolysis products:

Analytical Py-GC/MS study. *Journal of Analytical and Applied Pyrolysis*, **92**(2), 430-438.
Mante, O.D., Agblevor, F.A., McClung, R. 2013. A study on catalytic pyrolysis of biomass with Y-zeolite based FCC catalyst using response surface methodology. *Fuel*, **108**(0), 451-464.
Meng, J., Park, J., Tilotta, D., Park, S. 2012. The effect of torrefaction on the chemistry of fast-pyrolysis bio-oil. *Bioresource Technology*, **111**(0), 439-446.
Mihalcik, D.J., Mullen, C.A., Boateng, A.A. 2011. Screening acidic zeolites for catalytic fast pyrolysis of biomass and its components. *Journal of Analytical and Applied Pyrolysis*, **92**(1), 224-232.
Mochizuki, T., Atong, D., Chen, S.-Y., Toba, M., Yoshimura, Y. 2013. Effect of SiO2 pore size on catalytic fast pyrolysis of Jatropha residues by using pyrolyzer-GC/MS. *Catalysis Communications*, **36**(0), 1-4.
Nakano, J., Meshitsuka, G. 1992. The Detection of Lignin. in: *Methods in Lignin Chemistry*, (Eds.) S. Lin, C. Dence, Springer Berlin Heidelberg, pp. 23-32.
Ren, S., Lei, H., Wang, L., Bu, Q., Chen, S., Wu, J., Julson, J., Ruan, R. 2013. The effects of torrefaction on compositions of bio-oil and syngas from biomass pyrolysis by microwave heating. *Bioresource Technology*, **135**(0), 659-664.
Thangalazhy-Gopakumar, S., Adhikari, S., Gupta, R.B., Fernando, S.D. 2011. Influence of Pyrolysis Operating Conditions on Bio-Oil Components: A Microscale Study in a Pyroprobe. *Energy & Fuels*, **25**(3), 1191-1199.
Vassilev, S.V., Baxter, D., Andersen, L.K., Vassileva, C.G. 2010. An overview of the chemical composition of biomass. *Fuel*, **89**(5), 913-933.
Via, B.K., Adhikari, S., Taylor, S. 2013. Modeling for proximate analysis and heating value of torrefied biomass with vibration spectroscopy. *Bioresource Technology*, **133**(0), 1-8.
Widyaningrum, R.N., Church, T.L., Zhao, M., Harris, A.T. 2012. Mesocellular-foam-silica-supported Ni catalyst: Effect of pore size on H2 production from cellulose pyrolysis. *International Journal of Hydrogen Energy*, **37**(12), 9590-9601.
Zheng, A., Zhao, Z., Chang, S., Huang, Z., He, F., Li, H. 2012. Effect of Torrefaction Temperature on Product Distribution from Two-Staged Pyrolysis of Biomass. *Energy & Fuels*, **26**(5), 2968-2974.
Zheng, A., Zhao, Z., Chang, S., Huang, Z., Wang, X., He, F., Li, H. 2013. Effect of torrefaction on structure and fast pyrolysis behavior of corncobs. *Bioresource Technology*, **128**(0), 370-377.

Chapter 6- Summary and Future Directions

6.1. Summary

The main objective of this study was to understand the impact of torrefaction on aromatic hydrocarbon yield from catalytic pyrolysis of biomass and its individual component. This was divided into three specific objectives and in the first objective, biomass pre-treatment (torrefaction) was done at 225°C for 30 min on pine wood chips and the torrefied chips were used for catalytic pyrolysis process at four different temperatures (450, 500, 550 and 600°C) with three different feed to ZSM-5 ratio (1:4, 1:9 and 1:16). In addition to this, metal impregnated catalytic pyrolysis was done over raw pine wood using four different metals (Ni, Co, Mn and Fe) at 500, 550 and 600°C. Results showed that torrefied biomass gave higher yield of aromatics compared to raw pine on pyrolysis. Also, temperature and ZSM-5 amount promoted its yield. Total carbon yield from pyrolysis of torrefied pine was 1.45 times the total carbon from raw pine pyrolysis. Compounds like guaiacols and furans were found to be possible intermediates for aromatic production as they were formed only at low temperature and low feed to catalyst ratio. Aromatic hydrocarbon produced with the use of cobalt impregnated ZSM-5 was 13% more than that produced with ZSM-5 without impregnation.

In the next two objectives, the effect of torrefaction on biomass components (cellulose and lignin) was studied. This was done to understand the influence of

torrefaction on the structure and pyrolytic behavior of cellulose and lignin. It was observed that both cellulose and lignin showed few structural changes on torrefaction which promoted the yield of aromatic hydrocarbons during pyrolysis. Torrefaction of cellulose resulted in significant amount of aromatic hydrocarbons from pyrolyis, which were completely absent from raw cellulose pyrolysis. The primary product from non-catalytic pyrolysis of raw cellulose was levoglucosan and this compound was found to be traces from torrefied cellulose pyrolysis. An FTIR study concluded that certain bonds such as hemiacetyl bond (C-O-C) and C-OH bond in cellulose weaken during torrefaction which attributes for decreased levoglucosan and increased aromatic hydrocarbon yield from pyrolysis. Along with the torrefaction, effect of ZSM-5 acidity and temperature on the product distribution from pyrolysis of raw and torrefied cellulose and lignin was also studied. Acidity of ZSM-5 played a pivotal role in promoting aromatic hydrocarbon yield from pyrolysis of cellulose and lignin. In case of cellulose, presence of catalyst resulted in minimizing the levoglucosan yield to a larger extent from pyrolysis of raw cellulose. Also, highest aromatic hydrocarbon yield (~25 wt. %) was obtained with the most acidic zeolite while lowest yield (~7wt.%) was obtained with the least acidic zeolite. Similarly, lignin resulted in maximum aromatic hydrocarbon yield (~27 wt%) from pyrolysis of torrefied lignin with the use of most acidic zeolite at 600°C. Primary product from non- catalytic pyrolysis of lignin was guaiacols and it was relatively low from torrefied lignin pyrolysis. An FTIR study showed that torrefaction results in more of condensed guaiacyl lignin linkages, which was responsible for low guaiacols and higher phenols from pyrolysis.

6.2. Future directions

This research has shed light over biomass pre-treatment and catalytic pyrolysis for highly deoxygenated liquid product production. It was found that torrefaction and ZSM-5 catalyst enhanced the aromatic hydrocarbon yield to a larger extent. However, this study has to be further explored in the following areas

- Study the effect of torrefaction temperature and time on the products from pyrolysis

  Present study has focused only on the torrefaction process at one single temperature and time and has proved to have a significant impact on the yield of hydrocarbons. In future, biomass torrefied at various temperature and time can be used as feedstock for pyrolysis to study the effect of torrefaction time and temperature on the hydrocarbon yield.

- Study the effect of metals on ZSM-5 during pyrolysis

  In our study we have analyzed the effect of certain transition metals (Co, Ni, Mn and Fe), however, study can also be extended to analyze the effect of noble metals like ruthenium, palladium and bi-functional metals such as Ni-Co on ZSM-5 catalyst during pyrolysis process.

- Study the effect of metal concentration in the biomass

  Properties of biomass play a very important role during pyrolysis process. In this work we have discussed about the behavior of major components in the biomass—cellulose and lignin during pyrolysis. However, we can also analyze the effect of metal (alkali and alkaline earth metals) present in the biomass during

pyrolysis by doping the biomass with various proportions of metal on the biomass.

- Investigate the use of basic oxide as catalyst for upgrading

  The catalyst used throughout our study was ZSM-5. Study can be extended to the use of various basic oxides such as zinc oxide, magnesium oxide as catalyst to understand if the presence of basic medium helps in producing deoxygenated products.

Appendix A: Data for Graphs

Table A.1: Data for Figure 3.1

	Carbon Yield (wt.%)	
Group	Raw pine	Torrefied Pine
AH	0.85 ± 0.001	8.67 ± 0.17
PH	3.49 ± 0.23	3.49 ± 0.02
G	1.72 ± 0.002	2.19 ± 0.01
Naph	2.36 ± 0.06	2.07 ± 0.09
AS	0.45 ± 0.006	1.87 ± 0.04
FN	1.61 ± 0.004	

Table A.2: Data for Figure 3.2

	Carbon Yield (wt. %)			
	Tar Phase		Aqeuous Phase	
Group	Torrefied pine	Raw pine	Torrefied pIne	Raw pine
AH	2.05 ± 0.01	0.96 ± 0.001	1.06 ± 0.04	0.84 ± 0.001
PH	1.96 ± 0.002	2.09 ± 0.008	2.5 ± 0.012	1.59 ± 0.07
G	0.97 ± 0.0	0.75 ± 0.002	2.01 ± 0.09	0.94 ± 0.03
Naph	0.35 ± 0.005	-	1.61 ± 0.02	0.1 ± 0.008
AS	0.1 ± 0.004	0.94 ± 0.003	1.23 ± 0.007	0.025 ± 0.0
FN	1.42 ± 0.06	0.94 ± 0.0	1.29 ± 0.02	0.38 ± 0.07

Table A.3: Data for Figure 3.3

Temperature (°C)	Total carbon yield (wt.%) Biomass :Catalyst ratio		
	1:4	1:9	1:14
450	15.61 ± 2.3	20.32 ± 2.01	26.78 ± 2.91
500	17.77 ± 1.96	24.91 ± 2.78	29.83 ± 2.76
550	29.23 ± 2.01	38.62 ± 1.98	49.12 ± 2.99
600	29.571 ± 2.96	44.98 ± 3.96	46.38 ± 3.8

Table A.4: Data for Figure 3.4

Group	Carbon Yield (wt.%) Temperatures(°C)			
	450	500	550	600
AH	9.43 ± 0.91	15.1 ± 0.98	18.51 ± 1.87	23.97 ± 1.68
PH	1.048 ± 0.012	2.36 ± 0.07	6.12 ± 0.02	7.58 ± 0.76
G	5.23 ± 0.12	0.85 ± 0.001	0.82 ± 0.005	0.76 ± 0.008
Naph	5.66 ± 0.87	4.84 ± 0.76	10.55 ± 0.92	12.06 ± 0.87
AS	-	-	1.61 ± 0.05	-
FN	2.31 ± 0.14	0.56 ± 0.04	0.45 ± 0.009	0.4 ± 0.001

Table A.5: Data for Figure 3.5

Temperature (°C)	Carbon Yield (wt.%)				
	Benzene	Toulene	P-xylene	Naphthalenes	Indanes
450	35.18 ± 1.04	25.66 ± 1.32	14.22 ± 1.45	11.87 ± 1.98	6.81 ± 0.91
500	36.64 ± 1.26	24.93 ± 1.67	13.02 ± 0.74	10.34 ± 0.79	6.42 ± 0.86
550	36.51 ± 1.73	31.38 ± 2.03	12.38 ± 0.29	8.47 ± 0.72	6.37 ± 0.91
600	34.12 ± 0.39	36.17 ± 2.71	5.95 ± 0.92	8.12 ± 0.42	5.95 ± 0.69

Table A.6: Data for Figure 3.6

	Carbon Yield (wt.%)					
Biomass: catalyst ratio	AH	PH	G	Naph	AS	FN
1:4	17.92 ± 1.08	2.79 ± 1.56		5.97 ± 0.87	0.76 ± 0.006	1.85 ± 0.02
1:9	23.97 ± 1.63	7.58 ± 2.08	0.76 ± 0.004	12. ± 1.436		
1:14	30.37 ± 2.17	1.8 ± 0.37		14.11 ± 1.72		

Table A.7: Data for Figure 3.7

	Carbon Yield (wt.%)				
Biomass : Catalyst ratio	Benzene	Toulene	P-xylene	Naphthalenes	Benzene derivatives
1:4	10.2 ± 0.79	7.33 ± 0.18	5.16 ± 0.98	7.33 ± 0.87	28.13 ± 1.86
1:9	9.6 ± 0.02	8.16 ± 0.76	5.84 ± 0.43	4.25 ± 0.17	24.79 ± 2.06
1:14	8.64 ± 0.01	10.29 ± 0.29	8.64 ± 0.71	3.35 ± 0.01	22.2 ± 2.18

Table A.8: Data for Figure 3.10

Metal Impregnated	Temperature (°C)	Total Carbon Yield (wt.%)
Cobalt	500	36.28 ± 3.82
	550	21.22 ± 1.90
	600	44.96 ± 3.94
Iron	500	26.28 ± 3.09
	550	16.13 ± 1.96
	600	5.98 ± 0.26
Nickel	500	13.3 ± 1.52
	550	11.3 ± 1.95
	600	12.01 ± 1.08
Manganese	500	2.21 ± 0.5
	550	7.65 ± 0.59
	600	14.68 ± 0.27

Table A.9: Data for Figure 3.11

Metal impregnated	Temperature (°C)	Carbon Yield (wt.%)				
		aromatic hydrocarbon	Phenols	Furans	Naphthalenes	Anhydrous sugars
Cobalt	500	23.82 ± 1.34	3.09 ± 0.039		8.72 ± 0.09	0.6 ± 0.09
	550	16.78 ± 1.1	0.86 ± 0.28	0.77 ± 0.01	2.63 ± 0.73	0.22 ± 0.02
	600	33.78 ± 2.13	1.38 ± 0.29	0.42 ± 0.09	9.11 ± 1.35	0.24 ± 0.08
Iron	500	19.83 ± 0.25	2.36 ± 0.87	0.96 ± 0.001	2.83 ± 0.09	0.28 ± 0.01
	550	9.03 ± 1.09	4.36 ± 0.03	1.48 ± 0.002	0.6 ±0.001	0.64 ± 0.001
	600	4..44 ± 0.18	0.79 ± 0.089	0.1 ± 0.01	0.46 ± 0.002	0.17 ± 0.03
Nickel	500	11.08 ± 1.5	1.91± 0.18	0.03 ± 0.01	0.26 ± 0.02	
	550	9.51 ± 1.09	0.67±0.034	0.07 ± 0.003	0.61 ± 0.056	0.42 ± 0.02
	600	5.39 ± 0.127	3.90± 0.18	0.75 ± 0.037	1.96 ± 0.09	
Manganese	500	1.92 ± 0.203			0.29 ± 0.30	
	550	6.65 ± 0.34	0.13± 0.04		0.86 ± 0.21	
	600	13.14 ± 0.87	0.07± 0.001		1.46 ± 0.04	

Table A.10: Data for Figure 3.12

Groups	Metal impregnated on zeolite				
	Cobalt	Iron	Nickel	Manganese	Zeolite
Aromatic hydrocarbon	23.86 ± 1.34	19.83 ± 0.258	11.08 ± 1.5	1.92 ± 0.2	10.67 ± 0.87
Phenols	3.09 ± 0.18	2.36 ± 0.29	1.91 ± 0.08		5.01 ± 0.02
Furans		0.96 ± 0.001	0.03 ± 0.01		1.01 ± 0.01
Naphthalenes	8.72 ± 0.47	2.83 ± 0.09	0.26 ± 0.02	0.29 ± 0.03	3.9 ± 0.67
Anhydrous sugars	0.6 ± 0.09	0.28 ± 0.01			0.12 ± 0.001

Table A.11: Data for Figure 4.1

Sample	Moisture content (%)	Mass retained (% d.b)	Energy retained (%)	Carbon (% d.b)	Hydrogen (% d.b)	Oxygen (% d.b)
Raw cellulose	6.24	100	100 ± 0.12	42.66 ± 0.00	7.1 ± 0.00	56.84 ± 0
Torrefied cellulose	4.3	78.86	97.6 ± 0.06	44.2 ± 0.00	6.93 ± 0.162	53.34 ±0.162

Table A.12: Data for Figure 4.3

Groups	Raw cellulose (wt.% carbon)	Torrefied Cellulose (wt. % carbon)
Aromatics	-	10.43 ± 0.11
Furans	5.17 ± 0.33	3.84 ± 0.55
Anhydrous sugars	14.49 ± 0.36	0.57 ± 0.28

Table A.13: Data for Figure 4.5

Silica / Alumina	Temperature (°C)	Total carbon yield (wt. %)
30	500	28.61 ± 1.21
	550	40.47 ± 1.53
	600	41.92 ± 2.6
50	500	21.01± 2.98
	550	26.07 ±1.42
	600	26.98 ±1.02
80	500	23.52 ±1.82
	550	31.16 ±2.98
	600	30.22 ± 1.68
280	500	14.43 ± 1.13
	550	21.11 ± 0.43
	600	16.94 ± 0.95

Table A.14: Data for Figure 4.6

Silica:Alumina	Temperature (°C)	Total carbon yield (wt. %)
30	500	33.509 ± 2.08
	550	39.573 ± 2.71
	600	38.841 ± 2.44
50	500	25.74 ± 4.46
	550	28.6 ± 2.62
	600	27.43 ±2.34
80	500	23.65 ± 1.43
	550	21.89 ± 0.83
	600	15.11 ± 0.67
280	500	14.06 ± 0.68
	550	13.02 ± 0.94

	600	5.97 ± 0.33

Table A.15: Data for Figure 4.7

Silica:Alumina	Temperature (°C)	Carbon yield (wt. %)			
		Aromatics	Phenols	Furans	Anhydrous sugars
30	500	19.21 ± 0.78	7.53 ± 1.47	1.46 ± 0.11	0.41 ± 0.05
	550	24.59 ± 1.94	11.47 ± 1.27	3.82 ± 0.23	0.59 ± 0.04
	600	25.36 ± 1.33	13.29 ± 1.64	2.96 ± 1.04	0.31 ± 0.22
50	500	12.22 ± 2.15	5.2 ± 1.6	2.18 ± 1.57	1.41 ± 0.86
	550	22.93 ± 0.84	1.38 ± 0.46	1.36 ± 1.24	0.4 ± 0.05
	600	21.54 ± 1.67	2.98 ± 0.98	1.74 ± 0.01	0.72 ± 0.04
80	500	10.54 ± 0.5	7.84 ± 1.35	4.24 ± 1.73	0.9 ± 0.52
	550	20.07 ± 1.7	8.4 ± 0.87	2.2 ± 0.3	0.49 ± 0.16
	600	19.56 ± 0.81	8.97 ± 1.44	1.41 ± 0.69	0.28 ± 0.07
280	500	5.62 ± 0.82	3.04 ± 0.42	5.71 ± 1.32	0.06 ± 0.06
	550	7.12 ± 0.76	7.54 ± 1.55	6.45 ± 1.52	-
	600	7.99 ± 1.01	2.33 ± 0.32	6.55 ± 0.21	0.07 ± 0.05

Table A.16: Data for Figure 4.8

Silica:Alumina	Temperature (°C)	Carbon yield (wt. %)			
		Aromatics	Phenols	Furans	Anhydrous sugars
30	500	27.07 ± 0.1	5.69 ± 0.57	0.73 ± 0.09	0.019 ± 0.002
	550	30.14 ± 0.10	8.98 ± 0.57	0.43 ± 0.09	0.023 ± 0.001
	600	30.49 ± 0.5	8.13 ± 1.12	0.2 ± 0.001	0.021 ± 0.003
50	500	18.95 ± 1.69	2.02 ± 0.97	3.94 ± 1.02	0.83 ± 0.5
	550	21.59 ± 0.91	2.64 ± 1.32	2.81 ± 0.17	1.56 ± 0.58
	600	23.43 ± 1.87	2.82 ± 0.58	0.77 ± 0.14	0.41 ± 0.07
80	500	13.99 ± 0.63	2.99 ± 0.28	4.49 ± 1.82	2.18 ± 0.16
	550	13.95 ± 0.91	3.47 ± 0.44	2.18 ± 0.22	2.29 ± 0.61
	600	11.04 ± 0.87	2.51 ± 0.28	1.24 ± 0.16	0.32 ± 0.1
280	500	9.47 ± 0.09	1.17 ± 0.43	3.39 ± 0.03	0.03 ± 0.02
	550	10.24 ± 1.0	1.18 ± 0.91	1.34 ± 0.79	0.26 ± 0.08
	600	3.19 ± 0.43	0.98 ± 0.24	1.65 ± 0.24	0.15 ± 0.01

Table A.17: Data for Figure 4.9

Silica:Alumina	Temperature (°C)	Overall carbon yield (wt. %)	
		Raw cellulose	Torrefied cellulose
30	500	11.444	18.4265991
	550	16.188	21.7611927
	600	16.768	21.3597657
50	500	8.404	14.154426
	550	10.428	15.72714
	600	10.792	15.083757
80	500	9.408	13.005135
	550	9.408	13.005135
	600	12.464	8.308989
280	500	4.6176	7.92984
	550	8.444	7.332
	600	3.388	2.8059

Table A.18: Data for Figure 5.2

Samples	Raw lignin	Torrefied Lignin
Aromatics	2.07± 0.21	7.23 ± 1.67
Phenols	8.27 ± 0.24	13.58 ± 1.61
Guaiacols	23.02 ± 1.75	7.22 ± 0.61

Table A.19: Data for Figure 5.4

Silica:Alumina	Temperature (°C)	Total carbon yield (wt.%)
30	500	32.63 ± 2.45
	550	37.15 ± 1.11
	600	39.39 ± 4.91
50	500	22.76 ± 2.06
	550	28.53 ± 1.95
	600	30.18 ± 4.14
80	500	19.41 ± 0.29
	550	22.13 ± 2.27

	600	21.61 ± 2.56
280	500	16.23 ± 1.29
	550	18 ± 0.22
	600	14.74 ± 0.19

Table A.20: Data for Figure 5.5

Silica:Alumina	Temperature (°C)	Carbon yield (wt.%)		
		Aromatics	Phenols	Guaiacols
30	500	22.38 ± 0.8	6.3 ± 0.25	
	550	23.42 ± 1.36	7.6 ± 0.74	1.08 ± 0.05
	600	22.46 ± 2.2	9.16 ± 0.2	1.56 ± 0.22
50	500	18.64 ± 2.21	2.47 ± 0.03	0.27 ± 0.04
	550	19.89 ± 0.91	4.22 ± 0.1	0.8 ± 0.3
	600	16.69 ± 1.72	2.93 ± 0.10	1.46 ± 0.38
80	500	13.55 ± 0.81	0.47 ± 0.07	3.28 ± 0.51
	550	14.38 ± 0.763	2.04 ± 0.34	0.44 ± 0.02
	600	13.3 ± 0.5	1.67 ± 0.17	0.36 ± 0.04
280	500	7.74 ± 1.02	3.92 ± 0.35	1.84 ± 0.01
	550	5.59 ± 0.15	7.43 ± 0.03	1.09 ± 0.002
	600	7.2 ± 0.12	4.12 ± 0.07	0.5 ± 0.004

Table A.21: Data for Figure 5.6

Silica:Alumina	Temperature (°C)	Total carbon yield (wt.%)
30	500	32.63 ± 2.45
	550	37.15 ± 1.11
	600	39.39 ± 4.91
50	500	22.76 ± 2.06
	550	28.53 ± 1.95
	600	30.18 ± 4.14
80	500	19.41 ± 0.29
	550	22.13 ± 2.27
	600	21.61 ± 2.56
280	500	16.23 ± 1.29
	550	18 ± 0.22
	600	14.74 ± 0.19

Table A.22: Data for Figure 5.7

Silica:Alumina	Temperature	Carbon yield (wt.%)

	(°C)	Aromatics	Phenols	Guaiacols
30	500	22.38 ± 0.8	6.3 ± 0.25	
	550	23.42 ± 1.36	7.6 ± 0.74	1.08 ± 0.05
	600	22.46 ± 2.2	9.16 ± 0.2	1.56 ± 0.22
50	500	18.64 ± 2.21	2.47 ± 0.03	0.27 ± 0.04
	550	19.89 ± 0.91	4.22 ± 0.1	0.8 ± 0.3
	600	16.69 ± 1.72	2.93 ± 0.10	1.46 ± 0.38
80	500	13.55 ± 0.81	0.47 ± 0.07	3.28 ± 0.51
	550	14.38 ± 0.763	2.04 ± 0.34	0.44 ± 0.02
	600	13.3 ± 0.5	1.67 ± 0.17	0.36 ± 0.04
280	500	7.74 ± 1.02	3.92 ± 0.35	1.84 ± 0.01
	550	5.59 ± 0.15	7.43 ± 0.03	1.09 ± 0.002
	600	7.2 ± 0.12	4.12 ± 0.07	0.5 ± 0.004

Table A.23: Data for Figure 5.8

		Overall carbon yield (wt.%)	
Silica:Alumina	Temperature (°C)	Raw lignin	Torrefied lignin
30	500	17.66	20.42
	550	21.45	24.66
	600	26.09	29.7
50	500	14.62	17.13
	550	11.75	19
	600	19.99	28.07
80	500	17.08	20.11
	550	14.13	24.661
	600	21.61	29.38
280	500	10.71	9.425
	550	7.54	11.88
	600	9.76	17.41